UNIVERSIDAD DE LA REPÚBLICA URUGUAY

FACULTAD DE CIENCIAS
UDELAR | fcien.edu.uy

Doctorado en Biotecnología

Fotoliasas bacterianas antárticas: bioprospección, producción recombinante, caracterización y potencial biotecnológico

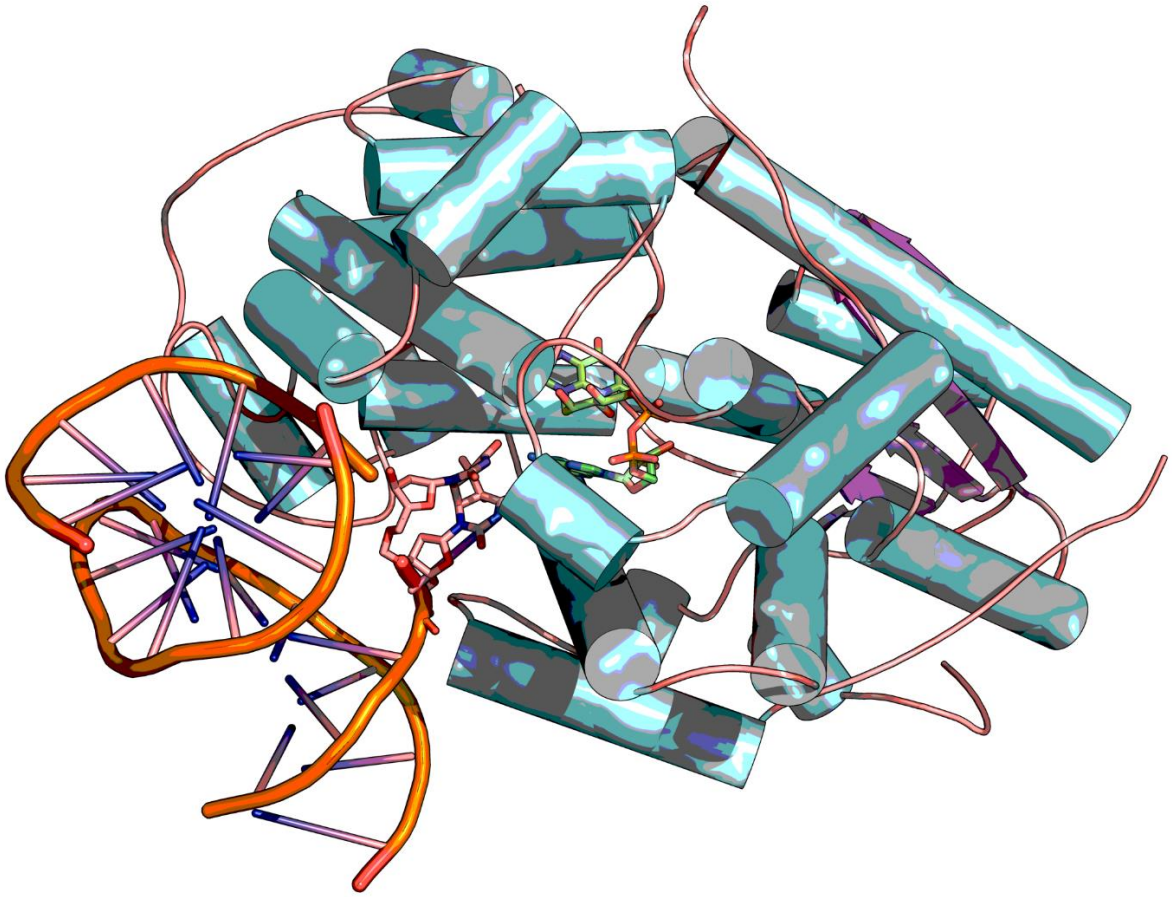

Lic. Juan José Marizcurrena

Tesis de Doctorado en Biotecnología

Posgrado en Biotecnología

Fotoliasas bacterianas antárticas: bioprospección, producción recombinante, caracterización y potencial biotecnológico

Juan José Marizcurrena

Orientadora: Dra. Susana Castro-Sowinski

Co-orientador: Dr. Wilner Martínez-López

Tribunal:

Dra. Beatriz Álvarez

Dra. Cecilia Abreu

Dr. Carlos Carmona

Sección Bioquímica y Biología Molecular

Facultad de Ciencias

UdelaR

Agradecimientos

A Susana Castro, por sus años dedicados a mi formación, empezando por mi tesis de grado y hasta culminar el Doctorado. Por saber aguantarme en los peores momentos, y por compartir su alegría en los buenos. Gracias por permitirme pensar por mí mismo, por dejarme seguir adelante con ideas que creías que no llegarían a buen puerto y por introducirme de puertas abiertas y sin dudar, a su tesoro más grande, su familia.

A los que estuvieron siempre: César García, Lorena Herrera, Bibiana, Célica, por su amistad, por los incontables momentos de payasadas que no voy a olvidar nunca, y por la infinita paciencia en los momentos de frustración en la ciencia.

A los de mayor experiencia: Manuel, Carolina, Diego, Uriel, Mario, Nati Fullana, por estar siempre bien dispuestos a esas dudas que surgen todo el tiempo cuando uno está haciendo mesada y por infundir las buenas prácticas e introducir nuevas preguntas.

A los nuevos: Matías, Marcos, Valentina, Mariana, Camila, Tania María, por aportar juventud y alegrar el día a día.

A los integrantes de Sección Bioquímica, por hacerme sentir parte siempre. Por las horas de trabajo, almuerzos y consejos compartidos.

A mi Familia, a mis padres, mis hermanos, y abuelos, por ser una familia unida y que siempre me alentaron a seguir luchando por mi sueño de hacer ciencia. A mi padre y a mi madre, gracias por mi crianza, por brindarme la mejor infancia que pude haber tenido, por contribuir a ser como soy, por permitirme estudiar, aunque eso requiriese alejarme de ustedes.

A Eloisa, amor de mi vida, madre de mis hijos. Gracias por compartir tu vida conmigo, por ayudarme a crecer, a superar mis trabas y animarte a construir una familia y un hogar juntos.

Finalmente, quiero agradecer a las agencias financiadores, ANII y CSIC, que brindaron el apoyo económico en forma de becas y de proyectos que permitieron realizar esta tesis.

Contenido

ESTRUCTURA DE LA TESIS

La presente tesis está organizada de la siguiente forma:

Se incluye un resumen, seguido de una introducción general que introduce la radiación UV como causante del daño al ADN, los sistemas de reparación de ADN dañado en hebra simple y finalmente profundiza en el mecanismo de fotorreparación y las fotoliasas. También incluye una breve reseña acerca de la historia y el descubrimiento de las fotoliasas. Posteriormente se incluyen la hipótesis de trabajo, el objetivo general y los objetivos específicos. Los resultados se presentan en tres capítulos. Los mismos se componen de los materiales y métodos, y los resultados a modo de artículos publicados. Dada mi afinidad por el arte, cada capítulo finaliza con una obra de bacterias en placa de agar, de ejecución propia.

La tesis concluye con una sección de discusión globalizadora que incluye aspectos ya discutidos en los manuscritos, así como de conclusiones y perspectivas al futuro.

El primer capítulo trata sobre la bioprospección e identificación de microorganismos antárticos resistentes a UVc (100-280 nm) y la búsqueda de genes codificantes para diversas fotoliasas, enzimas con potencial uso en la industria médica y cosmética.

El segundo capítulo trata sobre la caracterización del aislamiento UV-resistente *Hymenobacter* sp. UV11, el cual mostró mayor resistencia a UVc, la secuenciación y anotación del genoma y la búsqueda del gen codificante para la fotoliasa que produce. También incluye la producción, purificación y determinación de actividad de la fotoliasa recombinante.

El tercer capítulo trata sobre la búsqueda de fotoliasas en el aislamiento UV-resistente *Sphingomonas* sp. UV9, el cual mostró mayor capacidad fotorreparadora. También incluye la producción, purificación y determinación de actividad de la fotoliasa recombinante.

RESUMEN GRÁFICO

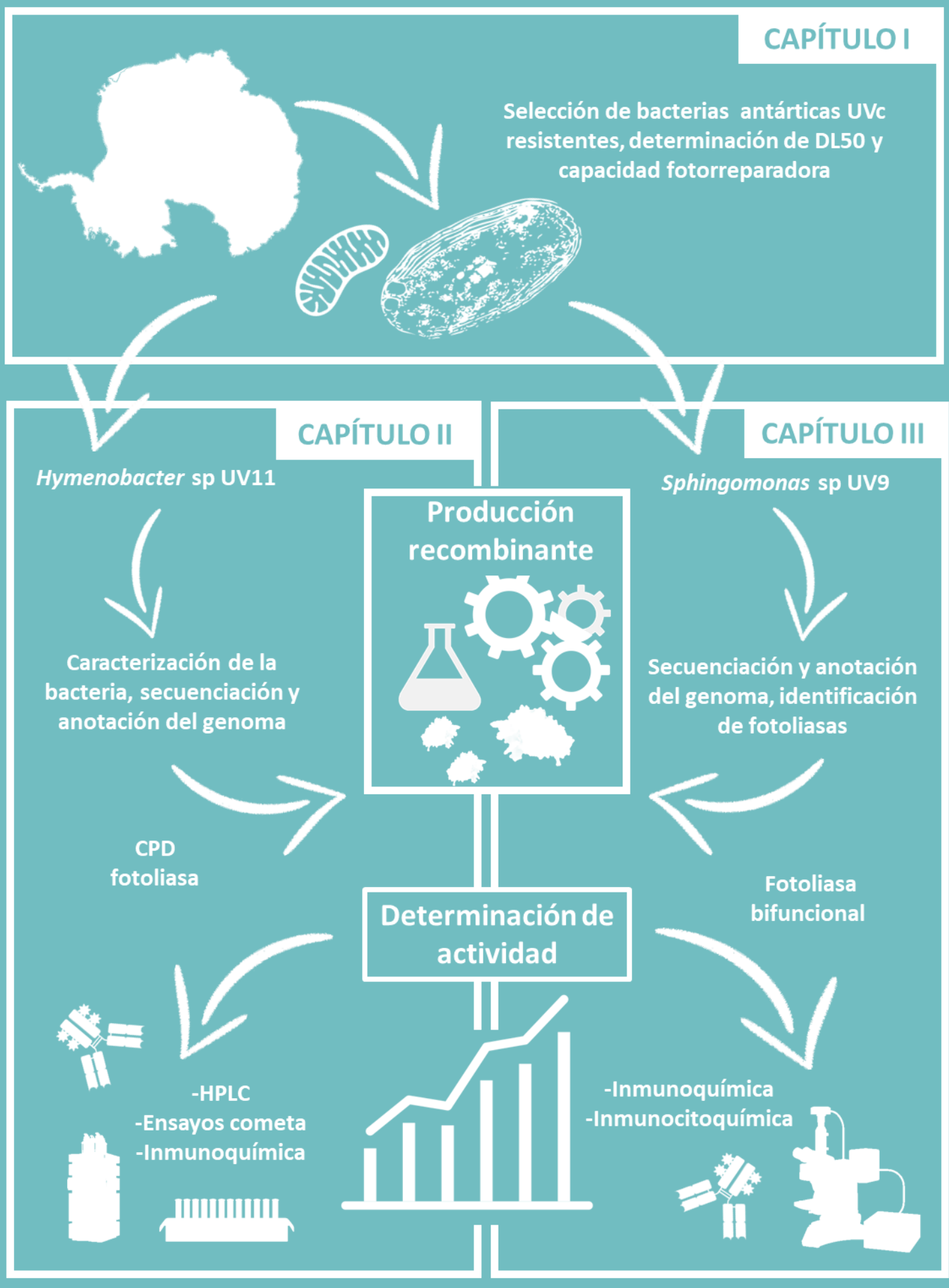

RESUMEN

A lo largo de la vida, lo seres vivos nos encontramos expuestos a diferentes tipos de estrés ambiental, como la exposición a la radiación solar. La luz solar está compuesta por la luz visible, la radiación infrarroja (que es responsable de hacernos sentir el calor) y la luz UV (que es responsable de generar el bronceado). El daño por radiación UV (formación de CPD- y 6,4-fotoproductos en el ADN, entre otros) es acumulativo y genera envejecimiento prematuro de la piel, aparición de manchas solares, arrugas e incluso en peores casos puede generar cáncer de piel.

Los organismos poseen diferentes mecanismos para reparar el daño por radiación UV. Entre estos, se encuentra un pequeño artefacto capaz de utilizar nuevamente la luz, pero en este caso para reparar el daño. Estas máquinas biológicas son denominadas fotoliasas, enzimas que no se encuentran en los mamíferos placentarios (entre los que se encuentra el Hombre). Su aplicación en forma tópica ha demostrado ser de gran utilidad reparando el daño causado por la irradiación UV al ADN.

En el desarrollo de esta tesis, se aislaron 12 microorganismos antárticos UV-resistentes y se identificaron por secuenciación y análisis del gen ADNr 16S. Se verificó que los mismos pertenecen a los siguientes géneros bacterianos: *Sphingomonas, Pseudomonas, Janthinobacterium, Hymenobacter* y *Flavobacterium*. Para los 12 microorganismos se realizaron curvas de muerte con dosis crecientes de radiaciones UVc, lo cual permitió la selección de dos bacterias con marcada resistencia y actividad fotorreparadora. Posteriormente, se procedió a la obtención de las secuencias codificantes de dichas fotoliasas, mediante una estrategia que incluyó el uso de cebadores degenerados y también de secuenciación completa del genoma. Se identificaron secuencias codificantes de CPD-fotoliasas de los géneros *Sphingomonas, Hymenobacter, Pseudomonas y Janthinobacterium*, así como una 6,4-fotoliasa del género *Sphingomonas*, enzimas encargadas de reparar los diferentes tipos de fotoproductos de ADN.

Luego se puso a punto la producción recombinante y purificación de fotoliasas presentes en los genomas de los géneros bacterianos que mostraron mayor resistencia y capacidad fotorreparadora, *Hymenobacter* sp. cepa UV11 y *Sphingomonas* sp. cepa UV9. La actividad de reparación de CPDs por la fotoliasa producida por *Hymenobacter* sp. UV11 se demostró por tres técnicas: HPLC, inmunoensayos y ensayos cometa. Por otro lado, la fotoliasa producida por *Sphingomonas* sp. UV11 demostró actividad reparadora de ambos, CPD- y 6,4-fotoproductos (fotoliasa bifuncional), algo novedoso, ya que no han reportado fotoliasas bifuncionales al momento.

Como resultado de esta propuesta se espera contribuir al desarrollo de una formulación con valor comercial para la industria farmacéutica, con fines cosméticos y médicos, incrementando el valor agregado de los productos actualmente disponibles en el mercado, y con aplicación en la prevención del foto-envejecimiento y cáncer de piel.

1. INTRODUCCIÓN

La presente introducción general está centrada en la radiación UV como el principal causante de daño directo en el ADN, profundizando en los sistemas de reparación del ADN, el mecanismo de la fotorreparación y algunas características generales de las fotoliasas. Se incluye también una reseña histórica de las fotoliasas. Los diferentes criterios de clasificación de fotoliasas según su taxonomía, tipo de sustratos que reconocen y los aminoácidos involucrados en las vías de fotorreparación, no son abordados en esta introducción, y se tratarán en detalle en las introducciones correspondientes del manuscrito que corresponda.

1.1. Cáncer de piel y la radiación ultravioleta

La incidencia del cáncer de piel se ha incrementado como consecuencia del adelgazamiento de la capa de ozono, así como por la mayor exposición a la luz ultravioleta (UV) en épocas estivales, por lo que se ha convertido en un problema de interés público. Si bien el desarrollo del cáncer es multifactorial, la irradiación UV juega un importante papel debido a su capacidad mutagénica, supresión del sistema inmunológico, estrés oxidativo y respuesta inflamatoria. Todos estos efectos desempeñan un rol en el envejecimiento prematuro de la piel (foto-envejecimiento), la aparición de manchas, la queratosis actínica y en el peor de los escenarios, el cáncer de piel. A nivel mundial, se estima que entre dos y tres millones de personas sufren de cáncer no-melanoma, la forma más benigna de la enfermedad y que en general no deriva en metástasis; existen 132.000 nuevos casos mundiales registrados de cáncer del tipo melanoma por año, con un promedio de una muerte por día (1). Sin embargo, estas cifra están muy subestimadas, ya que existe un registro inadecuado de esta enfermedad a nivel mundial (2). El índice de mortalidad por cáncer de piel es muy alto, sobre

todo si se considera que el melanoma es casi siempre curable si se trata durante las etapas incipientes de la enfermedad (3).

Existen diferentes tipos de cáncer de piel y sus diferencias radican en el tipo celular donde se originó el cáncer; ver Figura 1. 1. Si la célula originaria es un melanocito (células productoras del pigmento melanina), nos encontramos frente a un melanoma (4). Los cánceres de piel tipo no-melanoma, incluyen los carcinomas de células basales (ocho de cada diez casos) y los carcinomas de células escamosas (dos de cada diez) (5, 6); ver Figura 1. 1. Con menos frecuencia, también ocurren carcinomas de células de Merkel, Sarcoma de Kaposi, linfoma cutáneo, tumores de los folículos pilosos o glándulas de la piel (menos del 1 % de los cánceres de piel) (7).

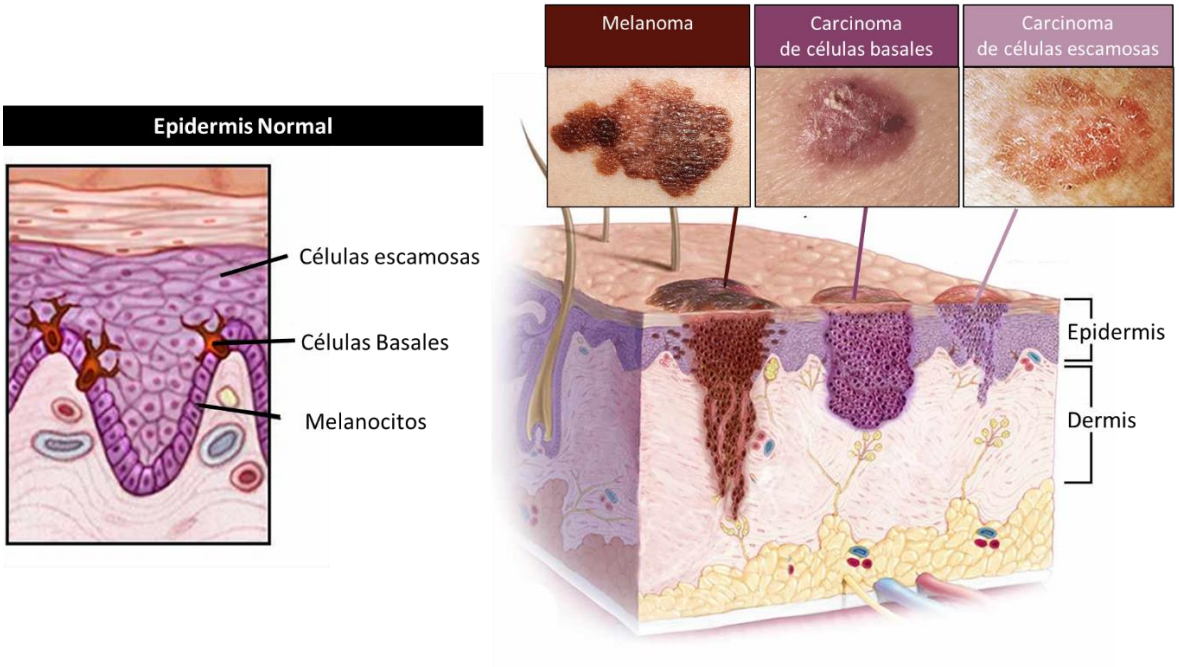

Figura 1. 1. Esquema de la piel y los tipos más comunes de cáncer piel. En la figura de la izquierda se esquematiza un corte de epidermis normal. En la figura de la derecha se muestra una sección donde se muestran los tipos más comunes de cánceres: melanoma, carcinoma de células basales y carcinoma de células escamosas.

En Uruguay muere una persona por cáncer de piel cada tres días (8), y según la Agencia Internacional de Investigación en Cáncer, se detectan aproximadamente 200 casos anuales de melanomas, con una mortalidad del 25 % (1).

Existen diversos tipos de radiaciones que alcanzan a la Tierra, entre ellas la luz proveniente del sol. La misma se compone principalmente de UV, visible e infrarroja. La luz UV se subdivide en: UVa (315 a 400 nm; produce principalmente estrés oxidativo), UVb (280 a 315 nm; produce estrés oxidativo y daño en el ADN) y UVc (100 a 280 nm, que produce daño oxidativo y fundamentalmente daño al ADN); esta última es absorbida por la capa de ozono presente en la atmósfera y que nos protege de sus efectos dañinos.

La forma de prevenir los riesgos y efectos de la irradiación UV sobre los humanos consiste en cambiar los hábitos de exposición al sol, evitando la exposición en horas críticas y usando protectores solares con filtros UVa y UVb en los horarios adecuados.

Las lesiones sobre el ADN más severas producidas por la irradiación UV son la formación de fotoproductos: dímeros de ciclo butano de pirimidinas (CPDs), y dímeros de pirimidina-pirimidona (6,4-fotoproductos; 6,4-FP); ver Figura 1. 2

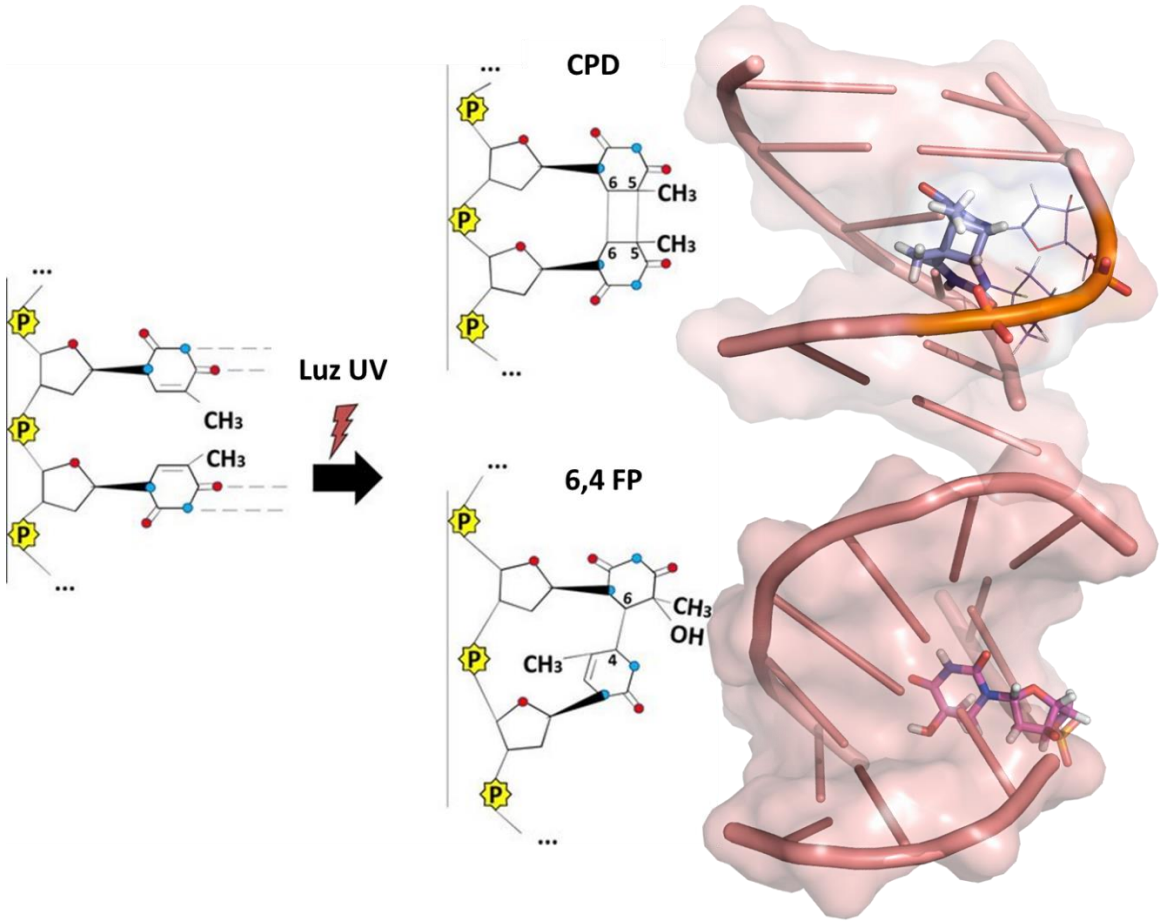

Figura 1. 2. Daño generado en el ADN frente a la exposición UV. Las bases nitrogenadas del ADN poseen un máximo de absorción a los 260 nm. Durante la excitación con UVc, se producen CPDs y 6,4-FP en aproximadamente un 75 % y 25 %, respectivamente. El molde utilizado para el CPD y el 6,4-FP corresponden a los números de acceso 1PIB y 1CFL. Los círculos rojos y celestes representan a los oxígenos y los nitrógenos, respectivamente. Adaptado de Quinet (9).

Este tipo de daño se repara principalmente de forma indirecta por el sistema de escisión de nucleótidos (NER). También se repara en forma directa a través de la enzima fotoliasa, una enzima que los mamíferos superiores no producimos (ver detalles más adelante). Las lesiones causadas por la exposición al UV conducen al rompimiento de los puentes de hidrógeno entre las dos hebras de ADN donde ocurrió el daño, impidiendo la complementariedad de bases en esa región del ADN. La distorsión causada sobre la estructura del ADN por estos fotoproductos termina impidiendo el desarrollo de los mecanismos básicos

para la vida de la célula, como son la replicación y la transcripción, resultando en la inducción de mutaciones, inestabilidad genómica y muerte celular (10).

1.1.1 Mecanismos de reparación del ADN

A continuación se presenta una breve reseña sobre los diferentes mecanismos o sistemas de reparación del daño presente en el ADN. Se tratará con mayor profundidad el mecanismo de reparación correspondiente a las fotoliasas.

1.1.1.1 Glicosilasas de ADN

Las glicosilasas son una familia de enzimas involucradas en la reparación por escisión de bases (BER). La escisión de bases es el mecanismo mediante el cual las bases dañadas presentes en el ADN se remueven y reemplazan; las ADN glicosilasas catalizan el primer paso de este proceso. Primero se remueve la base nitrogenada dañada, dejando el esqueleto del azúcar fosfato intacto y se crea un sitio apurínico-apirimidínico, comúnmente denominado sitio AP. La escisión se logra gracias a la torsión de la base dañada hacia afuera de la doble hélice, seguido de la ruptura del enlace N-glicosídico (11).

Varias glicosilasas evolucionaron para reconocer distintos tipos de bases oxidadas, las cuales se forman por el ataque de especies altamente oxidantes derivadas de la reducción parcial del oxígeno, generadas durante el metabolismo celular. Las lesiones más abundantes formadas a partir de residuos de guanina son el 2,6-diamino-4-hidroxi-5-formamidopirimidina (FapyG) y la 8-oxoguanina (12, 13). Esta última es frecuente en el ADN mitocondrial de personas de edad avanzada y es altamente mutagénica, ya que genera transiciones del tipo CG a AT (14).

1.1.1.2 Reparación por Escisión de Bases (BER)

La vía BER se encuentra en todos los dominios de la vida, es la principal responsable de la remoción de lesiones pequeñas en el ADN que no producen distorsiones en la hélice. La

vía BER la inicia una glicosilasa, que remueve las bases afectadas y deja un sitio AP, el cual posteriormente se cliva por una AP endonucleasa. El ADN resultante tiene entonces una rotura en una hebra y puede procesarse posteriormente por el mecanismo de parche corto (se reemplaza un solo nucleótido) o por parche largo (se sintetizan de 2 a 10 nucleótidos).

Generalmente esta vía actúa a continuación de los procesos de desaminación, oxidación y alquilación. Estas modificaciones afectan los enlaces de hidrógeno responsables de la complementariedad de bases, generando mutaciones. Las lesiones reparadas por la vía BER incluyen las bases oxidadas (8-oxoguanina; 2,6-diamino-4-hidroxi-5-formamidopirimidina, FapyG, FapyA), las bases alquiladas (3-metiladenina, 7-metilguanina), las bases desaminadas (hipoxantina formada a partir de adenina y xantina formada a partir de guanina) y el uracilo (por su incorporación errónea en el ADN o por desaminación espontánea de la citosina) (11).

1.1.1.3 Reparación por Escisión de Nucleótidos (NER)

El sistema de reparación conocido como NER se encuentra en todos los seres vivos y está formado por un complejo enzimático que cataliza múltiples pasos e involucra diversas enzimas; este sistema es capaz de reconocer grandes distorsiones en la estructura del ADN, como las lesiones inducidas por UV (CPDs y 6,4-FP) y aductos químicos voluminosos. Los individuos con deficiencias en el NER pueden presentar trastornos genéticos como el xeroderma pigmentosum (XP) o el síndrome de Cockayne (CS), con característicos síntomas clínicos. Estos trastornos se caracterizan por una mayor sensibilidad a la radiación UV, elevada incidencia en el desarrollo de cáncer y defectos en múltiples sistemas que pueden incluir alteraciones inmunológicas y neurológicas (15). Estas enfermedades muestran la importancia del sistema NER como un mecanismo fundamental para la protección de la integridad

funcional del genoma humano (16), proporcionando un apoyo importante para la teoría de la mutación somática del cáncer.

El sistema de reparación NER se compone de dos subvías. La reparación genómica global (GGR) opera en todo el genoma, pero tiene el inconveniente de que ciertos tipos de daños (como los CPDs inducidos por radiación UV) no se reconocen eficientemente y, en consecuencia, se reparan con baja eficiencia. Para evitar este tipo de lesiones que dificultan la transcripción por el estancamiento de la ARN polimerasa II, ha evolucionado una subvía de NER, denominada reparación acoplada a la transcripción (TCR). Este proceso dirige la maquinaria de reparación preferentemente a la polimerasa que se encuentra bloqueada en la plantilla activa de la cadena de ADN transcrita, y funciona como un sistema de copia de seguridad selectiva de las lesiones que son reparadas lentamente o no son reparadas por GGR (17).

1.1.1.4 Reparación por missmatch (MMR)

Consiste en un sistema, presente en todos los dominios de la vida, de reconocimiento y reparación de inserciones, deleciones y bases mal incorporadas que pueden aparecer durante la replicación y recombinación. La reparación por ¨missmatch¨ es específica de hebra, y puede distinguir la hebra parental de la hebra hija. Los ejemplos de reparación por ¨missmatch¨ incluyen G-T o A-C. Se reconoce la deformación de la doble hebra causada por el apareamiento erróneo, y posteriormente se repara escindiendo la base mal incorporada y reemplazándola con el nucleótido correcto.

Las bases mal apareadas son reconocidas por un dímero de MutS (proteínas descritas para *E. coli*), quien recluta las proteínas accesorias para formar el complejo MutSHL. A continuación, una helicasa (UvrD) separa las dos hebras y el complejo avanza hasta encontrar

la base mal apareada. A continuación, una exonucleasa (ExoI en eucariotas) sigue el complejo y degrada la cola de ss-DNA. Finalmente, la polimerasa pol III rellena el *gap* (18).

1.1.1.5 Fotorreparación

La fotorreparación es el proceso de reparación directa del ADN realizado por la enzima fotoliasa. La fotoliasas son flavoproteínas que utilizan la energía de la luz azul para reparar el ADN, catalizando la reparación de los fotoproductos resultantes de la formación de dímeros de ciclobutano de pirimidina (CPDs) y 6,4-fotoproductos. Las fotoliasas son específicas del tipo de daño que reconocen y reparan, y por ello se clasifican en CPD-fotoliasas o 6,4-fotoliasas, respectivamente. A diferencia de los mecanismos de reparación mencionados anteriormente, las fotoliasas están ausentes en los mamíferos superiores incluyendo a la especie humana. Por ser objeto de interés de esta tesis, las fotoliasas se abordarán en profundidad a continuación en la sección 1.2.

1.2. Proteínas y luz

En las últimas décadas, la ciencia ha hecho muchos aportes tendientes a comprender la importancia de la luz visible (400-700 nm) en la fisiología de plantas, animales y microorganismos. Se ha estudiado en profundidad el rol que cumple la luz visible en los procesos regulatorios generales, el ciclo circadiano, la fotosíntesis, así como en la producción de pigmentos en las especies fotótrofas (19, 20). Del mismo modo, los reportes de los cambios que se generan en respuesta a la luz azul, se conocen ya desde hace un largo tiempo y es bien conocida su influencia en el comportamiento y en el desarrollo de los organismos (21, 22).

Con el transcurso del tiempo, se han dado a conocer nuevas clases de receptores de luz azul y se ha visto que estos fotorreceptores se encuentran presentes en un amplio espectro de la filogenia microbiana; esto lleva a la idea de que la capacidad de percibir la luz azul es un atributo conservado en la evolución y por lo tanto de gran importancia (23–25). La

luz es una señal ubicua, tanto en ecosistemas terrestres como en acuáticos, y puede brindar información importante acerca de la posición del nicho ecológico. Por tanto, no resulta sorprendente que los sistemas sensores que detectan fotones en el rango visible se encuentren presentes en diferentes especies microbianas.

Existen muchos estudios del daño al ADN causado por exposición a la luz y cómo altera la estructura del material genético. Muchos microorganismos codifican fotorreceptores que regulan la síntesis de pigmentos protectores o bien que reparan directamente el ADN dañado en respuesta a la absorción de los fotones (26, 27).

1.2.1 Dominios sensores Luz-Oxígeno-Voltaje (LOV)

Los dominios LOV son sensores proteicos conservados en bacterias, arqueas, plantas, hongos y animales (incluyendo la especie humana); estos son capaces de detectar la luz azul a través de un cofactor flavina y cuyas funciones están principalmente asociadas a la percepción de las condiciones ambientales.

En cuanto a su estructura, los dominios LOV exhiben el plegado clásico Per-Arnt-Sim (PAS), nombrado así debido al nombre de las primeras proteínas descubiertas y que presentaban este dominio (Per – period circadian protein, Arnt – aryl hydrocarbon receptor nuclear translocator protein y Sim – single-minded protein) (28). Este arreglo, como se muestra en la Figura 1. 3a, consiste en cinco hojas beta antiparalelas (Aβ, Bβ, Gβ, Hβ and Iβ) con elementos conectores del tipo alfa hélice (Cα, Dα, Eα and Fα).

Este tipo de dominio presenta un cromóforo que contiene una flavina que se une de forma no covalente al bolsillo o cavidad de acceso al mismo; tras ser iluminado con luz azul, la energía de los fotones se traduce en la formación de un enlace covalente entre el C4 de la flavina y una cisteína que se encuentra en el motivo conservado GXNCRFLQ presente en la

hélice Eα (Figura 1. 3b, c). En la mayoría de los casos el enlace tiene vida media de minutos a horas, dependiendo de la proteína (29).

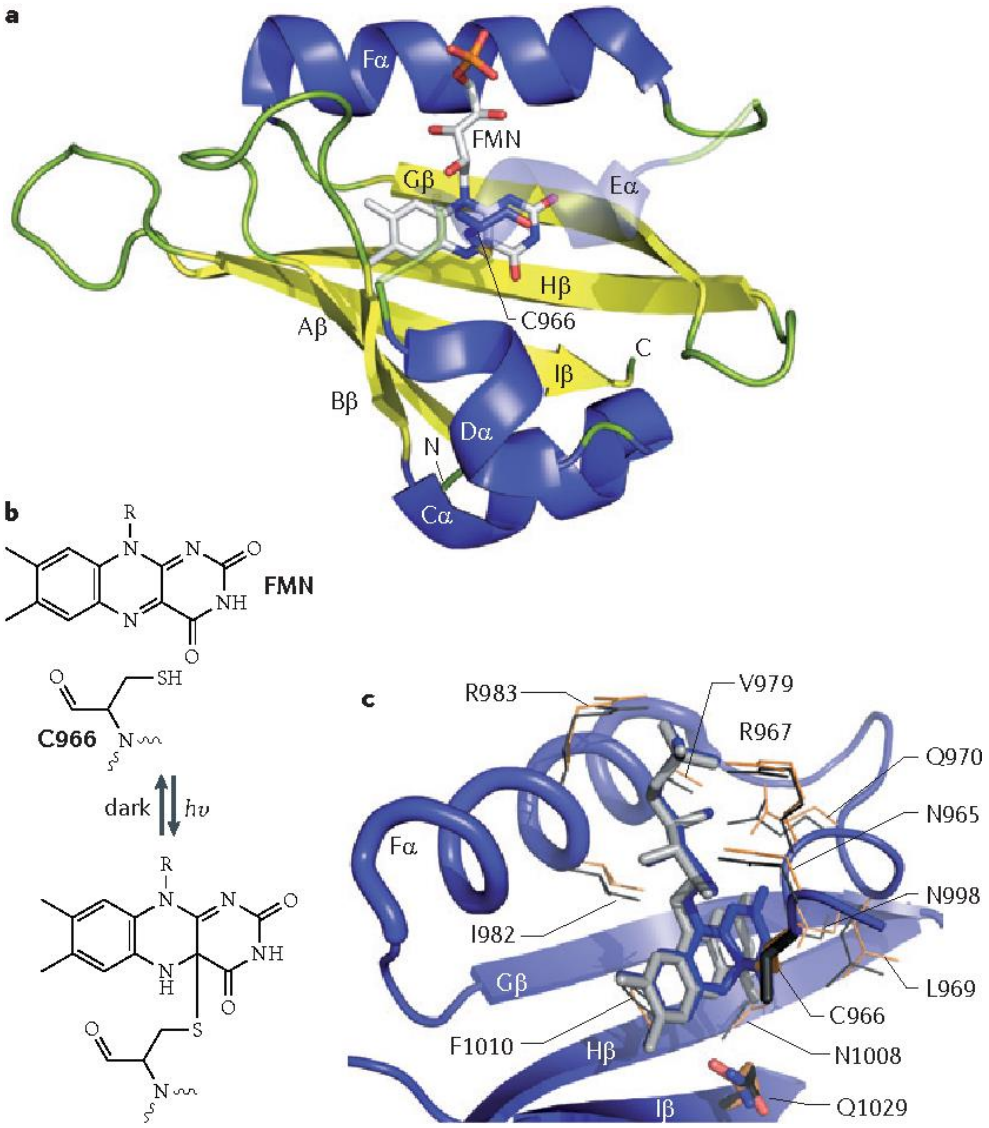

Figura 1. 3 Estructura de un dominio LOV. (A) Dominio LOV unido a un cromóforo de flavina en estado de iluminación (PDB 1JNU). Se muestran las hélices α en azul, las hojas β en amarillo y los bucles en verde. El mononucleótido de flavina (FMN) se muestra en gris. (B) Esquema del enlace covalente formado entre una cisteína y el C4 del FMN, en respuesta a la absorción de luz azul por parte del dominio LOV. (C) Bolsillo de unión a flavina del dominio LOV2 del fitocromo A (phy3). Los residuos que interaccionan con el cofactor FMN se muestran en naranja para el estado iluminado (PDB 1JNU) y en gris para el estado de oscuridad (PDB 1G28). Tomado de Herrou (30).

Entonces, cuando una proteína con dominios tipo LOV recibe una señal luminosa, se generan cambios conformacionales que modulan una función efectora. En bacterias, estas

funciones principalmente forman parte de sistemas de dos componentes que incluyen, entre otras, la adhesión celular, la esporulación y la respuesta a estrés (31, 32).

1.2.2 Criptocromos

Los criptocromos son receptores de luz azul y ultravioleta (UVa) que comparten estrecha identidad de secuencia y estructura con las fotoliasas; sin embargo, no poseen actividad catalítica (33–36). Los criptocromos, junto con las fotoliasas, constituyen la superfamilia de las fotoliasas/criptocromos que actúan como receptores de luz (37).

De acuerdo a la identidad de secuencias, los criptocromos se agrupan en tres subfamilias: los criptocromos de plantas, los criptocromos animales y CRY-DASH (ver Figura 1. 4).

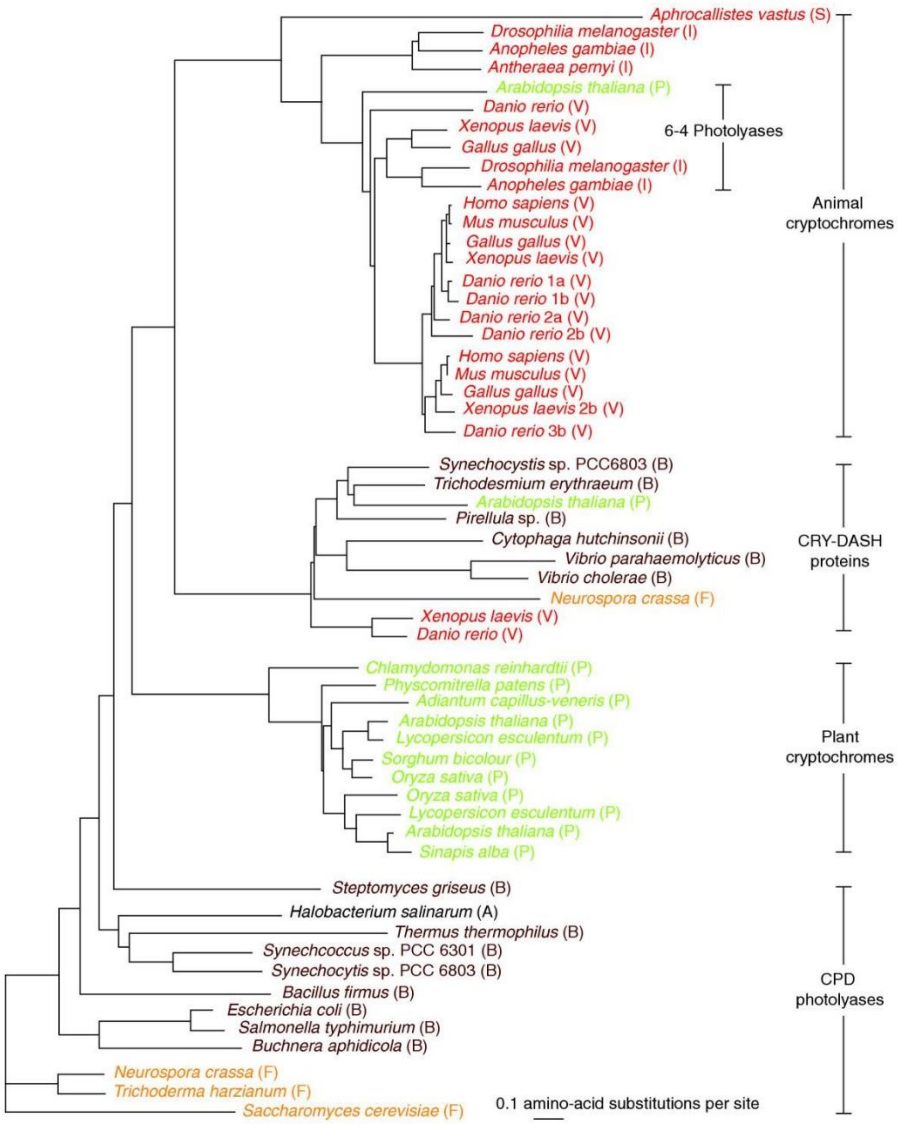

Figura 1. 4. Árbol filogenético de la subfamilia de fotoliasas/criptocromos. Abreviaciones: A, arqueas; B, bacteria; F, hongos; I, insectos; P, plantas; S, esponjas; V, vertebrados. Tomado de Lin (38).

Los criptocromos se encuentran ampliamente distribuidos en procariotas y eucariotas, pero no se han encontrado en arqueas (aunque éstas últimas sí poseen fotoliasas). El primer gen CRY1 de criptocromo identificado fue el de *Arabidopsis thaliana* (39), y posteriormente se encontraron por homologías en otras especies de plantas, animales y microorganismos. Los criptocromos animales son componentes fundamentales del reloj circadiano, capaces de controlar los ritmos fisiológicos y comportamentales diarios (35).

Inicialmente se creía que solo los eucariotas superiores poseían criptocromos, pero estudios posteriores revelaron la presencia de un gen de criptocromo en la cianobacteria *Synechocystis* sp. (25). A este nuevo tipo de criptocromo se le denominó CRY-DASH. Los CRY-DASH se han encontrado en cianobacterias fotosintéticas, bacterias, hongos, plantas y algunos animales; ver Figura 1. 4. Hasta el momento, no existe evidencia que indique cuál es la función biológica de los CRY-DASH.

Los criptocromos exhiben una estructura cristalina casi idéntica a las fotoliasas (ver Figura 1. 5a, b), pero no poseen actividad reparadora del ADN. La mayoría de los criptocromos (con excepción de los CRY-DASH), se componen de dos dominios, uno N-terminal relacionado a las fotoliasas (PHR) y uno C-terminal de tamaño variable (ver Figura 1. 5c). La región PHR de los criptocromos puede unir cromóforos (40, 41), mientras que las fotoliasas también pueden unir un FAD. El dominio C-terminal de los criptocromos se encuentra en general menos conservado que el dominio PHR; también es considerablemente más largo en criptocromos de plantas que en animales, y los CRY-DASH carecen completamente de este dominio.

Las estructuras cristalinas se han determinado para los tres miembros de la superfamilia: CPD fotoliasas (*E. coli*; Figura 1. 5b), CRY-DASH *(Synechococcus* sp.; Figura 1. 5d) y criptocromos de plantas (*A. thaliana* CRY1; Figura 1. 5a). Todos los dominios PHR poseen el mismo tipo de plegamiento, un dominio α/β seguido de un dominio hélices α conectados por un ¨*loop*¨ (Figura 1. 5c, d). Los dos lóbulos de la hélice α forman un bolsillo denominado cavidad de acceso del FAD (42, 43), que es donde se ubica esta molécula. El FAD se une de forma no covalente a la proteína adoptando una conformación atípica en forma de U, de tal modo que la adenina y el anillo isoaloxazina se posicionan también orientados hacia la parte inferior de la cavidad (ver Figura 1. 5d), desde donde puede acceder al solvente.

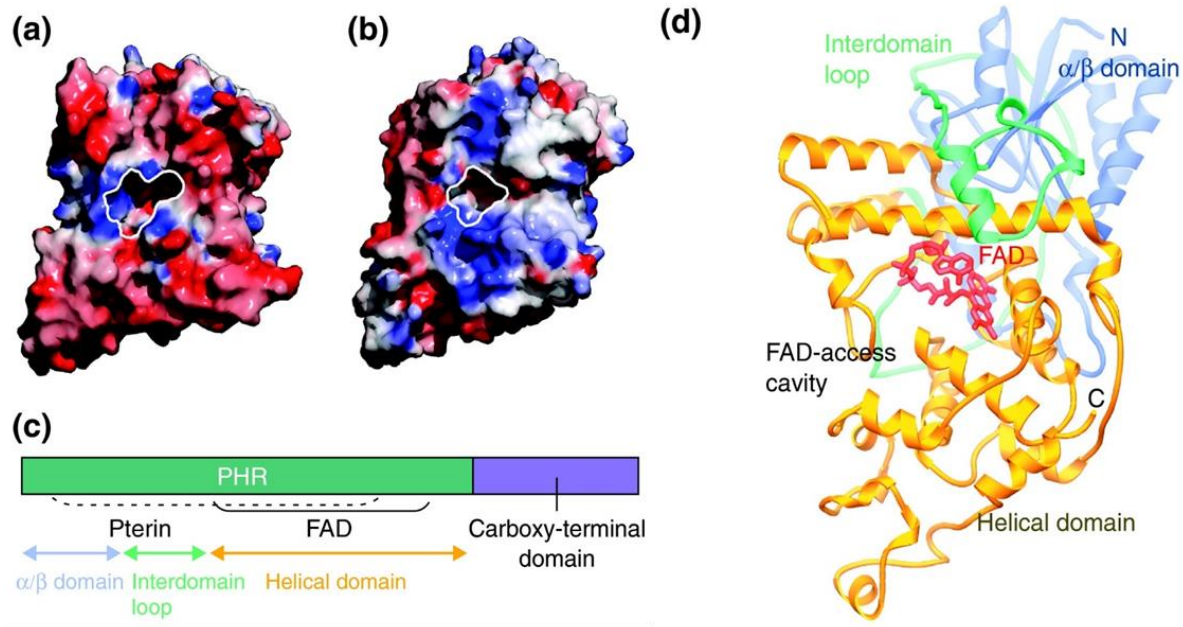

Figura 1. 5. Estructura de fotoliasas/criptocromos. Comparación de las estructuras de las regiones PHR de (a) CRY1 de *A. thaliana* y (b) la ADN fotoliasa de *E. coli*. Las líneas blancas indican la cavidad de acceso al FAD; los colores rojo y azul representan las áreas de potencial electrostático negativo y positivo, respectivamente. (c) Representación esquemática de una proteína típica de la superfamilia fotoliasa/criptocromo. Las partes de la región PHR donde se une la pterina y el FAD se indican con llaves y los dominios se indican debajo. (d) Estructura cristalina del CRY-DASH de *Synechocystis* sp. PCC6803. Tomado de Chentao (38).

A pesar de las similitudes estructurales, la región PHR de CRY1 de *A. thaliana* posee algunas diferencias con las fotoliasas y los CRY-DASH. En primer lugar, las fotoliasas poseen un surco cargado positivamente que se ubica por debajo de la cavidad de acceso del FAD (Figura 1. 5a), y que es la encargada de interaccionar con el ADN. El CRY-DASH también posee un surco similar con potencial electrostático positivo en la superficie que rodea a la cavidad, lo cual es consistente con la observación de que los CRY-DASH pueden unirse al ADN, aunque aún no se haya descifrado cual sea su función (44).

La región PHR de CRY1 carece de este surco (ver Figura 1. 5a), sugiriendo que esta proteína no tendría la capacidad de unirse directamente con el ADN. Otra distinción es que la cavidad donde se ubica el FAD en las fotoliasas/CRY-DASH no es tan larga y profunda como en CRY1 (ver, Figura 1. 5a).

1.2.3 Descubrimiento e historia de las fotoliasas

Las fotoliasas pueden imaginarse como nanomáquinas alimentadas por fotones de luz azul y que reparan los fotoproductos formados en el ADN por la exposición a luz UV. Claud Rupert fue quien describió a esta enzima por primera vez en 1958, y este descubrimiento marcó el comienzo del campo del estudio de la reparación del ADN como una disciplina científica. Anteriormente se conocía que el UV era capaz de eliminar de forma muy eficiente a las bacterias; pero en 1949, Alber Kelner (Cold Spring Harbor) observó que luego de la desinfección con UV y posterior exposición a la luz "las bacterias muertas volvían a la vida" (45, 46). En ese momento, este fenómeno no pudo explicarse, y se lo denominó fotorreactivación. Un tiempo después, Rupert analizó este fenómeno en profundidad y demostró que el UV causaba la muerte de las bacterias debido a que se producía daño en su material genético. Rupert también propuso que existía una enzima capaz de utilizar la energía de la luz azul (presente en la luz visible) responsable de reparar el ADN dañado. Hasta este momento la conclusión era que la luz azul era capaz de traer de nuevo a la vida a las células muertas, y que la resurrección de las bacterias no era un fenómeno milagroso que necesitaba de una explicación metafísica (47, 48), demostrándose que había una razón regida por las leyes de la física capaz de explicarlo. Rupert propuso entonces un mecanismo de reacción en donde la exposición a UV convertiría dos pirimidinas adyacentes en un dímero de ciclobutano de pirimidina (CPD), a través de la formación de un enlace C5_C5 y C6_C6. Posteriormente, la fotoliasa rompería los dos enlaces anormales que mantienen unidas a las pirimidinas, convirtiendo dicho dímero en dos pirimidinas normales (49, 50), reparando el ADN dañado y eliminando así los efectos dañinos del UV (Figura 1. 6).

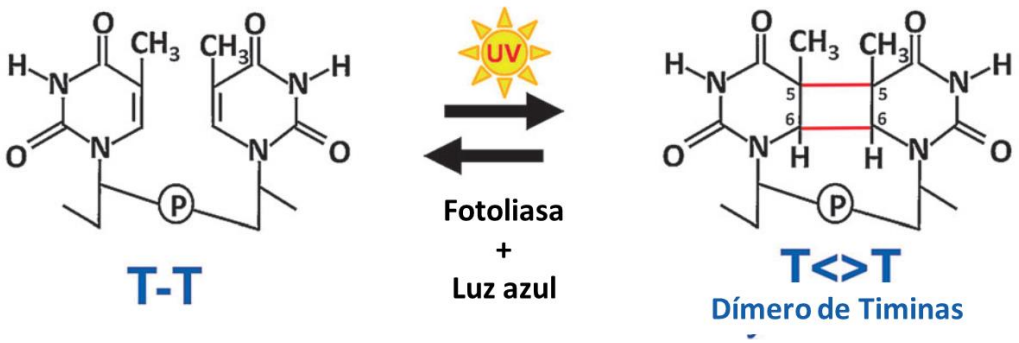

Figura 1. 6. Reparación mediada por fotoliasa, modelo general de Rupert. El UV induce la formación de CPDs, la fotoliasa se une al dímero, absorbe un fotón de luz azul y convierte el dímero en dos timinas canónicas. Adaptado de Sancar (51).

Si bien esto era una respuesta un tanto satisfactoria para el fenómeno de la fotorreactivación, generaba una pregunta que aún carecía de una explicación física. Si la fotoliasa es una proteína, ¿cómo se explica entonces su capacidad de absorber la luz azul? En las siguientes décadas, Rupert y colaboradores enfocaron sus esfuerzos en identificar el componente responsable de la absorción de la luz azul presente en las fotoliasas. Lamentablemente, estos esfuerzos no fueron productivos, pues determinaron que la bacteria *Escherichia coli* producía solo entre 10 y 20 moléculas de fotoliasa por célula, lo cual dificultaba purificar y caracterizar la enzima. Años más tarde, el Dr. Aziz Sancar, en esa época un joven estudiante (Premio Nobel de Química en el 2015 por sus contribuciones a los mecanismos de reparación del ADN), se incorporó al grupo del profesor Rupert. En esa época se encontraba en auge el clonado de genes y, meses después a finales de los 70´, Sancar produjo la primera fotoliasa recombinante (52). En los años siguientes, en la Universidad del Norte de Carolina (USA), Sancar y colaboradores purificaron la enzima en grandes cantidades, y observaron que la enzima tenía un característico color azul brillante (53–55). Este hallazgo respondió a la pregunta física, la presencia de un color azul indicaba que la proteína podía absorber la luz. A través de estudios de química analítica, el grupo se propuso identificar el

componente que absorbía la luz, y se encontraron no con uno, sino dos cofactores cromóforos, uno de ellos el meteniltetrahidrofolato (MTHF) y el otro un dinucleótido de flavina y adenina (FAD) (56, 57). También observaron que la fotoliasa exhibía colores que iban desde el violeta hasta el naranja, y que esto dependía del estado redox del FAD (58), ver Figura 1. 7.

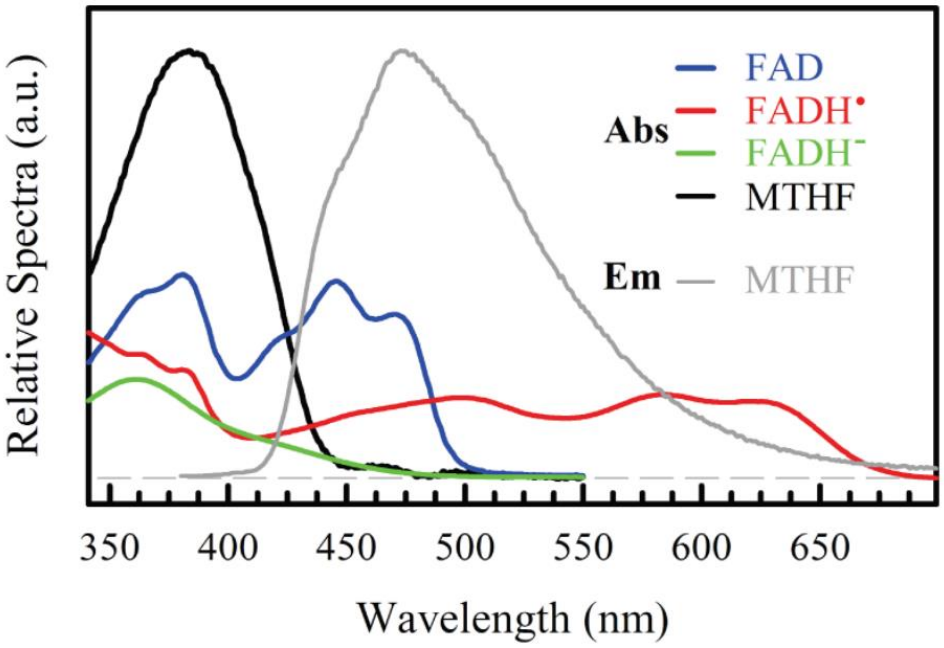

Figura 1. 7. Espectros del estado estacionario de la fotoliasa de *E. coli*. Se muestran los espectros relativos del FAD oxidado (azul), la semiquinona FADH• (rojo), la hidroquinona aniónica $FADH^-$ (verde), el MTHF (negro), y el espectro de emisión del MTHF (gris). La longitud de onda de excitación para el MTHF fue de 360 nm. Los espectros de absorción para el $FADH^-$ se registraron en condiciones aeróbicas, mientras que los espectros para FAD, FADH• y MTHF se registraron en condiciones anaeróbicas. Tomado Zhong (58).

Finalmente, las funciones de los dos cofactores se determinaron mediante experimentos fotoquímicos, donde se usó el folato como análogo a un panel solar que absorbía la energía presente en la luz y la transfería al FADH (59, 60). Realizando estos experimentos se determinó que la flavina cumple el rol de catalizador (aunque también es capaz de absorber fotones, pero de forma menos eficiente), llevando a cabo la reparación del

CPD. Esta reparación se realiza a través de un mecanismo de reacción radicalaria, en una serie de reacciones tipo redox (61, 62).

A mediados de 1995 se cristalizó la primera fotoliasa, y la información estructural apoyaba el mecanismo de reacción descrito hasta el momento (42). En la Figura 1. 8, se muestra la primera estructura 3D de la fotoliasa de *E. coli*, en un diagrama de cintas y de carga superficial. Tal como se había predicho bioquímicamente, el folato cumplía el rol de panel solar y se situaba sobre la parte superior de enzima, absorbía la luz, y luego transferiría la energía a la flavina que se encontraba enterrada en el centro de la enzima. Con esta información estructural se refinó el mecanismo de reacción, como se muestra en la Figura 1. 8. Se propuso que la fotoliasa se une a la hebra de ADN que contiene el CPD, debido a que es capaz de reconocer la distorsión del esqueleto generada por las T<>T. Luego de la unión, a través de interacciones iónicas entre el surco de la fotoliasa cargado positivamente y el esqueleto de fosfodiéster cargado negativamente del ADN, la enzima tornea las T<>T por fuera de la hélice, exponiéndolas hacia el centro de la enzima. De este modo las T<>T permanecen interaccionando a través de fuerzas de Van der Waals con el $FADH^-$ (reducido). El complejo resultante es muy estable, y permanecerá así hasta que el folato absorba el fotón y comience la transferencia de energía. El estado excitado de la flavina ($FADH^{-*}$), repara las T<>T mediante una reacción redox cíclica ($FADH^- \rightleftharpoons$CPD), permitiendo luego a la enzima disociarse del ADN para continuar con la búsqueda de otros sitios dañados del ADN.

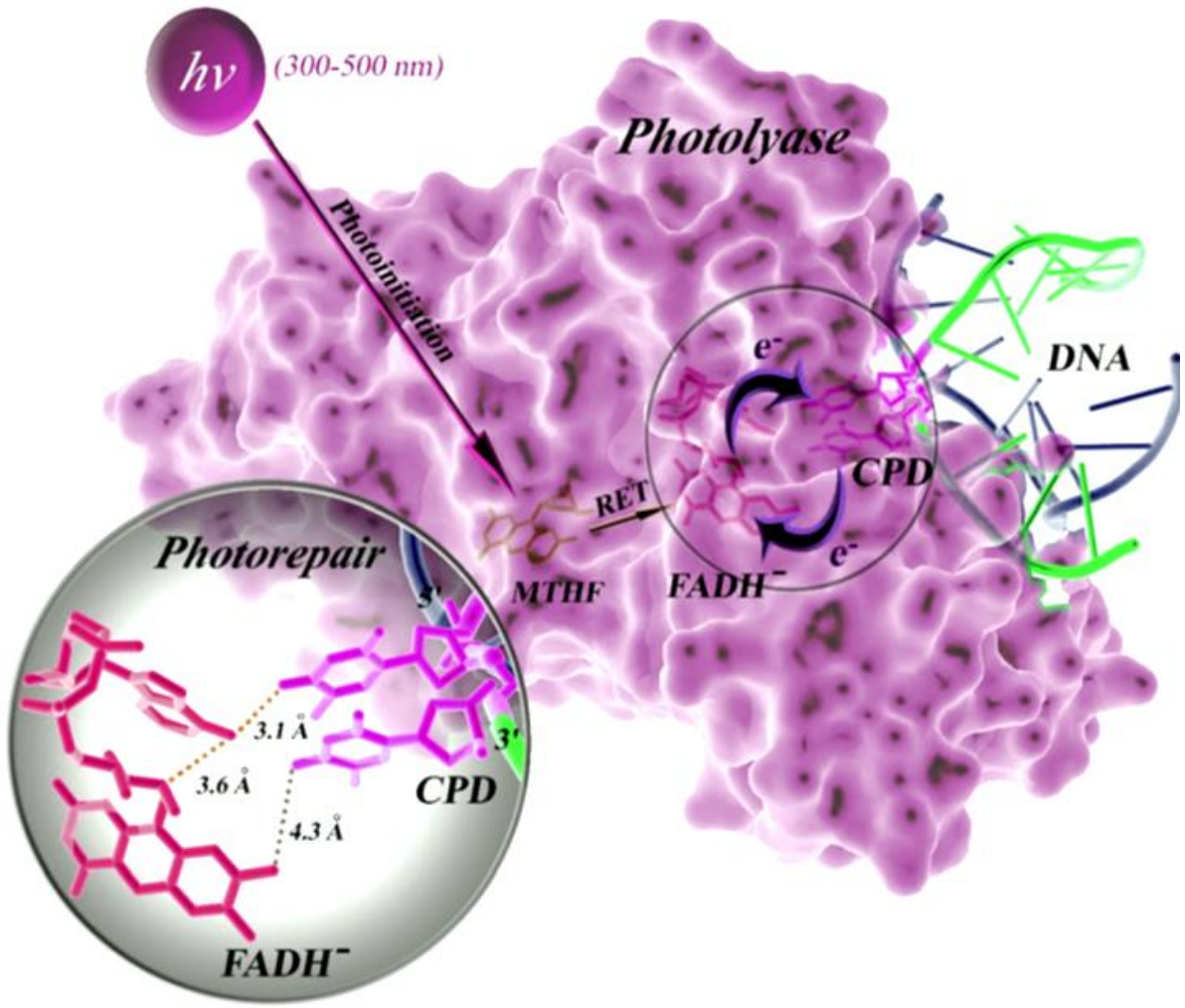

Figura 1. 8. Mecanismo de reacción de la fotoliasa. La enzima interacciona mediante enlaces iónicos con los residuos de fosfato del ADN dañado y gira los dímeros de pirimidina hacia la cavidad catalítica, para exponerlos al $FADH^{-}$. La catálisis se inicia por parte del folato, a través de la absorción de un fotón (300-500 nm). El estado excitado del MTHF transfiere la energía al $FADH^{-}$ mediante resonancia de Förster (FRET). Luego, el $FADH^{-}$* excitado repara el ciclobutano de pirimidina mediante una reacción cíclica redox convirtiendo las T< >T en T–T. La enzima luego se disocia del ADN reparado. También se muestran las distancias entre los átomos del $FADH^{-}$ y del CPD. Tomado de Zhong (58, 63).

Actualmente puede decirse que las fotoliasas están entre las enzimas mayormente estudiadas y comprendidas, gracias a las contribuciones del Dr. Sancar y el Dr. Zhong de la Universidad de Ohio, también determinaron las constantes microscópicas (así se denomina a la constante de velocidad de cada etapa) de la reparación por parte de las fotoliasas. Como

se muestra en la Figura 1. 9, el ciclo catalítico completo tarda unos 1.2 ns y la enzima repara las T<>T con un rendimiento cuántico de 0.9 (42, 58, 63–67).

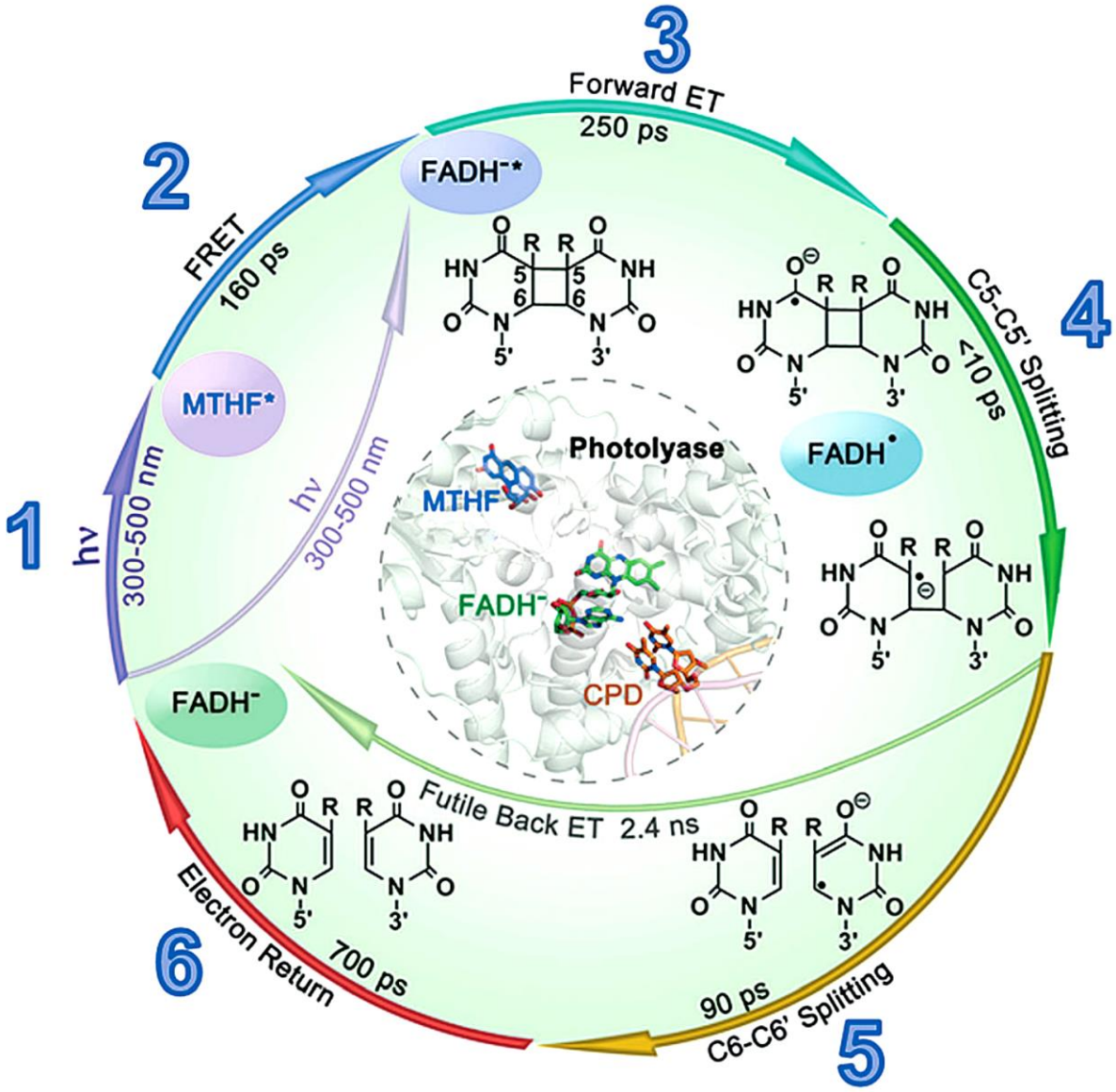

Figura 1. 9. Constantes de velocidad microscópicas para la fotoliasa de *E. coli*. Las constantes microscópicas se determinaron por "ultrafast time-resolved absorption and fluorescence up-conversion spectroscopy". El clivaje del anillo de ciclobutano de pirimidina se realiza por un mecanismo de reacción asincrónico que acopla el clivaje del enlace C5_C5 en menos de 10 ps para inmediatamente romper el enlace C6_C6 en 90 ps. La reacción fotoquímica completa tarda 1.2 ns con un rendimiento cuántico de 0.9. El círculo interno muestra la localización espacial de la antena (MTHF), el catalizador ($FADH^{-}$) y el dímero de ciclobutano de pirimidinas (CPD). Tomado de Sancar (51).

1.2.4 La Antártida como fuente de fotoliasas

La Antártida es un ambiente hostil para la especie humana, no solo por las bajas temperaturas reinantes, sino también porque en esta zona del planeta la capa de ozono se encuentra adelgazada, permitiendo así un mayor pasaje de la radiación UV proveniente del sol. Esta presión selectiva favorece la supervivencia de microorganismos que se hayan adaptado a la alta radiación. Como resultado, los microorganismos resistentes a la irradiación UV desarrollaron y/o perfeccionaron los mecanismos de protección (producción de pigmentos y fotoprotectores) y reparación (como los descritos en la sección 1.1.1).

1.2.5 Usos potenciales de las fotoliasas

En pocas palabras, las fotoliasas utilizan la luz azul para reparar el daño causado al ADN por la luz UV. Esta introducción comenzó comentando los efectos nocivos de la irradiación UV sobre la piel, y su participación en el foto-envejecimiento y posible desarrollo de cáncer de piel. Estos efectos son consecuencia del estrés oxidativo y de la formación de fotoproductos en el ADN. Entonces, cabe preguntarnos: ¿puede el uso de antioxidantes y reparadores de ADN, como las fotoliasas, ser una respuesta al avance del cáncer de piel en el mundo?

Los antioxidantes tópicos y las enzimas de reparación del ADN se han explorado como posibles fotoprotectores. La aplicación de antioxidantes como flavonoides, resveratrol (fitoalexina polifenólica) y extractos de té verde demostraron disminuir el daño al ADN causado por la irradiación UV, pero estos compuestos son inestables y difunden pobremente a través de la piel.

También se ha explorado el uso de enzimas exógenas para su incorporación a la piel humana, a través del uso de liposomas que han permitido atravesar el estrato córneo (68). Se

ha utilizado la T4 endonucleasa V y fotoliasa, donde luego de uso se ha evidenciado una disminución en el daño al ADN por exposición a la luz UV (69).

Se ha señalado que la aplicación de T4 endonucleasa V tiene un efecto clínico beneficioso, protegiendo a pacientes con lesiones de piel malignas y pre-malignas. Sin embargo, la aplicación de fotoliasa reduce el daño al ADN inducido por la irradiación UV en forma más efectiva (70). Varios experimentos, llevados a cabo *in vivo*, han demostrado que la aplicación de fotoliasa liposomada (proveniente de la cianobacteria *Anacystis nidulans*), en forma tópica en la piel humana, contribuye en forma estadísticamente significativa a la prevención del daño al ADN inducido por la irradiación UV y de la muerte celular por apoptosis (71–73). Actualmente existen en el mercado mundial varias cremas cosméticas y protectores solares conteniendo fotoliasas: Ladival®Serum Regenerador Post-solar (Laboratorios Stada, con fotoliasa extraída de un alga), Eryfotona® AK-NMSC (ISDIN; con fotoliasa encapsulada en liposomas), Celfix DNA® (PrecisionMD) y DermADN de la empresa nacional Dermur, entre otras.

También existen patentes actualmente disponibles donde se describe la producción y usos de fotoliasas provenientes de *A. nidulans* (patente 0423214A), así como de formulaciones que la incluyen (WO 2014011611 A1). También se ha patentado el uso de fotoliasas para el tratamiento de determinadas enfermedades, como es el caso de la queratosis actínica (patente WO2012168401 A1).

Hipótesis

La Antártida es una fuente natural de microorganismos productores de fotoliasas novedosas, y estas enzimas podrían formar parte de la oferta existente en el mercado de moléculas reparadoras del daño al ADN causado por la radiación UV.

Objetivo general

Contribuir al desarrollo de una formulación de aplicación tópica para la profilaxis del daño causado por la exposición a luz solar.

Objetivos específicos

I. Realizar la bioprospección de microorganismos resistentes a la radiación UVc, identificarlos en forma molecular y caracterizar su comportamiento frente a la irradiación UVc.
II. Identificar las secuencias codificantes de las fotoliasas de los microorganismos con mayor resistencia a la radiación UVc.
III. Producir en forma recombinante y purificar una CPD- y una 6,4-fotoliasa.
IV. Caracterizar la actividad de fotorreparación del ADN de las diferentes fotoliasas siguiendo diferentes líneas de evidencia o estrategias, tanto *in vitro* como *in vivo*.

CAPÍTULO I

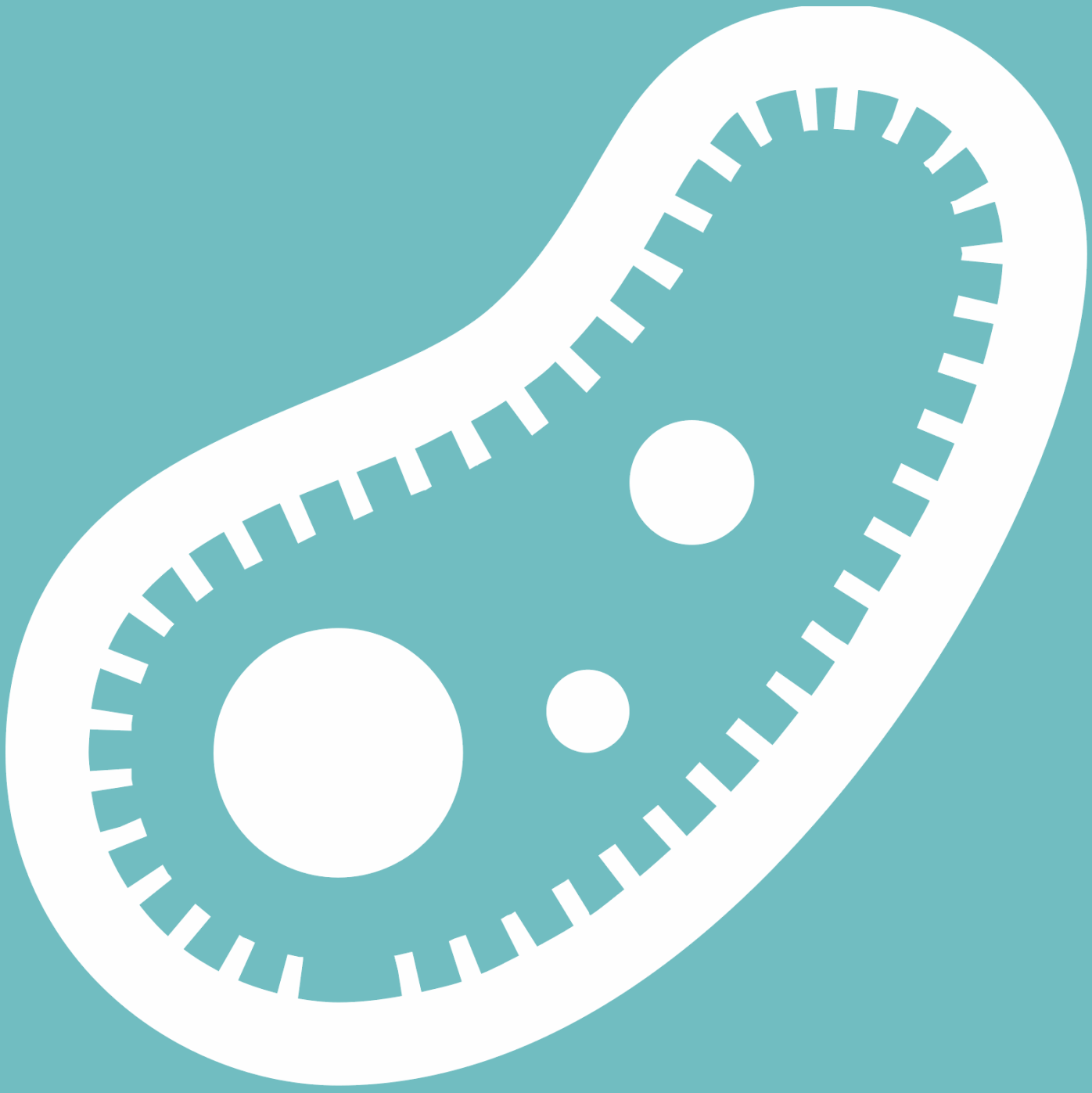

2. BIOPROSPECCIÓN DE MICROORGANISMOS UV-RESISTENTES

El trabajo se inició con la bioprospección de bacterias UV-resistentes, la caracterización de su comportamiento frente a la irradiación UVc y la identificación de las secuencias codificantes para las fotoliasas (Objetivos específicos I y II). Se presentan a continuación, los Materiales y Métodos, y los Resultados obtenidos en la forma de un trabajo publicado.

2.1. Materiales y Métodos

2.1.1 Muestreo, aislamiento e identificación de bacterias UVc-resistentes

En enero del año 2010, integrantes del nuestro grupo de laboratorio colectaron muestras del lago Uruguay y del glaciar Collins (Isla Rey Jorge, Península de Fildes, Antártida) en las cercanías de la Base Científica Antártica Artigas (BCAA; 62°11'4''S; 58°51'7''W), para la bioprospección de bacterias UV-resistentes. Las coordenadas de GPS junto con las propiedades físicas y químicas de las muestras (pH, temperatura y conductividad) se describen en Morel et al. (74).

Las muestras se colectaron en condiciones de asepsia y se refrigeraron para su posterior tratamiento en el laboratorio. Un volumen de 10 mL de muestra se transfirió a una placa de Petri estéril y vacía, y se irradió con una lámpara UVc (254 nm), de Spectroline (modelo ENF-260C/FE). Las muestras se colectaron a dosis de radiación creciente, comenzando por 50, 100, 150 y 200 J m^{-2}. Posteriormente, se sembraron con rastrillo en medio de cultivo TSA (Triptosa Soja Agar; Sigma, Cat No 22092) y se incubaron a 4 °C durante 20 días. Las colonias que mostraron la mayor sobrevida y diferencias en la morfología de la colonia, se purificaron dos veces por el método de estría en placas nuevas conteniendo TSA.

Las colonias puras se preservaron en glicerol 15% a -80 °C. Las bacterias se identificaron mediante morfología y forma de colonia, así como por secuenciación del gen 16S (usando los cebadores: 1401R: 5´ CGG TGT GTA CAA GGC CCG GGA ACG 3´; 784F: 5´ AA A CAG GAT TAG ATA CCC 3´; 907R: 5´ CCG TCA ATT CCT TTR AGT TT 3´; 63F 5´ CAG GCC TAA CAC ATG CAA GTC 3´). Todas las secuencias se encuentran depositadas en la base de datos de la NCBI (75).

Respecto a la caracterización de la población bacteriana, se determinó el número de microorganismos mediante conteo de viables por el método de unidades formadoras de colonias (UFC) para los diferentes tiempos de irradiación (diferente intensidad de radiación). Para las curvas de dosis respuesta frente a la radiación UVc, se graficó el porcentaje de sobrevida versus la dosis de irradiación.

2.1.2 Curvas dosis-respuesta y determinación de la dosis letal 50 para la irradiación UVc, para cada uno de los aislamientos UV-resistentes

Los aislamientos se crecieron en 2 mL de caldo TSB (Caldo Triptosa Soja; en caso de tratarse de medio sólido el TSB se suplementó con agar al 1.5%, y se denominó TSA) a 20 °C y 200 rpm hasta la aparición de turbidez; posteriormente se transfirieron a 200 mL de medio, manteniendo las mismas condiciones. Luego de 48 h (correspondiente a la fase exponencial tardía) las células se colectaron por centrifugación a 6000 rpm (15 min a 4 °C), el sedimento celular se lavó dos veces con NaCl 1 M y la cantidad de bacterias se normalizó a 10^6 células mL^{-1} en NaCl 0,9 %, tomando en cuenta que 0.05 UA (Unidades de Absorbancia) a 620 nm equivalen a $1x10^8$ UFC mL^{-1}. Un volumen de 10 mL de suspensión celular se transfirió a una placa de Petri estéril de 90 mm de diámetro (asegurando una monocapa de bacterias), y se irradió con una dosis de 0,4 J s^{-1} con agitación a temperatura ambiente (la irradiación se verificó con un dosímetro de UVc, Spectroline DIX-254A). Se tomaron alícuotas cada 15 seg y

la sobrevida se determinó mediante conteo de viables por el método de UFC en placas de Petri conteniendo TSA, a 20 °C. A modo de control se utilizó la cepa de *Escherichia coli* K12. Con los datos obtenidos se realizaron las curvas de dosis respuesta y se determinó la dosis letal 50 (DL_{50}).

2.1.3 Ensayo de fotorreparación

Tomando en cuenta que las fotoliasas necesitan la luz azul para reparar el ADN (fotorreparación), la actividad fotorreparadora se determinó comparando curvas de dosis respuesta en presencia y ausencia de luz, como lo describe Miller (76).

Brevemente, se estriaron 100 µL de una suspensión de 10^9 células mL^{-1} en forma de línea recta en placas de TSA. Inmediatamente se irradiaron con diferentes dosis de UVc y se incubaron a 20 °C en presencia y ausencia de luz azul (FastGene Blue/Green LED GelPic Imaging System, 515 nm). Luego de 48 h se observó el crecimiento y se registró hasta qué intensidad de irradiación crece el microorganismo. La capacidad fotorreparadora se definió como la cantidad máxima de irradiación UVc que puede tolerar el aislamiento (cuando crece en presencia de luz azul) si se lo compara con el ensayo realizado en ausencia de luz azul.

2.1.4 Identificación de genes de fotoliasas mediante PCR utilizando cebadores degenerados

Con el fin de encontrar las secuencias codificantes de fotoliasas de los aislamientos de mayor resistencia a UVc, se purificó su ADN y se realizaron reacciones de PCR con cebadores degenerados. Para el diseño de los mismos, se seleccionaron genes de referencia para fotoliasas de la base de datos de la NCBI, se alinearon sus secuencias proteicas, y se escogieron las zonas de alta conservación para los diferentes géneros bacterianos.

Teniendo en cuenta estas regiones conservadas y los diferentes géneros bacterianos, se diseñaron los siguientes juegos de cebadores, para: *Pseudomonas* (PseFFwr: 5´ CAY GAY GAY GCN CCN TGY AA 3´; PseFRev: 5´ NSW CCA YTG CCA NCC NCC RTT RTT 3´), *Sphingomonas* (SphFFwr: 5´ TGG TGG YTN CAY CAY WSN YT 3´; SphFRev: 5´ NGC NAR NGG NAC CCA 3´) e *Hymenobacter* (HymFFwd: 5´ TGG TGG YTN CAY CAY WSN YT 3´; HymFRev: 5' ARY TGN CKC ATN GCR TC 3´). También se utilizaron juegos de cebadores reportados previamente en la literatura (PHPR1: 5´TGG YWY MGV RBG AYY TVC G 3´; PHPR2: 5´GAR GCG YCC ACT GCC ARC CRC C 3´) (77).

El ADN genómico se extrajo utilizando el kit "DNA Miniprep" de Zymo Research (Cat. No D6005) y se usó como molde para las reacciones de PCR, utilizando el RANGER Mix de Bioline (Cat. No 25051) como reactivo para la amplificación. Los productos de amplificación se controlaron por electroforesis, se clonaron usando el kit "InsT/Aclone PCR Cloning" de Thermo Scientific (Cat. No K1213) y se enviaron para su secuenciación, utilizando los cebadores universales M13, a Macrogen, en Corea. Los resultados de la secuenciación del ADN se analizaron con las herramientas BLASTx y BLASTn de la NCBI (78). Las secuencias nucleotídicas y aminoacídicas se depositaron en la base de datos del GenBank (75).

2.1.5 Identificación de genes de fotoliasas mediante búsqueda en el *borrador* del genoma

Los genomas de los aislamientos (*Sphingomonas* sp. UV9 e *Hymenobacter* sp. AU11) se secuenciaron en Macrogen (Corea), se ensamblaron usando Spades (79) y se anotaron en la base de datos de la NCBI y del RAST (80). Los números de acceso de la NCBI corresponden a SCIN01000000 y SRII00000000, respectivamente. Esta actividad la realizó Danilo Morales, en el marco de su tesis de Maestría.

Las secuencias codificantes (CDS) para las fotoliasas se identificaron por búsqueda manual en el genoma anotado. Además, se buscaron otras secuencias de interés, según se verá en la sección Resultados de otros capítulos.

2.1.6 Análisis *in sílico* y relaciones filogenéticas de fotoliasas de bacterias antárticas

Las posibles secuencias de las fotoliasas se analizaron utilizando los servidores de la NCBI. Además, se realizó una predicción de la estructura y función mediante modelado por homología, utilizando el servidor de la HHpred [Homology detection & structure prediction by HMM-HMM comparison; https://toolkit.tuebingen.mpg.de/tools/hhpred (81)]. Como genes de referencia, se seleccionaron secuencias de referencia de fotoliasas depositadas en las bases de datos del NCBI. Todas las secuencias de fotoliasas se alinearon con el servidor ClustalW (https://www.ebi.ac.uk/Tools/msa/clustalo/ (82)) y los árboles filogenéticos se infirieron con los algoritmos de Neighbor Joining (NJ), Maximum-Likelihood (ML) y Unweighted Pair Group Method with Arithmetic mean (UPGMA), con un *bootstrap* de 1000 réplicas, utilizando MEGA 7.0 (83). Las ramas con valores de *bootstrap* menores al 50% se colapsaron.

2.2. Resultados

Ver Artículo

-Searching for novel photolyases in UVC-resistant Antarctic bacteria

ÁRBOL DE LA VIDA

Arte en placa de agar. Se sembraron y se crecieron las bacterias UVc resistentes de los géneros *Hymenobacter* (rojo), *Sphingomonas* (naranja y amarillo), *Janthinobacterium* (violeta/negro) y *Pseudomonas* (blanco/crema).

Extremophiles
DOI 10.1007/s00792-016-0914-y

ORIGINAL PAPER

Searching for novel photolyases in UVC-resistant Antarctic bacteria

Juan José Marizcurrena[1,2,3] · María A. Morel[4] · Victoria Braña[4] · Danilo Morales[1] · Wilner Martinez-López[2,3] · Susana Castro-Sowinski[1,4]

Received: 5 September 2016 / Accepted: 31 December 2016

Abstract Ultraviolet (UV) light irradiation has serious consequences for cell survival, including DNA damage by formation of cyclobutane pyrimidine dimers (CPD) and pyrimidine (6,4) pyrimidone photoproducts. In general, the Nucleotide Excision Repair pathway repairs these lesions; however, all living forms, except placental mammals and some marsupials, produce a flavoprotein known as photolyase that directly reverses these lesions. The aim of this work was the isolation and identification of Antarctic UVC-resistant bacteria, and the search for novel photolyases. Two Antarctic water samples were UVC-irradiated (254 nm; 50–200 J m^{-2}) and 12 UVC-resistant bacteria were isolated and identified by 16S rDNA amplification/analysis as members of the genera *Pseudomonas, Janthinobacterium, Flavobacterium, Hymenobacter* and *Sphingomonas*. The UVC 50% lethal dose and the photo-repair ability of isolates were analyzed. The occurrence of photolyase coding sequences in *Pseudomonas, Hymenobacter* and *Sphingomonas* isolates were searched by PCR or by searching in the draft DNA genome. Results suggest that *Pseudomonas* and *Hymenobacter* isolates produce CDP-photolyases, and *Sphingomonas* produces two CPD-photolyases and a 6,4-photolyase. Results suggest that the Antarctic environment is an important source of genetic material for the identification of novel photolyase genes with potential biotechnological applications.

Keywords Antarctic microbiology · Photolyase · UVC-resistant bacteria · Photo-repair

Communicated by M. da Costa.

Electronic supplementary material The online version of this article (doi:10.1007/s00792-016-0914-y) contains supplementary material, which is available to authorized users.

✉ Susana Castro-Sowinski
s.castro.sow@gmail.com

[1] Biochemistry and Molecular Biology, Faculty of Sciences, Universidad de la República, Igua 4225, 11400 Montevideo, Uruguay

[2] Epigenetics and Genomics Instability Laboratory, Institute Clemente Estable, Av. Italia 3318, 11600 Montevideo, Uruguay

[3] Biodosimetry Service. Institute Clemente Estable, Av. Italia 3318, 11600 Montevideo, Uruguay

[4] Molecular Microbiology, Institute Clemente Estable, Av. Italia 3318, 11600 Montevideo, Uruguay

Introduction

Ultraviolet (UV) light is a form of radiation with a wavelength between 40 and 400 nm. This is divided into Vacuum UV (40–190 nm), Far UV (190–220 nm), UVC (220–290 nm), UVB (290–320), and UVA (320–400 nm). UV radiation has serious consequences for cell survival, producing DNA damage, mutations and oxidative stress (base oxidation, lipoperoxidation, among others).

UVB causes direct and indirect DNA damage (oxidative stress and protein denaturation), meanwhile UVC mainly causes direct DNA damage by formation of cyclobutane pyrimidine dimers (CPD) and pyrimidine (6,4) pyrimidone photoproducts (6,4 photoproducts). These bulky DNA lesions produce RNA polymerase II halting during transcription (Budden and Bowden 2013). CPDs also induce the transcriptional regulation of genes associated with repair and signaling of SSBs (single-strand breaks) and DSBs (double-strand breaks), thus during DNA replication, unrepaired CPD lesions can induce DSBs and S-phase cell cycle arrest (Garinis et al. 2005). In general, the Nucleotide

Published online: 11 February 2017

Excision Repair (NER) system repairs these lesions, but if the repair is incomplete and the damaged bases are misread during replication, the resulting mutations may produce different diseases such as skin cancer (Yang 2011; Narayanan et al. 2010).

In addition to NER, bacteria, fungi and bacteriophages produce glycosylases (T4 endonuclease or DNA endonuclease UVDE) that specifically create a nick at the 5′ edge of a CPD. Then, enzymes of the Base Excision Repair (BER) pathway are recruited for removing the lesion, restoring the native DNA conformation (Yang 2011). However, the simplest way to repair a CPD lesion is carried out by the enzyme photolyase (EC 4.1.99.3). This enzyme directly reverses the lesion by cleaving the covalent bonds between pyrimidines bases (Benjdia 2012). Photolyases are found in all living forms, except placental mammals and some marsupials. They belong to the superfamily cryptochrome/photolyase of flavoproteins, which contains a non-covalently bound flavin adenine dinucleotide (FAD), or flavin mononucleotide (FMN) responsible for a direct electron transfer to the DNA lesion. Photolyases possess two domains, the antenna and the DNA binding domain. The antenna contains a chromophore (5,10-methenyl-tetrahydrofolate, the MTHF found in *Escherichia coli*; 6,7-dimethyl-8-ribityl-lumazine, the DMRL found in *Agrobacterium tumefaciens* or 8-hydroxy-7,8-didemethyl-5-deazariboflavin, the 8-HDF found in *Anacystis nidulans*) which is able to absorb blue light and transfer the energy by resonance to $FADH^{-}$ producing the electron excitation and further transfer to the dimer (Wang et al. 2015; Zhang et al. 2013; Brettel and Byrdin 2010). In brief, the UV irradiation produces CPD lesions and blue-light activates the photolyase responsible of photo-repair. This phenomenon is widely known, and allows the direct reversal of UV-induced DNA lesions.

Photolyases are classified based on different criteria: (1) according the photoproduct they recognize, they are classified as CPD-photolyases (e.g. Phr of *E. coli*; Brash et al. 1985) or 6,4-photolyases (e.g. PhrB of *Agrobacterium fabrum*; Graf et al. 2015); (2) based on sequence analysis of the CPD-photolyases, they are divided into three classes: I, II and III. CPD-photolyase class I are found in microorganisms (e.g. *Anacystis nidulans* and *E. coli)*, class II are mainly present in higher eukaryotic organisms, but also in prokaryotes and viruses, and CPD-photolyases type III (PhrA of *Agrobacterium tumefaciens*) are closely related to Cryptochromes plant photoreceptors (Wang et al. 2015). Finally, photolyases are also classified based on the chromophore present in the antenna domain, MTHF, DMRL or 8-HDF.

About 50% of the analyzed eubacterial species have shown photolyase homologous (Goosen and Moolenaar 2008). *Escherichia coli* photolyase was the first one to be purified (Sancar et al. 1984), but other prokaryotic photolyases have been also purified and characterized, such as the enzymes produced by *A. nidulans* (Yasui et al. 1988) and *Thermus thermophilus* (Kato et al. 1997). For a long list of photolyase producing eubacteria and archaea isolates see Goosen and Moolenaar (2008).

These enzymes have potential biotechnological applications on the cosmetic and pharmaceutical industries. A few experiments have been performed in vivo showing that the addition of bacterial photolyase to sunscreen increases the protection of human skin exposed to UV radiation, repairing CPDs and subsequently preventing apoptosis (Stege et al. 2000; Berardesca et al. 2012; Puig-Butillé et al. 2013).

Among places exposed to high UV radiation on Earth, Antarctica has shown an increasing UV-radiation at ground level, mainly due to the continuous depletion of the ozone layer (the sun's harmful UV-radiation shield). In addition, ice reflection can lead to an increased UV intensity. Thus, Antarctica may be a hotspot for natural selection of UV-resistant microbes, among other places. We have worked under the following hypothesis: Antarctic UVC-resistant bacteria may produce efficient photolyases. The aim of this work was the isolation of Antarctic UVC-resistant bacteria, the characterization of their photorepair ability and the genomic identification of photolyases with potential biotechnological applications in the medical and cosmetic industries.

Materials and Methods

Sampling, isolation and identification of UVC-resistant bacteria

Water samples from Uruguay Lake and Collins Glacier (King George Island, Fildes Peninsula, Antarctica) were collected in January 2010 at various locations near the Artigas Antarctic Scientific Base [Base Científica Antártica Artigas (BCAA); 62°11′4″S; 58°51′7″W]. The GPS location, physical and chemical properties (pH, temperature and conductivity) and bacterial abundance of water samples were described by Morel et al. (2015).

Briefly, water samples were aseptically collected and refrigerated until their processing at the lab. Ten mL of samples were aseptically transferred to empty petri dishes and exposed to UVC radiation (254 nm) using a Spectroline lamp (model ENF-260C/FE). Samples were taken after the exposure at 50, 100, 150 and 200 J m^{-2}, spread on TSB-agar (Tryptic soy broth) and incubated at 4 °C during 20 days. The number of heterotrophic bacterial populations was recorded by CFU counting and the profile of UVC-resistant bacteria was analyzed by plotting the % survival vs dose irradiation. Surviving colonies, showing different

morphological appearances, were transferred to new TSB-agar plates twice to assure purity. Isolates were storage in 15% glycerol at −80 °C. All bacteria were identified by sequencing a 1500 bp 16 S rDNA fragment as described by Martínez-Rosales and Castro-Sowinski (2011). All sequences were submitted to the NCBI database and the accession numbers are shown in Table 1.

UVC dose–response relationships and 50% lethal dose determination

Isolates were grown in 2 mL TSB at 20 °C and 200 rpm, and then transferred to 200 mL TSB and grown in similar conditions. After 48 h growth (late exponential phase), cells were harvested by centrifugation at 6000 rpm (15 min at 4 °C), pellets were washed twice using 1 M NaCl and cell concentrations were fixed at 10^6 cells/mL using 0.9% NaCl. Ten mL of cell suspensions were placed in 90 mm diameter sterile glass Petri dishes (ensuring a bacterial monolayer), and irradiated at 0.4 J/s (controlled with a UVC dosimeter, Spectroline DIX-254A) with stirring at room temperature. Aliquots were taken every 15 s and cell survival rate was determined by CFU counting on TSB-agar (TSA) at 20 °C. *Escherichia coli* K12 cells were used as control strain. Time-dependent survival curves were done and the Lethal Doses 50% (LD50) were calculated.

Photo-reactivation activity assay

As photolyases repair DNA using blue light, the contribution of photolyase activity on DNA repair can be determined comparing the survival rate of UVC-irradiated cells grown under blue light and darkness conditions. Briefly, 100 µL aliquots of 10^9 cells per mL were streak in straight lines on TSA, irradiated at different UVC-doses and incubated (20 °C) under blue light or darkness as described by Miller (1972). Growth was controlled after 48 h and the highest UVC-dose tolerated by each isolate, growing under blue light and darkness, were recorded. Photo-reactivation activity was defined as the amount of the total UVC dose (in J m^{-2}) that the isolate tolerates due the exposition to blue light, in comparison to darkness. This value was

Table 1 Characterization of UVC-resistant isolates

Isolate	Accession number	Phylogenetic affiliation	Closest relative in database (accession number)	% 16S rDNA similarity	Pigmentation	UVC LD50 (J m^{-2})	Photo-reactivation activity (J ml^{-2})
UV1	KX085031	*Janthinobacterium* sp.	*Janthinobacterium svalbardensis (N* R_132608.1)	99	Creamy	36	nd
UV2	KX085032	*Pseudomonas* sp.	*Pseudomonas brenneri (N* R_025103.1)	99	Creamy	36	30
UV3	KX085033	*Flavobacterium* sp.	*Flavobacterium frigidarium (N* R117853.1)	99	Creamy	12	nd
UV4	KX085034	*Pseudomonas* sp.	*Pseudomonas brenneri (N* R025103.1)	93	Creamy	36	54
UV5	KX085035	*Pseudomonas* sp.	*Pseudomon as extremaustralis (*NR_114911.1)	99	Creamy	90	54
UV6	KX085036	*Pseudomonas* sp.	*Pseudomonas frederiksbergensis (N* R_117177.1)	99	Creamy	72	90
UV7	KX085037	*Pseudomonas* sp.	*Pseudomonas brenneri (N* R_025103.1)	99	Creamy	42	nd
UV8	KX085038	*Pseudomonas* sp.	*Pseudomonas frederiksbergensis (N* R_117177.1)	99	Creamy	36	nd
UV9	KX086567	*Sphingomonas* sp.	*Sphingomonas aerolata (NR_042130.1)*	98	Orange	78	150
UV10	KX085039	*Sphingomonas* sp.	*Sphingomonas faeni (N* R_042129.1)	93	Orange	18	nd
UV11	KX085040	*Hymenobacter* sp.	*Hymenobacter metalli (* NR_108905.1)	96	Red/pink	126	90
UV12	KX085041	*Sphingomonas* sp.	*Sphingomonas glacialis (* NR_117270.1)	99	Yellow	90	150

The table shows the 16S rDNA accession number for each isolate; the proposed phylogenetic affiliation based on BLASTn results performed in the NCBI webpage, including the closest relative and their 16S rDNA accession number; the pigmentation of colonies; and the behavior of isolates under UVC-irradiation (LD50 and photo-reactivation assay). *Escherichia coli* K12 was used as control strain, showing LD50 and photo-reactivation values of 6 J m^{-2} and 12 J m^{-2}, respectively. *nd* non-determined

determined as the difference between the J m^{-2} tolerated (growth) under blue light minus the J m^{-2} tolerated under darkness, in the assay conditions.

Identification of photolyase genes by PCR using degenerate primers

Reference photolyase sequences were downloaded, aligned and then degenerate primers were designed to anneal highly consensus regions of different bacterial genus. Consensus primers for *Pseudomonas* (PseFFwr: 5′ CAY GAY GAY GCN CCN TGY AA 3′; PseFRev: 5′ NSW CCA YTG CCA NCC NCC RTT RTT 3′), *Sphingomonas* (SphFFwr: 5′ TGG TGG YTN CAY CAY WSN YT 3′; SphFRev: 5′ NGC NAR NGG NAC CCA 3′) and *Hymenobacter* (HymFFwd: 5′ TGG TGG YTN CAY CAY WSN YT 3′; HymFRev: 5′ ARY TGN CKC ATN GCR TC 3′) photolyases were found. Previously reported degenerate primers were also used (PHPR1: 5′TGG YWY MGV RBG AYY TVC G 3′; PHPR2: 5′GAR GCG YCC ACT GCC ARC CRC C 3′) (Yasui et al. 1994).

Genomic DNA was extracted using the DNA Miniprep kit from ZymoResearch (Catalog No D6005) and used as template in PCR reactions, using the high-performance RANGER Mix of Bioline. Amplification products were cloned using the InsTAclone PCR Cloning Kit (Catalog No K1213) and sequenced with M13 forward and reverse primers. DNA sequences were analyzed using BLASTx and BLASTn tools at the NCBI web site (http://www.ncbi.nlm.nih.gov/) and the cryptochrome database dbCRY (http://www.dbcryptochrome.org). Aminoacid sequences were submitted to GenBank and the accession numbers are currently shown in Table 2 and the branches of the phylogenetic tree shown in Fig. 2.

Identification of photolyase genes by searching in the draft genome

The genome of two isolates (*Sphingomonas* sp. UV9 and *Hymenobacter* sp. AU11) were sequenced, annotated and functionally categorized as described by Morel et al. (2016). The coding sequences for photolyases were searched in the RAST server (Aziz et al. 2008). Photolyase aminoacid sequences were submitted to GenBank and the accession numbers are currently shown in Table 2 and the branches of the phylogenetic tree shown in Fig. 2.

In silico analyses and phylogenetic affiliation of bacterial Antarctic photolyases

Photolayse sequences were analyzed in the NCBI and Cryptochrome (dbCRY) databases. In addition, the protein function and structure prediction of sequences were analyzed in the HHpred server (Homology detection & structure prediction by HMM–HMM comparison; https://toolkit.tuebingen.mpg.de/hhpred), using default parameters.

Class I, II and III CPD-photolyases and 6,4-photolyases reference sequences were searched in the NCBI and dbCRY servers. These and our photolyase sequences were aligned using ClustalW and the phylogenetic trees were inferred using the Neighbor Joining (NJ), Maximum-Likelihood (ML) and Unweighted Pair Group Method with Arithmetic mean (UPGMA) algorithms, with bootstrap analysis for 1000 replicates, in the MEGA 7.0 software (Kumar et al. 2016). Branches with less than 50% bootstrap replicates were collapsed.

Results

The influence of UVC light on the heterotrophic microbial populations of water samples collected in Uruguay Lake and Collins Glacier was analyzed. After the exposure to 50, 100, 150 and 200 J m^{-2} (at 254 nm), 5, 0.1. 0.1 and 0.1% of microbial population (initially 10^5 CFU/mL), respectively, did survive to UVC-irradiation (Fig. 1).

Twelve microbial colonies, showing different morphology, were able to grow beyond 100 and 200 J m^{-2} UVC-exposure (UVC-resistant isolates). These isolates were identified as members of the genera *Janthinobacterium, Pseudomonas, Flavobacterium, Sphingomonas* and *Hymenobacter* based on their 16S rDNA sequence similarities with reference strains (Table 1). The phylogenetic affiliation of isolates was reinforced by the construction of a phylogenetic tree, using reference sequences as shown in Supplementary Material (Fig. S1). The identification at specie level has not been designated yet, at least until a further assessment of concluding identification using a polyphasic approach.

The UVC surviving performance of the isolates was analyzed taking in account the UVC LD50 values and photo-reactivation ability. The LD50 values showed that *Pseudomonas* sp. UV5 and UV6 (90 and 72 J m^{-2}), *Sphingomonas* sp. UV9 and UV12 (78 and 90 J m^{-2}), and *Hymenobacter* sp. UV11 (126 J m^{-2}), are UVC-resistant microbes, rather than the *E. coli* K12 control strain (6 J m^{-2}; data not shown) and other UVC-resistant isolates (Table 1).

We also analyzed the contribution of photolyase activity in UVC-resistance performing photo-reactivation assays. Only isolates that showed the highest LD50 values were analyzed. Both *Sphingomonas* sp. UV9 and *Hymenobacter* sp. UV11 have showed the highest photo-reactivation activities, in comparison to other UVC-resistant isolates and the *E. coli* control strain, suggesting that they may produce highly efficient photolyases (Table 1).

Table 2 In silico characterization of photolyases

Isolate	Accession number	Closest relative in NCBI	Similarity (%)	Closest relative in the Cryptochrome Database (dbCRY)	Similarity (%)	HHpred	Identity (%)
UV2	KX443995	CPD-Photolyase of *Pseudomonas fluorescens* (WP_063033117.1)	96	Class I Photolyase of *Pseudomonas fluorescens* (PFLU_0750)	87.1	(1owl_A) Class I CPD- Photolyase of *Anocystis nidulans* (8-HDF;FAD)	39
UV4	KX443996	CPD-Photolyase of *Pseudomonas fluorescens* (WP_063033117.1)	96	Class I Photolyase of *Pseudomonas fluorescens* (PFLU_0750)	87.50	(1owl_A) Class I CPD- Photolyase of *Anocystis nidulans* (8-HDF;FAD)	38
UV5	KX443997	CPD-Photolyase of *Pseudomonas veroni* i (WP_057005762.1)	96	Class I Photolyase of *Pseudomonas fluorescens* (PFLU_0750)	90,17	(1owl_A) Class I CPD- Photolyase of *Anocystis nidulans* (8-HDF;FAD)	39
UV6	KX443998	CPD-Photolyase of *Pseudomonas* sp.(WP_054045661.1)	89	Class I Photolyase of *Pseudomonas fluorescens* (PFLU_0750)	84.77	(1owl_A) Class I CPD- Photolyase of *Anocystis nidulans* (8-HDF;FAD)	39
UV9	KX118296	CPD-Photolyase of *Sphingomonas* sp. (WP_056058598.1)	93	Class I Photolyase of *Sphingobium japonicum* (SJA_C1-17570)	61.67	(4u63_A) Class III CPD- Photolyase of *Agrobacterium tumefaciens* (MTHF;FAD)	50
UV9	KX118297	Photolyase of *Sphingomonas* sp. (WP_056479988.1)	96	Non found		(4dja_A) 6,4- Photolyase of *Agrobacterium tumefaciens* (DMRL;Fe-S cluster)	59
UV9	KX118298	CPD-Photolyase of *Sphingomonas* sp. (WP_056526775)	82	Class II Photolyase of *Pirellula staleyi* (Psta_1310)	36.94	(2xrz_A) Class II CPD- Photolyase of Archea *Methanosarcina mazei* (FAD;8-HDF)	27
UV11	KX118295	CPD-Photolyase of *Hymenobacter* sp. (AMR25685.1)	92	Class I Photolyase of *Gramella forsetii* (YP_861859.1)	49.88	(1owl_A) Class I CPD- Photolyase of *Anocystis nidulans* (8-HDF;FAD)	35

The table shows the accession number of *Pseudomonas, Hymenobacter* and *Sphingomonas* photolyases, as deposited in the NCBI database; the closest relative by searching protein homology in the NCBI, dbCRY and HHpred servers, including % similarity and the accession numbers of closest relatives in parenthesis. For HHpred, the antenna and cofactor are also indicated in parenthesis. DMRL means "6,7-dimethyl-8-ribityllumazine"

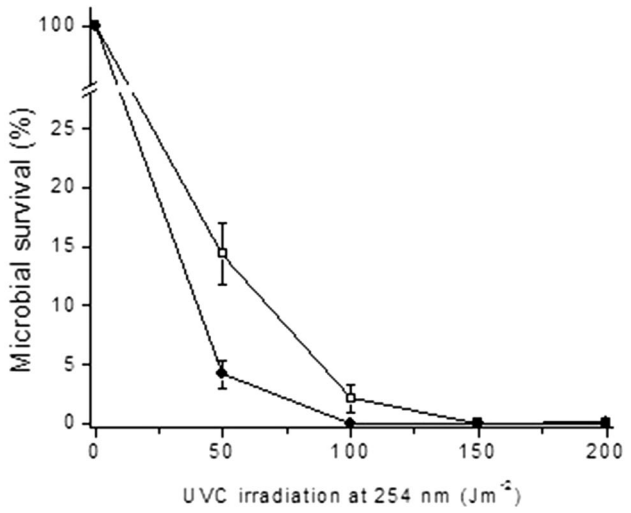

Fig. 1 Influence of UVC light on the heterotrophic microbial populations of water samples. Percentage of survival and irradiation dose was *plotted*. Empty *squares* and *filled circles* represent Uruguay Lake and Collins Glacier water samples, respectively

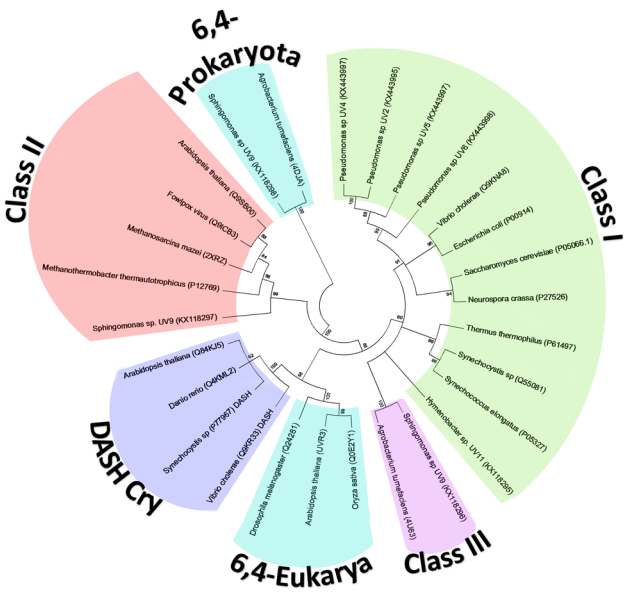

Fig. 2 Phylogenetic tree of photolyases. The reconstruction was based on aminoacid sequences. The *numbers* settled in branches represent nodal support values. Phylogenetic analysis was performed using different methods, but only maximum likelihood is shown. All methods reached trees with similar topology. *Accession numbers* are shown in parenthesis

Degenerated primers, designed based on conserved amino acid sequences of bacterial photolyases and previously reported primers (PHPR1/PHPR2; Yasui et al. 1994), were used to amplify partial gene sequences. This strategy was only successful using the primer set PseFFwr/PseFRev, designed to amplify *Pseudomonas* photolyases. Almost complete coding sequences of *Pseudomonas* spp. (strains UV2, UV4, UV5 and UV6) photolyases were found. The analysis of sequences showed that *Pseudomonas* may produce Class I CPD-photolyases (probably containing a cofactor FAD) homologous to other *Pseudomonas* and *Anacystis nidulans* photolyases (Table 2).

The occurrence of photolyase genes in *Hymenobacter* sp. UV11 and *Sphingomonas* sp. UV9 were assessed by genome sequencing and searching in the annotated genome using RAST. The analysis of *Sphingomonas* sp. UV9 genome suggests that this microbe produces three photolyases: two CPD-photolyases and a 6,4-photolyase (Table 2). HHpred analysis predicted that both CPD-photolyases from UV9 may contain a FAD cofactor, but they probably have different functional antenna chromophore (8-HDF and MTHF) (Table 2). A putative 6,4-photolyase carrying a 4Fe-4S cluster as cofactor (in addition of FAD) and an uncommon DMRL (6,7-dimethyl-8-ribityllumazine) antenna chromophore, as shown in *A. tumefaciens* (Zhang et al. 2013), was found. The analysis of the draft genome of UV9 suggests that this bacterium has only the information for the synthesis of MTHF and DMRL (data not shown), suggesting that both CPD-photolyses uses a MTHF as antenna chromophore.

In addition, the evolutionary history of photolyases was assessed (Fig. 2). The cryptochrome/photolyase family has been divided in seven major classes: three CPD-photolyases (I–III), CRY-DASH proteins (photoreceptor, but also repair CPD lesions on single-stranded DNA), 6,4-photolyases that clusters with animal cryptochromes, plant cryptochromes, and FeS-BCPs (FeS bacterial cryptochrome and photolyases) composed by bacterial 6,4-photolyases and photoreceptors with an iron-sulfur cluster. The phylogenetic tree showed that the identified photolyases cluster with Class I, II and III CPD-photolyases, and prokaryotic 6,4-photolyases, in agreement with the results obtained by BLAST in the NCBI and the CRY DataBase.

Discussion

The occurrence of UVC-resistant heterotrophic microbes in two Antarctic water samples was analyzed during this work. Morel et al. (2015) had previously reported the physical–chemical properties and culturable heterotrophic microbial populations of these samples (meltwater from the protected area under the Collins Glacier, and from Uruguay Lake, the source of drinking water for the BCAA personnel). The current study contributes to the knowledge regarding the water quality of BCAA waterworks. The UVC dosage in drinking water disinfection varies among samples, but the guidelines for drinking-water quality of the World Health Organization states a 99% baseline

removal for disinfection of bacteria, viruses and protozoa using 7, 59 and 10 J m^{-2}, respectively. Thus, the values of microbial survival after UVC-irradiation suggest that the water samples collected in Uruguay Lake and Collins Glacier present a high population of UVC-resistant heterotrophic bacteria; these samples could be considered a disinfected drinking water only after UVC irradiation of 50 and 100 J m^{-2}. Notwithstanding, our results are comparable with the data obtained by Lehtola et al. (2003). The authors showed that UVC-irradiation doses of 50 J m^{-2} (50 mW s/cm^2) inactivated 10% of the microbial population of Finnish waterworks.

UVA and UVB accounts for about 95 and 5% of the total UV energy that reaches the Earth's surface, meanwhile UVC hardly reaches the troposphere (Albarracin et al. 2016). As the UVC region is not environmentally relevant, most reports show data assessing the UVA and UVB sensitivity of bacteria. However, despite the low UVC incidence on Earth, the isolation of UVC-resistant microbes has been widely reported. During this work, 12 UVC-resistant isolates of the genera *Janthinobacterium, Pseudomonas, Flavobacterium, Sphingomonas* and *Hymenobacter* were identified. Bacteria of these genera have previously been identified as UV-resistant microbes (Dai et al. 2009; Ordoñez et al. 2009; Santos et al. 2011). In a similar work, Santos et al. (2013) studied the survival under UV-irradiation of bacteria displaying different UV sensitivities, isolated from the surface water of an estuarine system in Portugal, showing that *Micrococcus* sp., *Pseudomonas* sp. and *Sphingomonas* sp. isolates were highly UVC-resistant microbes with UVC LD50 of 45, 40.6 and 40.6 J m^{-2}, respectively. Our isolates showed higher UVC LD50 values, suggesting that the water samples collected in Antarctica possess bacteria displaying highest UVC-resistance as compared to bacteria of estuarine water in Portugal.

Altogether, determination of LD50 and photo-reactivation assays (Tables 1 and 2), suggest that *Hymenobacter, Sphingomonas* and a few *Pseudomonas* isolates are highly UVC-resistant bacteria that may produce active photolyases involved in this phenotype.

The genus *Hymenobacter* belongs to the phylum Bacteroidetes, order Sphingobacteriales, family Cytophagaceae, and comprises 40 recognized species (with at least five UV-resistant species: *H. actinosclerus, H. xinjiangensis, H. tibetensis, H. rubidus* and *H. kanuolensis*; Dai et al. 2009, Su et al. 2014). Among our UVC-resistant bacteria, the bloody-red colony-forming *Hymenobacter* sp. UV11 isolate showed greater resistance to UVC (63% survival at 300 J m^{-2}) as compared to *H. rubidus* strain DG7BT (0.1% at 300 J m^{-2}), a pink-red colored bacteria isolated from a soil collected in Seoul (Republic of Korea) and other *Hymenobacter* strains (Lee et al. 2016). The production of bright red-pink pigments by Antarctic *Hymenobacter* strains have been previously reported, and the chemical characterization of carotenoids showed that they derive from a common backbone of 2′-hydroxyflexixanthin (Klassen and Foght 2008).

The genus *Sphingomonas*, a member of the family Sphingomonadaceae, order Sphingomonadales, class Alphaproteobacteria contains 89 validly named species, which form pigmented colonies. These bacteria produce yellow to orange pigments such as nostoxanthin [(2R,3R,2′R,3′R)-β,β-Carotene-2,3,2′,3′-tetrol] or astaxanthin with potential applications in medicine (Mageswari et al. 2015). *Sphingomonas* sp. UV9 and UV12 produce orange and yellow colonies, respectively, that might contribute to the UV-resistant phenotype. However, the relationship between pigment production and UV-resistance of our isolates has still to be probe by the analysis of deficient pigment-producing bacteria.

The genus *Pseudomonas*, a member of the family Pseudomonadaceae, order Pseudomonadales, class Gammaproteobacteria has been continuously under taxonomic revisions. Among member of this genus, pigmented and non-pigmented colonies, and UV-resistant and –sensitive bacteria have been described. The *Pseudomonas* sp. isolates described during this work showed to be high UVC-resistant non-pigmented bacteria (Table 1).

When exposed to blue light, UVC-exposed cells may survive due to the NER system and by the direct DNA repair ability of photolyase, but the production of UV-protecting pigments also shields cells from UVC damage (Dillon and Castenholz 1999). On the other hand, when UVC-exposed cells are incubated in darkness conditions, the photolyase is barely active (needs blue light for activity) and cell growth is mainly due their repair and resistance mechanisms, not linked to their photo-repair ability. These characteristics allowed, by performing photoreactivation assays, to estimate the contribution of photolyase activity in UV-resistance. Thus, with the aim to better understanding the role of photolyase activity in UVC-resistance, the coding sequence of photolyases from different UVC-resistant isolates of our collection were searched. The information supports that *Hymenobacter* sp. UV11 possesses a unique Class I CPD-photolyase, homologous to *Hymenobacter* sp. PAMC 26,554 (NCBI) and to the reference sequence of the Bacteroidete *Gramella forsetii* KT0803 photolyase (dbCRY) (Table 2). As protein structure diverges far slower than primary sequence, we included a secondary structural prediction analysis using HHpred, which allocates 15% of the profile weighting at each residue to predicted structure. HHpred detected homology between the photolyases produced by *Hymenobacter* sp. UV11 and the cyanobacteria *A. nidulans*, suggesting that UV11 may produce a photolyase containing a cofactor FAD and probably an 8-HDF antenna (Table 2). However, by searching in the UV11

genome using RAST, the information for the synthesis of the MTHF antenna (but not 8-HDF) was found (data not shown). This result shows the limitation of *in silico* comparison analyses. In summary, the results suggest that *Pseudomonas* spp. isolates and *Hymenobacter* sp. UV11 produce Class I CPD-photolyases, meanwhile *Sphingomonas* sp. UV9 produces three photolyases (two CPD-photolyases and a 6,4-photolyase). Currently, we are producing the UV11 CPD-photolyase by DNA recombinant technology for further biochemical characterization.

Bacterial photolyases have not been systematically studied, and most reports have been focused in *E. coli* (Sancar et al. 1984; Brash et al. 1985), *A. tumefaciens* (Zhang et al. 2013; Wang et al. 2015), *A. nidulans* (Yasui et al. 1988), *Acinetobacter* sp. (Albarracin et al. 2012, 2014) and *T. thermophilus* (Kato et al. 1997) photolyases. However, the occurrence of photolyase genes in many microbial genomes has been shown. The occurrence of 6,4-photolyases has been mainly reported in eukaryotes, but also in the bacterium *Agrobacterium* (Zhang et al. 2013). In addition to 6,4-photolyases, the production of Class III CPD-photolyases has also been reported in *Agrobacterium* species (Oberpichler et al. 2011; Zhang et al. 2013; Graf et al. 2015; Scheerer et al. 2015). These *Agrobacterium* CPD- and 6,4-photolyases clearly cluster with *Sphingomonas* sp. UV9 photolyases, suggesting that these proteins have a common evolutionary history, although they are proteins produced by microorganisms that belong to unrelated phylogenetic families.

Our phylogenetic analysis confirms most of the known features of the evolutionary history of photolyases, as shown by Scheerer et al. (2015). The tree also supports the fact that our *Pseudomonas* isolates produce Class I CPD-photolyases, and that *Sphingomonas* sp. UV9 possesses a 6,4-photolyase, which clearly clustered with a bacterial 6,4-photolyase produced by *A. tumefaciens*, and did not cluster with eukaryotic 6,4-photolyases as expected. In addition, the two UV9 CPD-photolyases clustered with Class II and Class III bacterial photolyases. Interestingly, the Chryptocrome database does not recognize Class III photolyases, and classify the *A. tumefaciens* Class III photolyase (accession number 4U63) as Class I photolyase. The phylogenetic tree supports that this Class III *A. tumefaciens* photolyase are closely related to Class I enzymes, including the *Hymenobacter* sp. UV11 CPD-photolyase.

Conclusion

Native microbial Antarctic communities are challenged by a combination of physical stresses, including the exposure to UV radiation, and probably they develop cooperative strategies to deal with. Among mechanisms involved in UV-resistance (cell protection, tolerance through the production of antioxidant enzymes, and DNA repair; Albarracin et al. 2016), this work was focused on the isolation and identification of UVC-resistant Antarctic bacteria, and the in silico characterization of their photolyases. A few UVC-resistant bacteria (*Pseudomonas, Hymenobacter, Sphingomonas, Flavobacterium* and *Janthinobacterium* isolates) have been isolated, and showed high UVC LD50 values. The results suggest that the Antarctic environment possesses a diverse group of UVC-resistant bacteria. Among the highest resistant bacteria found in the Antarctic water samples, the photo-reactivation assays showed that a few microorganisms might produce highly active photolyases. The identification and *in silico* analysis of *Pseudomonas, Hymenobacter* and *Sphingomonas* photolyase genes suggest that the Antarctic environment is an important source of genetic material for the identification of different photolyase genes. Inefficient repair of CPD- and 6,4-photoproducts could lead to human skin cancer, a matter of clinical concern (Narayanan et al. 2010), therefore these photolyases might have potential biotechnological applications in the cosmetic and pharmaceutical industries.

Currently, we are analyzing the biochemical properties of the UV11 photolyase, and describing the physiology of *Hymenobacter* sp. UV11 and *Sphingomonas* sp. UV9 isolates through the analysis of the draft genomes. This information will be available soon.

Acknowledgements This work was partially supported by PEDECIBA (Programa de Desarrollo de las Ciencias Básicas) and Celsius Laboratory (http://www.celsius.uy/). The work of JJM was supported by the National Agency of Investigation and Innovation (ANII, Agencia Nacional de Investigación e Innovación). The authors thank the Uruguayan Antarctic Institute for the logistic support during the stay in the Artigas Base. S. Castro-Sowinski, M. A. Morel and W. Martínez-López are members of the National Research System (SNI, Sistema Nacional de Investigadores, of ANII).

References

Albarracin VH, Pathak GP, Douki T, Cadet J, Borsarelli CD, Gärtner W (2012) Extremophilic *Acinetobacter* strains from High-Altitude lakes in Argentinean puna: remarkable UV-B resistance and efficient DNA damage repair. Life Evol Biosph 42: 201. doi:10.1007/s11084-012-9276-3

Albarracin VH, Simon J, Pathak GP, Valle L, Douki T, Cadet J, Borsarelli CD, Farias ME, Gärtner W (2014) First characterisation of a CPD-class I photolyase from a UV-resistant extremophile isolated from High-Altitude Andean Lakes. Photochem Photobiol Sci 13:739–750. doi:10.1039/C3PP50399B

Albarracin VH, Gärtner W, Farias ME (2016) Forged under the sun: life and art of extremophiles from Andean lakes. Photochem Photobiol 92:14–28. doi:10.1111/php.12555

Aziz RK, Bartels D, Best AA et al (2008) The RAST server: rapid annotations using subsystems technology. BMC Genom 9:75. doi:10.1186/1471-2164-9-75

Benjdia A (2012) DNA photolyases and SP lyase: structure and mechanism of light-dependent and independent DNA lyases. Curr Opin Struct Biol 22:711–720 doi:10.1016/j.sbi.2012.10.002

Berardesca E, Bertona M, Altabas K, Altabas V, Emanuele E (2012) Reduced ultraviolet-induced DNA damage and apoptosis in human skin with topical application of a photolyase-containing DNA repair enzyme cream: clues to skin cancer prevention. Mol Med Rep 5: 570–574 doi:10.3892/mmr.2011.673

Brash DE, Franklin WA, Sancar GB, Sancar A, Haseltine WA (1985) *Escherichia coli* DNA photolyase reverses cyclobutane pyrimidine dimers but not pyrimidine-pyrimidone (6–4) photoproducts. J Biol Chem 260:11438–11441

Brettel K, Byrdin M (2010) Reaction mechanisms of DNA photolyase. Curr Opin Struct Biol 20:693–701 doi:10.1016/j.sbi.2010.07.003

Budden T, Bowden NA (2013) The role of altered nucleotide excision repair and UVB-induced DNA damage in melanomagenesis. Int J Mol Sci 14:1132–1151. doi:10.3390/ijms14011132

Dai J, Wang Y, Zhang L, Tang Y, Luo X, An H, Fang C (2009) *Hymenobacter tibetensis* sp. nov., a UV-resistant bacterium isolated from Qinghai–Tibet plateau. Syst Appl Microbiol 32:543–548. doi:10.1016/j.syapm.2009.09.001

Dillon JG, Castenholz RW (1999) Scytonemin, a cyanobacterial sheath pigment, protects against UVC radiation: implications for early photosynthetic life. J Phycol 35:673–681. doi:10.1046/j.1529-8817.1999.3540673.x

Garinis GA, Mitchell JR, Moorhouse MJ et al (2005) Transcriptome analysis reveals cyclobutane pyrimidine dimers as a major source of UV-induced DNA breaks. EMBO J 24:3952–3962. doi:10.1038/sj.emboj.7600849

Goosen N, Moolenaar GF (2008) Repair of UV damage in bacteria. DNA Repair 7: 353–379 doi:10.1016/j.dnarep.2007.09.002

Graf D, Wesslowski J, Ma H, Scheerer P, Krauß N, Oberpichler I, Lamparter T (2015) Key Amino Acids in the Bacterial (6–4) Photolyase PhrB from *Agrobacterium fabrum*. PloS One 10:e0140955. doi:10.1371/journal.pone.0140955

Kato R, Hasegawa K, Hidaka Y, Kuramitsu S, Hoshino T (1997) Characterization of a thermostable DNA photolyase from an extremely thermophilic bacterium, *Thermus thermophilus* HB27. J Bacteriol 179:6499–6503. doi:10.1128/jb.179.20.6499-6503.1997

Klassen JL, Foght JM (2008) Differences in carotenoid composition among *Hymenobacter* and related strains support a tree-like model of carotenoid evolution. Appl Environ Microbiol 74:2016–2022. doi:10.1128/AEM.02306-07

Kumar S, Stecher G, Tamura K (2016) MEGA7: molecular evolutionary genetics analysis version 7.0 for bigger datasets. Mol Biol Evol 33:1870–1874. doi:10.1093/molbev/msw054

Lee J-J, Joe ES, Kim EB, Jeon SH, Srinivasan S, Jung H-Y, Kim MM (2016) *Hymenobacter rubidus* sp. nov., bacterium isolated from a soil. Antonie Van Leeuwenhoek 109:457–466. doi:10.1007/s10482-016-0652-2

Lehtola MJ, Miettinen IT, Vartiainen T, Rantakokko P, Hirvonen A, Martikainen PJ (2003) Impact of UV disinfection on microbially available phosphorus, organic carbon, and microbial growth in drinking water. Water Res 37:1064–1070. doi:10.1016/S0043-1354(02)00462-1

Mageswari A, Subramanian P, Srinivasan R, Karthikeyan S, Gothandam KM (2015) Astaxanthin from psychrotrophic *Sphingomonas faeni* exhibits antagonism against food-spoilage bacteria at low temperatures. Microbiol Res 179:38–44. doi:10.1016/j.micres.2015.06.010

Martínez-Rosales C, Castro-Sowinski S (2011) Antarctic bacterial isolates that produce cold-active extracellular proteases at low temperature but are active and stable at high temperature. Polar Res 30:7123. doi:10.3402/polar.v30i0.7123

Miller JH (1972) Experiments in Molecular Genetics. Cold Spring Harbor Laboratory, Cold Spring Harbor

Morel MA, Braña V, Martinez-Rosales C, Cagide C, Castro-Sowinski S (2015) Five-year bio-monitoring of aquatic ecosystems near Artigas Antarctic Scientific Base, King George Island. Adv Polar Sci 26: 102–106 doi:10.13679/j.advps.2015.1.00102

Morel MA, Iriarte A, Jara E, Musto H, Castro-Sowinski S (2016) Revealing the biotechnological potential of *Delftia* sp. JD2 by a genomic approach. AIMS Bioeng, 3: 156–175 doi:10.3934/bioeng.2016.2.156

Narayanan DL, Saladi RN, Fox JL (2010) Review: ultraviolet radiation and skin cancer. Int J Dermat 49:978–986. doi:10.1111/j.1365-4632.2010.04474.x

Oberpichler I, Pierik AJ, Wesslowski J, Pokorny R, Rosen R, Vugman M, Zhang F, Neubauer O, Ron EZ, Batschauer A, Lamperter T (2011) A photolyase-like protein from *Agrobacterium tumefaciens* with an iron-sulfur cluster. PLoS One 6:e26775. doi:10.1371/journal.pone.0026775

Ordoñez OF, Flores MR, Dib JR, Paz A, Farías ME (2009) Extremophile culture collection from Andean Lakes: extreme pristine environments that host a wide diversity of microorganisms with tolerance to UV radiation. Microb Ecol 58:461–473. doi:10.1007/s00248-009-9527-7

Puig-Butillé JA, Malvehy J, Potrony M, Trullas C, Garcia-García F, Dopazo J, Puig S (2013) Role of CPI-17 in restoring skin homoeostasis in cutaneous field of cancerization: effects of topical application of a film-forming medical device containing photolyase and UV filters. Exp Dermatol 22:482–501. doi:10.1111/exd.12177

Sancar A, Smith FW, Sancar GB (1984) Purification of *Escherichia coli* DNA photolyase. J Biol Chem 259:6028–6032

Santos AL, Lopes S, Baptista I, Henriques I, Gornes NCM, Almeida A, Correia A, Cunha A (2011) Diversity of UV sensitivity and recovery potential among bacterioneuston and bacterioplankton isolates. Lett Appl Microbiol 52:360–366. doi:10.1111/j.1472-765X.2011.03011.x

Santos AL, Oliveira V, Baptista I, Henriques I, Gomes NCM, Almeida A, Correia A, Cunha A (2013) Wavelength dependence of biological damage induced by UV radiation on bacteria. Arch Microbiol 195:63–74. doi:10.1007/s00203-012-0847-5

Scheerer P, Zhang F, Kalms J, von Stetten D, Krauβ N, Oberpichler I, Lamparter T (2015) The Class III cyclobutane pyrimidine dimer photolyase structure reveals a new antenna chromophore binding site and alternative photoreduction pathways. J Biol Chem 290:11504–11514. doi:10.1074/jbc.M115.637868

Stege H, Roza L, Vink AA, Grewe M, Ruzicka T, Grether-Beck S, Krutmann J (2000) Enzyme plus light therapy to repair DNA damage in ultraviolet-B-irradiated human skin. PNAS 97:1790–1795. doi:10.1073/pnas.030528897

Su S, Chen M, Teng C, Jiang S, Zhang C, Lin M, Zhang W (2014) *Hymenobacter kanuolensis* sp. Nov., a novel radiation-resistant bacterium. Int J Sys Evol Microbiol 64:2108–2112. doi:10.1099/ijs.0.051680-0

Wang J, Du X, Pan W, Wang X, Wu W (2015) Photoactivation of the cryptochrome/photolyase superfamily. J Photochem Photobiol C Photochem Rev 22: 84–102 doi:10.1016/j.jphotochemrev.2014.12.001

Yang W (2011) Surviving the sun: Repair and bypass of DNA UV lesions. Protein Sci 20:1781–1789 doi:10.1002/pro.723

Yasui A, Takao M, Oikawa A, Kiener A, Walsh CT, Eler APM (1988) Cloning and characterization of a photolyase gene from the cyanobacterium *Anacystis nidulans*. Nucl Acids Res 16:4447–4463. doi:10.1093/nar/16.10.4447

Yasui A, Eker AP, Yasuhira S, Yajima H, Kobayashi, T, Takao M, Oikawa A (1994) A new class of DNA photolyases present in

various organisms including aplacental mammals. The EMBO J 13:6143–6151

Zhang F, Scheerer P, Oberpichler I, Lamparter T, Krauβ N (2013) Crystal structure of a prokaryotic (6,4) photolyase with an Fe-S cluster and a 6,7-dimethyl-8-ribityllumazine antenna chromophore. Proc Nat Acad Sci 110: 7217–7222 doi:10.1073/pnas.1302377110

CAPÍTULO II

3. CARACTERIZACIÓN DE LA BACTERIA UV-RESISTENTE IDENTIFICADA COMO *HYMENOBACTER* SP. UV11. PRODUCCIÓN RECOMBINANTE Y CARACTERIZACIÓN DE LA CPD-FOTOLIASA PRODUCIDA POR UV11

El trabajo se continuó con la caracterización del aislamiento UV resistente *Hymenobacter* sp. UV11, así como la producción y la caracterización de la fotoliasa recombinante codificada por UV11 (Objetivo específico III). Se presentan a continuación, los Materiales y Métodos, y los Resultados obtenidos en la forma de dos trabajos publicados.

3.1. Materiales y Métodos

3.1.1 Condiciones de crecimiento de *Hymenobacter* sp. UV11

Las bacterias se crecieron en el medio de cultivo oligotrófico denominado R2 (extracto de levadura 0.5 g/L, proteosa peptona 0.5 g/L, casaminoácidos 0.5 g/L, dextrosa 0.5 g/L, almidón soluble 0.5 g/L, pirUVato de sodio 0.3 g/L, K_2HPO_4 0.3 g/L, $MgSO_4$ anhidro 0.05 g/L) a 200 rpm y 20 ^oC, durante 72 h; o en placa utilizando el medio R2A (medio R2 suplementado con agar al 1.5%) e incubación en estufa a 20 ^oC.

3.1.2 Búsqueda de la producción de enzimas hidrolíticas extracelulares

La habilidad de UV11 para producir enzimas hidrolíticas se analizó creciendo la cepa en medio R2A (para la identificación de producción de amilasas) o SFR2 (R2A sin almidón) suplementado con leche descremada al 5% o carboximetilcelulosa al 2% (para la identificación de proteasas y celulasas, respectivamente) por 72 h y 20 ^oC. La producción de enzimas extracelulares se evidenció por la presencia de un halo de transparencia (proteólisis de la

leche) rodeando la colonia para la producción de proteasas. Para la determinación de celulasas o amilasas, las placas se trataron con Rojo Congo o solución de Lugol y se evidenció la producción de estas enzimas por la presencia de un halo de transparencia alrededor de la colonia.

3.1.3 Cuantificación de la actividad celulasa y proteasa en medio líquido

Un inóculo al 1% de un pre-cultivo fresco de la cepa UV11 se transfirió a 500 mL de medio R2 y se creció a 20 ºC y 200 rpm, por 72 h. El cultivo se centrifugó a 10.000 rpm y 4 ºC durante 5 min y se filtró (tamaño de poro 0.45 µm). El sobrenadante libre de células se utilizó para la determinación de actividad proteolítica y celulolítica. Las determinaciones de estas actividades las realizaron otros estudiantes y colaboradores del grupo de trabajo.

3.1.4 Microscopía Electrónica de Transmisión (MET)

La cepa UV11 se creció en 3 mL de medio R2 a 20 ºC y 200 rpm, por 72 h. El cultivo se centrifugó a 10.000 rpm y 4 ºC durante 5 min. El sedimento bacteriano se usó para realizar la microscopía. El procesamiento de las muestras y la obtención de las imágenes se realizaron en el servicio de MET de la Facultad de Ciencias.

3.1.5 ¨Shotgun¨ de las proteínas secretadas (secretoma)

Se crecieron pre-cultivos de UV11 en medio R2 a 20 °C y 220 rpm. Una alícuota del 1% se transfirió a 200 mL de medio R2 y se creció a 20 ºC por 48 h a 220 rpm. El cultivo se centrifugó durante 30 min, a 6000 rpm y 4 ºC. El sobrenadante se filtró (tamaño de poro 0,22 µM) y se determinó la cantidad de proteína por el método de Bradford (Amresco, M172), utilizando seroalbúmina bovina (BSA) como estándar. Se prepararon geles de poliacrilamida con una concentración de acrilamida-bisacrilamida del 5% en el gel concentrador y de 12% para el gel separador. Luego, se cargaron 40 µL de las muestras. La corrida electroforética se realizó a 70V hasta que el frente de corrida alcanzo el gel separador y luego se aumentó el

voltaje a 100V y se dejó ingresar 1 cm en el gel separador. Para la tinción, se utilizó una solución coloidal de Coomassie G, preparada de la siguiente forma: se disolvieron 0.2g de Coomassie Blue G-250 en 100 mL de agua destilada, a 50 °C; luego se dejó enfriar a temperatura ambiente, se adicionaron 100 mL de ácido sulfúrico (H_2S0_4) 2N y se incubó a temperatura ambiente por 3 h; se filtró, y se agregaron 22.2 mL de hidróxido de potasio (KOH) 10N, y 28.7g de ácido tricloroacético (TCA). El gel se tiñó por inmersión en la solución coloidal durante 15 min y la banda conteniendo las proteínas se cortó para su análisis por espectrometría de masas (Exactive hybrid quadrupole-Orbitrap, de Thermo Scientific). El análisis se realizó en la unidad de proteómica CEQUIBIEM, en la Universidad de Buenos Aires/CONICET, como se describe en Ghio et al. (84). Los datos crudos se procesaron utilizando el programa ¨Proteome Discoverer¨ (version 1.4 de Thermo Scientific) y la búsqueda de las proteínas presentes en el secretoma se realizó tomando en cuenta el proteoma obtenido luego de la anotación del genoma de *Hymenobacter* sp. UV11.

Los resultados del ¨*shotgun*¨ de las proteínas secretadas se analizaron con la dbCAN (base de datos curada para enzimas activas en carbohidratos CAZymas; http://bcb.unl.edu/dbCAN2 (85)), MEROPS (base de datos curada para proteasas; https://www.ebi.ac.uk/merops/ (86)) y MoonProt (base de datos para proteínas con funciones diversas; http://www.moonlightingproteins.org/ (87)), para la identificación de posibles celulasas, proteasas y las proteínas *moonlight* presentes en el secretoma. También se analizó la presencia de regiones transmembrana utilizando el paquete TMHMM (http://www.cbs.dtu.dk/services/TMHMM/ (88).

3.1.6 Extracción y análisis del pigmento

La cepa UV11 se creció en 2 L de medio R2 como se describió anteriormente, se centrifugó y el sedimento celular se liofilizó. A los 1.21 g de sedimento seco obtenido, se le

agregó 100 mL de metanol y se incubó a 65 ^{o}C durante 5 min para extraer el pigmento. El resto del procesamiento (la purificación) y la identificación del pigmento se realizaron en el Laboratorio de Química Orgánica, de la Facultad de Química (gentileza de Dr. Danilo Davyt y la estudiante Agustina Eizmendi).

3.2. Producción recombinante y caracterización de la CPD-fotoliasa

3.2.1 Cepas, líneas celulares eucariotas y condiciones de cultivo

Las cepas de *Escherichia coli* DH5α y BL21 (DE3) (ambas adquiridas de Invitrogen, USA) se utilizaron para la amplificación de plásmidos y para la producción recombinante de proteínas, respectivamente. Las mismas se mantuvieron en medio LB (Luria–Bertani; Sigma, Cat. No L3147) y se almacenaron a 4 ^{o}C.

Para demostrar la remoción *in vitro* de los CPDs, formados luego de la irradiación con UVc, por parte de la fotoliasa recombinante, se realizaron ensayos cometa, utilizando las líneas celulares CHO (Chinese Hamster Ovary) (89) y HaCaT. Esta última es una línea celular de queratinocitos aneuploides inmortales transformados espontáneamente de piel humana adulta (90).

Las líneas celulares CHO y HaCat se cultivaron con los medio McCoy's 5A (GIBCO, Cat. No. 12330031) y Dulbecco's modified Eagle medium (DMEM, GIBCO, Cat. No. 12430062), respectivamente. Los medios se suplementaron con suero fetal bovino 10% (GIBCO), 100 U mL^{-1} de penicilina y 100 U mL^{-1} de estreptomicina. Las células se cultivaron a 37 °C en cámara húmeda y gaseada (aire 95% y CO_2 5%). Los pasajes celulares se realizaron disgregando las células con una solución de tripsina 0.1 %, ácido etilendiaminotetraacético (EDTA, 0.05 %) en tampón fosfato libre de Ca^{2+}/Mg^{2+}.

3.2.2 Construcción y mantenimiento del plásmido

La CDS correspondiente a la fotoliasa producida por *Hymenobacter* sp. UV11 (Número de acceso de GenBank KX118295) se envió a sintetizar en el servicio de GenScript (91). El gen optimizado (optimización del uso de codones para su expresión en *Escherichia coli*) se fusionó en el vector de expresión pET28a(+); de este modo se añadió una etiqueta de seis histidinas en el extremo N-terminal. Al vector de expresión se le denominó PhotoHymeno_pET-28a(+).

Para permitir el mantenimiento y la expansión del plásmido, se transformó en cepas quimiocompetentes de *E. coli* DH5α (92), y se mantuvo en placas de LB suplementadas con 50 μg mL^{-1} de kanamicina. Para la expresión del plásmido, se transformaron cepas quimicompetentes de *E. coli* BL21. A la bacteria recombinante se la denominó *Escherichia coli* BL21 (DE3) cepa PhotoUV11 (Número de Acceso de Depósito: CECT 9643).

Las cepas transformadas se encuentran almacenadas en el repositorio internacional de patentes (Parc Científic Universitat de Valencia, Spain), bajo el tratado de Budapest de 1977. Las cepas DH5α y BL21 conteniendo el plásmido recombinante también se almacenaron en glicerol al 15% a -80 °C, en nuestro laboratorio.

3.2.3 Producción y purificación de la fotoliasa recombinante

Para la producción recombinante de la fotoliasa, el plásmido PhotoHymeno_pET-28a(+) se transformó a la cepa para expresión de *E. coli* BL21 (DE3). Se realizaron pre-cultivos de *E. coli* BL21, conteniendo el plásmido, en LB a 37 °C y 220 rpm. Una alícuota del 1% se transfirió a 200 mL de medio auto-inductor Zym-5052 (triptona 10 g, extracto de levadura 5 g, glicerol 5 g, glucosa 0.5 g, lactosa 0.2 g, $MgCl_2$ 2mM, Na_2HPO_4 0.45 g, KH_2PO_4 0.34 g, NH_4Cl 0.27 g, Na_2SO_4 0.07 g, $CaCl_2$ 20 μM, $MnCl_2$ 10 μM, $ZnSO_4$ 10 μM, $CoCl_2$ 2 μM, $CuCl_2$ 2 μM, $NiCl_2$ 2μM, Na_2MoO_4 2 μM, Na_2SeO_3 2 μM, H_3BO_3 2 μM, y agua csp 1L (93)), suplementado con kanamicina (50 mg mL^{-1}), y se creció a diferentes temperaturas (37, 20, 14 ^oC) y 220 rpm.

El crecimiento a 37 °C se realizó durante toda la noche, el crecimiento a 20 °C se realizó por 24 h, y para 14 ºC primero se creció durante 2 h a 37 ºC y luego por 72 h a 14 ºC. Las células se cosecharon, se lavaron dos veces y se lisaron por sonicación (40% amplitud) utilizando el tampón fosfato de sodio 50 mM, suplementado con NaCl 50 mM (pH 7.4), y se centrifugaron a 7000 g durante 10 min a 4 °C. Al sobrenadante se le denominó TF (Fracción Total). Las fracciones soluble (SF) e insoluble (IF; correspondiente a los cuerpos de inclusión) se separaron mediante centrifugación a 16000 g durante 30 min a 4 °C. La fracción insoluble se suspendió en tampón de solubilización (tampón fosfato de sodio 50 mM, NaCl 50 mM, urea 8 M, pH 8). Todas las fracciones se analizaron mediante electroforesis desnaturalizante (SDS-PAGE), utilizando un gel separador al 12 % y gel concentrador al 5%, y tinción con Azul de Coomasie (94).

La fotoliasa recombinante de UV11 se purificó desde la fracción soluble, incubando ésta con una resina de afinidad Ni-NTA (Invitrogen, Cat. No. R907). Se utilizó una relación de 20 mL de fracción soluble por mL de resina, en tampón de unión (tampón fosfato de sodio 50 mM, NaCl 50 mM, Imidazol 40 mM) y la incubación se realizó durante una hora a 4 °C. Luego, la resina se dejó decantar en una columna de purificación. La resina se lavó con cuatro volúmenes de tampón de unión, y se eluyó con tampón de unión suplementado con imidazol a una concentración final de 250 mM. El eluato resultante se desaló inmediatamente en una columna tipo PD-10 (GE Healthcare, 17-0851-01), siguiendo las instrucciones del fabricante. Todas las fracciones se controlaron mediante SDS-PAGE. La concentración proteica se determinó mediante el método de Bradford (Amresco, M172), utilizando BSA como estándar. La identidad de la proteína recombinante se verificó por análisis por espectrometría de masas MALDI/TOF-TOF, en la unidad de Bioquímica Analítica y Proteómica (UByPA) del Institut Pasteur (Montevideo, Uruguay). La masa de la proteína y la composición aminoacídica se

determinaron con los valores m/z utilizando el programa MASCOT (95). Finalmente, la fotoliasa recombinante se almacenó en tampón PBS suplementado con glicerol 50% a -80°C.

3.2.4 Determinación de actividad fotoliasa. Ensayo cometa con modificaciones menores

Se establecieron células de la línea HaCat o CHO tal cual se describió más arriba, se lavaron dos veces con PBS frío y se irradiaron con UVc (254 nm), con una dosis de 4 J m^{-2} utilizando una lámpara Spectroline (modelo ENF-260C/FE). Posteriormente, las células se lavaron y se colectaron con un rastrillo para su transferencia a tubos Eppendorf conteniendo 1 mL de PBS. Se ajustó la cantidad celular a 2×10^6 células mL^{-1} y se mezclaron cuidadosamente 20 µL de la suspensión celular con 80 µL de agarosa de bajo punto de fusión (Ultrapure LMP, Life Technologies, Cat No 16520) al 1 %. Inmediatamente se esparcieron en portaobjetos pre cubiertos con agarosa al 1.5%, se colocó un cubreobjetos y se dejaron solidificar por 5 min a 4 °C. A continuación, se removió el cubreobjetos, y los portaobjetos se sumergieron en solución de lisis (tampón Tris 10 mM, NaCl 2.5 M, Na_2EDTA 100 mM, Triton X-100 1% a pH 10) y se incubaron a 4 °C durante 2 h. Los portaobjetos se lavaron dos veces con tampón NET (Tris-HCl 10 mM, NaCl 100 mM, EDTA 10 mM; pH 8.0) durante 5 min a temperatura ambiente. Para los tratamientos con fotoliasa, se aplicaron 50 µL de la CPD-fotoliasa recombinante a diferentes concentraciones (1, 1,5, 2 µg mL^{-1} en tampón NET) y se irradió con lámpara UVa (ULTRA-VITALUX OSRAM 300W) durante 10 min en cámara húmeda para permitir la fotorreparación. La fotoliasa se removió lavando dos veces con tampón NET. Todos los portaobjetos se trataron con 50 µL de T4 endonucleasa V en tampón NET, se cubrieron con cubreobjetos y se incubaron en cámara húmeda durante 30 min a 37 °C.

La endonucleasa es capaz de reconocer el CPD y de cortar el ADN en hebra simple hacia el extremo 5´. Por tanto, en un gel desnaturalizante, la presencia de CPDs se revelará

como un patrón de ADN fragmentado, de diferentes tamaños y con capacidad de migrar en un campo electroforético. El ADN intacto se observa como un núcleo intacto al microscopio, mientras que el ADN dañado se observará como un cometa.

Se sumergieron los portaobjetos durante 15 min en tampón de separación para permitir el desenrollamiento del ADN. Luego, se realizó la electroforesis desnaturalizante alcalina (a pH 13-14 para permitir la desnaturalización del ADN), en tampón de separación (Na_2EDTA 1 mM, NaOH 0.3 N, a pH 13-14). La electroforesis se realizó a 0.7 V cm^{-1}, 300 mA durante 20 min, en baño frío a 4 °C. Una vez finalizada la electroforesis, los portaobjetos se neutralizaron en tampón de neutralización (Tris-HCl 0.4 M; pH 7.5) durante 5 min a temperatura ambiente y se tiñeron con 50 µL de una solución de bromuro de etidio (10 mg mL^{-1}). Las láminas se analizaron por microscopía de epifluorescencia utilizando el software Comet Imager (MetaSystems). Se contaron al menos 50 núcleos por lámina, y por duplicado para cada tratamiento y para los controles. Se realizaron tres réplicas biológicas independientes. El daño se cuantificó utilizando como parámetro el ¨olive tail moment¨ (momento oliva), que representa la cantidad de daño al ADN de cada célula. Como control positivo (reparación del daño causado por la irradiación UV) se utilizaron los Photosomes-V (preparado comercial conteniendo la fotoliasa de *Anacystis nidulans*) de Barnet, Protec Ingerdia (96).

3.2.5 Determinación de actividad fotoliasa. Detección de CPDs mediante cromatografía líquida de alta resolución (HPLC)

El oligonucleótido ¨t repair¨ (AGGTTGGC) se irradió con UVc para inducir la formación de CPDs y 6,4-fotoproductos. Ambos fotoproductos se separaron y purificaron por HPLC para ser utilizados como sustratos para los ensayos de reparación con la fotoliasa recombinante.

Los productos reparados y no reparados se detectaron nuevamente por HPLC como se describe en Ma et al. (97). Los detalles se describen a continuación.

Preparación y purificación de los fotoproductos:

Una solución de 50 µM del oligonucleótido "t-repair" se disolvió en agua estéril apirógena y se des-gaseó con argón. Luego se colocó una fina capa en una placa de petri, dentro de una caja sellada con una atmósfera de argón sobre un gel de enfriamiento y se irradió durante 6 h con una lámpara a UVc (GE Healthcare, G15T87B, 15 W) colocada a 12 cm por encima de la muestra. El oligonucleótido irradiado se concentró con speedvac (30 min a 45 ^{o}C) y se inyectó en el HPLC (series 1200 Agilent Technologies system) para su purificación utilizando una columna 100-3 C18ec (250 x 10, de Macherey-Nagel). La separación de los CPDs y los 6,4-fotoproductos se realizó con un gradiente de 4-18% de solución B (acetato de trietilamonio o TEAA 0.1 M preparada en agua y acetonitrilo –ACN - 20/80) en solución A (TEAA 0.1 M en agua); el gradiente se aplicó durante 45 min y el flujo se estableció en 5 mL min^{-1}. El perfil de elución se monitoreó a 260 nm y 325 nm (que es el segundo máximo de absorción para los 6,4-fotoproductos). El pico correspondiente a los CPDs se identificó utilizando el ensayo de fotorreparación, como se describe más abajo. Los eluídos colectados, correspondientes a los CPDs y los 6,4-fotoproductos purificados, se congelaron a -20 °C.

Para el ensayo de fotorreparación, se mezclaron los oligunucleótidos purificados conteniendo los CPDs o 6,4-fotoproductos a una concentración final de 5 µM en solución de reparación (Tris-HCl 50 mM, EDTA 1 mM, NaCl 100 mM, glicerol 5% (w/v), ditiotreitol (DTT) 14 mM, a pH 7.0). La fotoliasa recombinante se añadió para alcanzar concentraciones finales de entre 1 a 40 µg mL^{-1}. Luego de agregar la enzima, el ensayo se mantuvo en oscuridad hasta irradiarse con diodos de luz azul (400 nm) a una intensidad de 250 µmol m^{-2} s^{-1} durante 30 min. La reacción se detuvo por ebullición a 100 °C por 10 min. Las muestras se centrifugaron

a 13.000 rpm por 10 min a 4 °C y se filtraron (filtros de poro de 0.45µm), el sobrenadante obtenido se inyectó en el HPLC utilizando el mismo equipo descrito más arriba, pero equipado con una columna Gemini C18 de 50 x 4.60 mm, 110 Å (Phenomenex). Las condiciones de separación fueron las mismas que las descritas por Ma et al. (97): ACN 7% en TEAA 0.1 M, pH 7.0, durante 0–5 min; ACN 7–10% en TEAA 0.1 M, pH 7.0, durante 5–35 min; con un flujo de 0.75 mL min^{-1}; temperatura de columna de 27 °C y longitudes de onda de detección de 260 nm y 325 nm. La eficiencia de reparación se determinó tomando en cuenta el área bajo la curva de los picos correspondientes al ADN dañado y no dañado, como se describió anteriormente por Ma (98).

3.2.6 Determinación de actividad fotoliasa. Detección de CPDs por inmunoquímica

Se realizaron ensayos inmunoquímicos sobre ADN de timo de ternero como sustrato. Para cuantificar CPDs o 6,4-FPs se utilizaron anticuerpos monoclonales. Se trabajó con los kits "High Sensitivity CPD/Cyclobutane Pyrimidine Dimer ELISA" (NM-MA-K001) y "High Sensitivity 6,4 photoproduct ELISA" (NM-MA-K003), de la empresa CosmoBio, con algunas modificaciones como se describen a continuación.

El ADN de timo de ternero no irradiado e irradiado con UVc (10 Joules), se desnaturalizaron por incubación a 100 °C por 10 min e inmediato enfriamiento en hielo por 15 min. Para la sensibilización se aplicaron 50 µL de ADN en placas de ELISA protaminadas, a una concentración final de 0.4 µg mL^{-1} o 4 µg mL^{-1} para la detección de CPDs o 6,4-FP, respectivamente. En los pocillos donde se quería determinar la actividad fotorreparadora, se colocaron 150 µL de CPD-fotoliasa recombinante (a diferentes concentraciones), el resto de los pocillos se completaron con tampón PBS y se irradiaron durante 5 min con un LED azul (FastGene Blue/Green LED GelPic Imaging System, 515 nm) a temperatura ambiente. También se realizaron ensayos a modo de control en ausencia de luz, trabajando en cuarto oscuro.

Posteriormente se removió la fotoliasa con el tampón de lavado, y se incubó con los anticuerpos monoclonales anti-CPD (o anti-6,4) por 30 min, y se lavó nuevamente. El revelado se realizó mediante una segunda incubación con un anticuerpo secundario biotinilado, seguido de estreptavidina-peroxidasa e incubación con el sustrato 3,3',5,5'-tetrametillbenzidina (TMB). El producto final desarrolla un color amarillo que puede detectarse a 450 nm. Los reactivos, soluciones, el ADN, anticuerpos y soluciones tampón se utilizaron siguiendo las instrucciones del fabricante del Kit (CosmoBio). Los análisis estadísticos se realizaron con One-way ANOVA, con un valor $p < 0.05$.

3.3. Resultados

Ver artículos:

- Validating biochemical features at the genome level in the Antarctic bacterium *Hymenobacter sp*. strain UV11
- A highly efficient and cost-effective recombinant production of a bacterial photolyase from the Antarctic isolate *Hymenobacter sp*. UV11

SABANA AFRICANA

Arte en placa de agar. Se sembró *Janthinobacterium* (violeta/negro) con indicador rojo Congo incorporado en el agar (vira a violeta, rojo y amarillo a pHs básicos, neutros, ácidos. respectivamente). Se utilizaron gotas de NaOH y H_2SO_4 para conseguir el efecto de ocaso.

FEMS Microbiology Letters, 366, 2019, fnz177

doi: 10.1093/femsle/fnz177
Advance Access Publication Date: 9 August 2019
Research Letter

RESEARCH LETTER – Physiology & Biochemistry

Validating biochemical features at the genome level in the Antarctic bacterium *Hymenobacter* sp. strain UV11

Juan José Marizcurrena[1], Lorena M. Herrera[1], Alicia Costábile[1], Danilo Morales[1], Carolina Villadóniga[2], Agustina Eizmendi[3], Danilo Davyt[3] and Susana Castro-Sowinski[1,2,*]

[1]Biochemistry and Molecular Biology, Faculty of Sciences, Universidad de la República, Igua 4225, 11400 Montevideo, Uruguay, [2]Hydrolytic Enzymes Laboratory, Faculty of Sciences, Universidad de la República, Igua 4225, 11400 Montevideo, Uruguay and [3]Organic Chemistry Department, Faculty of Chemistry, Universidad de la República, General Flores 2124, 11800 Montevideo, Uruguay

*Corresponding author: Biochemistry and Molecular Biology, Faculty of Sciences, Universidad de la República, Igua 4225, 11400 Montevideo, Uruguay. Tel: +598-25252095; E-mail: scs@fcien.edu.uy

One sentence summary: Combining *in silico* and bench lab experiments to understand the Antarctic bacterium *Hymenobacter* sp. UV11.

Editor: Yu-Zhong Zhang

ABSTRACT

We present experimental data that complement and validate some biochemical features at the genome level in the UVC-resistant Antarctic bacterium *Hymenobacter* sp. UV11 strain. The genome was sequenced, assembled and annotated. It has 6 096 246 bp, a GC content of 60.6% and 5155 predicted genes. The secretome analysis, by combining *in silico* predictions with shotgun proteomics data, showed that UV11 strain produces extracellular proteases and carbohydrases with potential biotechnological uses. We observed the formation of outer membrane vesicles, mesosomes and carbon-storage compounds by using transmission electron microscopy. The *in silico* analysis of the genome revealed the presence of genes involved in the metabolism of glycogen-like molecules and starch. By HPLC–UV–Vis analysis and ^{1}H-NMR spectra, we verified that strain UV11 produces xanthophyll-like carotenoids such as 2′-hydroxyflexixanthin, and the *in silico* analysis showed that this bacterium has genes involved in the biosynthesis of cathaxanthin, zeaxanthin and astaxanthin. We also found genes involved in the repair of UV-damaged DNA such as a photolyase, the nucleotide excision repair system and the production of ATP-dependent proteases that are important cellular components involved in the endurance to physiological stresses. This information will help us to better understand the ecological role played by *Hymenobacter* strains in the extreme Antarctic environment.

Keywords: *Hymenobacter*; UV irradiation; hydrolytic enzymes; Antarctica; pigments

INTRODUCTION

Microorganisms belonging to the genus *Hymenobacter* (phylum Bacteroidetes, family Cytophagaceae) are aerobic, non-motile, Gram-negative and rod-shaped bacteria, which form red-to-pinkish colonies. *Hymenobacter* cells grow in liquid media forming flocs/aggregates and a slime-like extracellular polymer (Garrity 2005). These microorganisms grow in oligotrophic media, using a limited number of carbon sources such as some sugars, sugar alcohols, organic acids, isoprene and a few amino acids. In addition, it has been reported that *Hymenobacter* cells may hydrolyze gelatin, starch, xylan, Tween 80 and Tween 60, suggesting the production of extracellular proteases, amylases, xylanases and lipases (Brenner *et al.* 2005).

Received: 11 April 2019; **Accepted:** 8 August 2019

Currently, 65 *Hymenobacter* species have been identified (http://www.bacterio.net/hymenobacter.html), *Hymenobacter roseosalivarius*, a strain isolated from the Dry Valleys region in Antarctica being the type species (Hirsch *et al.* 1998). *Hymenobacter* strains have been isolated from air (Buczolits *et al.* 2002), soil (Jin *et al.* 2014; Srinivasan *et al.* 2015; Kim *et al.* 2017) and estuarine water samples (Kang *et al.* 2013), including extreme environments such as arid lands (Zhang *et al.* 2009; Reddy and Garcia-Pichel 2013), glaciers (Klassen and Foght 2011), Antarctic soils (Hirsch *et al.* 1998), highly UV-irradiated areas (Collins *et al.* 2000; Zhang *et al.* 2007), uranium mines (Chung *et al.* 2010), oily and heavy metal contaminated places (Zhang *et al.* 2011) and also in sanitized clean-room facilities (Venkateswaran *et al.* 2003). What does these places have in common? They are all oxidative stressful environments, which may suggest that bacteria from this genus possess the genetic machinery to cope with oxidative stress resistance, among others (Klassen and Foght 2011).

The aim of this work was to describe some biochemical and phenotypic characteristics and to explore the draft genome of the UVC-resistant strain *Hymenobacter* sp. UV11 (Marizcurrena *et al.* 2017), isolated from water samples from Uruguay Lake (King George Island, Fildes Peninsula, Antarctica) (Morel *et al.* 2015). UV11 is a psychrotolerant, aerobic, rod-shaped, Gram-negative bacterium that grows in solid media forming bloody-red colonies (Marizcurrena *et al.* 2017), as expected for a *Hymenobacter* strain. Here, we describe the bacterial ultrastructure, the resistome and CAZome (all carbohydrate-active enzymes of a genome) analyses, the secretome, the identification of pigments and the production of extracellular hydrolytic enzymes, with a focus on cellulolytic and proteolytic enzymes. This information will give insights into the biotechnological potential of this microorganism, as well as to understand how it adapts to its environment.

MATERIALS AND METHODS

Growth conditions

Hymenobacter sp. UV11 cells were grown in R2 broth (0.5 g/L yeast extract, 0.5 g/L proteose peptone 3, 0.5 g/L casamino acids, 0.5 g/L dextrose, 0.5 g/L soluble starch, 0.3 g/L sodium pyruvate, 0.3 g/L K_2HPO_4, 0.05 g/L anhydrous $MgSO_4$) at 200 rpm and 20°C. When 1.5% agar was added, the medium was called R2A (Nishioka *et al.* 2016).

Production of extracellular hydrolytic enzymes

The ability to produce extracellular hydrolytic enzymes was analyzed in R2A (for the identification of amylase production) or SFR2 (starch-free R2A) supplemented with 5% skim milk or 2% carboxymethylcellulose (for the identification of extracellular proteases and cellulases, respectively), as described by Herrera *et al.* (2017), at 20°C.

Quantification of protease and cellulase activities in liquid medium

A 10% inoculum from a starter culture of strain UV11 was added to 500 mL of R2 medium and grown at 20°C and 200 rpm, for 3 days. The culture was centrifuged at 10 000 rpm and 4°C for 5 min and filtered using a sterile 0.45-μm membrane; the cell-free supernatant was used for the quantification of cellulolytic or proteolytic activities.

The cellulolytic activity was determined using carboxymethylcellulose as a substrate; the reaction was run at pH 5.5 and 40°C, and the amount of released reducing sugars was determined by the 3,5-dinitrosalicylic acid assay (Miller *et al.* 1960) at 550 nm. One unit of enzyme activity was defined as the amount of enzyme required for the release of 1 μmol of reducing sugars in 1 h, under the assay conditions.

The proteolytic activity was determined using azocasein as a substrate; the reaction was run at pH 7.5 and 40°C, and the amount of the azo chromophore released was detected at 337 nm. One enzymatic unit was defined as the amount of enzyme required for 0.6 absorbance unit increase at 337 nm per hour, under the assay conditions.

Protein concentration was determined by the Bradford method (1976) using bovine serum albumin as standard.

Transmission electron microscopy

A bacterial pellet obtained from 3 mL of *Hymenobacter* grown in R2 at 20°C was fixed in 2.5% glutaraldehyde (prepared in 0.1 M phosphate buffer at pH 7.2) at 20°C overnight. Then, it was washed with phosphate buffer (five times, 5 min each) and was post-fixed in 1% OsO_4 for 1 h, washed with phosphate buffer again and dehydrated in a gradient of ethanol (25%, 50%, 75%, 95% and 100%), followed by two washings with anhydrous acetone (pure for analysis grade). Then, it was impregnated in successive passages of Araldite–acetone mixtures with increasing concentrations of Araldite (25%, 50%, 75%). Finally, the sample was embedded in Araldite resin. Thin and ultrathin sections (350 μm and 70 nm thickness) were cut with an RMC-MT-X ultramicrotome. The different sections were stained with 1% borax–methylene blue. Ultrathin sections were contrasted with 4% aqueous uranyl acetate during 30 min at 60°C and then by soaking in lead citrate for 10 min in a CO_2-free chamber. All analysis were performed on a JEOL transmission electron microscope (JEM 1010 model) at an acceleration voltage of 100 kV at the transmission electron microscopy (TEM) facilities of Faculty of Sciences, Montevideo, Uruguay.

Sequencing, annotation and functional categorization of *Hymenobacter* sp. UV11

The genomic DNA extraction and purification, library preparation and sequencing (performed at Macrogen facilities, Seoul, Korea), the raw reads preprocessing and the initial draft genome assembly (a conservative approach for *k*-mer selection using only *k*-mer above 91 bases and mismatch correction in SPAdes was used) were done as described by Marizcurrena *et al.* (2019c). The overall quality of the assembly was assessed using QUAST (Gurevich *et al.* 2013). The UV11 genome was annotated using RAST Version 2.0 (Rapid Annotation using Subsystem Technology) server (Aziz *et al.* 2008) and the NCBI Prokaryotic Genome Annotation Pipeline. This whole-genome shotgun project has been deposited at DDBJ/ENA/GenBank under the accession number SRII00000000. The version described in this paper is version SRII00000000.1. The total proteome, as obtained from the RAST annotation, was uploaded to the KAAS-KEGG Automatic Annotation Server (Kanehisa and Goto 2000; Kanehisa *et al.* 2017, 2019) for orthologous assignment and pathway mapping. In addition, the proteome deduced from the genome of strain UV11 was challenged against different databases such as dbCAN (http://csbl.bmb.uga.edu/dbCAN/annotate.php) and MEROPS (https://www.uniprot.org/database/DB-0059). Blastp searches were performed with parameters max_target_seqs 1 and e-value $1e^{-3}$.

Shotgun of secreted proteins (secretome)

The cell-free supernatant obtained from cells grown in R2 was run on a 10% SDS-PAGE and those portions of gels containing proteins were excised for shotgun mass spectrometry analysis as described in Herrera *et al.* (2019), in the Proteomics Core Facility CEQUIBIEM, at the University of Buenos Aires/CONICET (National Research Council), as described by Ghio *et al.* (2018). The raw data were processed using the Proteome Discoverer software (version 1.4 from Thermo Scientific) and searched against the *Hymenobacter* sp. UV11 protein sequence database obtained by genome annotation. The results obtained by shotgun of secreted proteins and by the analyses obtained using the dbCAN, MEROPS and MoonProt (https://www.uniprot.org/database/DB-0189) databases were compared to identify possible cellulases, proteases and moonlighting proteins already present in the secretome; the transmembrane topology search was analyzed using TMHMM database (http://www.cbs.dtu.dk/services/TMHMM).

Pigment extraction and analysis

Strain UV11 was grown in R2 as previously described, centrifuged and the pellet was lyophilized. A total of 1.21 g of dried bacteria was incubated three times with 100 mL of methanol at 65°C for 5 min for pigment extraction. The extract was evaporated under reduced pressure and 175.4 mg was collected and stored (protected from light in an amber vial). The extract was further fractioned by vacuum chromatography on silica gel (70 g) using 150 mL portions of different proportions of hexane:ethyl acetate (10%, 30%, 50%, 100%) and finally with ethyl acetate:methanol (95:5). The colored fraction (1.5 mg) was analyzed by HPLC–DAD as described by Klassen and Foght (2008), using a Waters HPLC equipment, with binary pumps (Waters 1525) and a photodiode array detector (Waters 2996, detection ranging from 200 to 800 nm). A C18 reverse phase separation column was used (Luna C18, 5 μm, 100 A, 4.6 mm × 150 mm). Mobile phase A was a mixture of methanol:water (80:20) and mobile phase B was methanol:ethyl acetate (80:20). The extract was eluted at a flow rate of 1 mL/min with a 0–100% gradient of B, in 20 min.

^{1}H-NMR spectra of the fraction (1.5 mg) suspended in deuterated chloroform were recorded with a Bruker Avance 400. Chemical shifts are given in ppm relative to tetramethylsilane, *J* in Hz.

RESULTS

General features of the UV11 genome

Analysis of the raw data enables us to identify 64 contigs that were assembled (minimum length: 1000 bp) with L50 and L75 of 7 and 14, respectively. The final assembly yielded a total length of 6 096 246 bp. After FASTP preprocessing, we obtained a Q20/Q30 of 94.79%/91.46% and a GC content of 60.6%. We identified a total of 5155 genes (5030 protein-coding genes and 43 tRNAs, one 5S, 16S and 23S each, three ncRNAs and two partial 16S rRNA genes) and 74 pseudogenes.

Production of extracellular hydrolytic enzymes: the potential of UV11 for the production of hydrolytic enzymes

We detected the production of extracellular proteases and cellulases in SFR2 medium and also the liquid medium. Results showed that the UV11 cell-free supernatant has values of 0.57 ± 0.17 and 1.07 ± 0.64 UE/mL of cellulase and protease activities, respectively. The CAZome analysis of strain UV11 showed that this bacterium harbors the information for the production of 157 glycosyl hydrolases, 91 glycosyltransferases, 81 carbohydrate esterases, 7 polysaccharide lyases and 41 carbohydrate-binding modules. Regarding proteases, we found 1129 or 523 coding sequences (CDSs) when using an e-value $<1e^{-15}$ or when using an e-value between $1e^{-15}$ and $1e^{-3}$, respectively; however, 313 proteases were found when using an e-value $<1e^{-3}$.

Among carbohydrases, we detected a set of proteins with β-glucosidase, α-amylase, β-hexosaminidase, β-galactosidase, chitinase, mannosidase, malto-oligosyltrehalose trehalohydrolase, endo-1,4-β-xylanase, cellulase andO-glycosyl hydrolase activities, among others (Table 1), in the UV11 secretome as searched by shotgun mass spectrometry analysis. In addition to carbohydrases, we found many proteases in the secretome from strain UV11 by shotgun mass spectrometry, including several metallopeptidases (Table 1). We also found a few moonlighting proteins (multifunctional proteins that perform unrelated functions) and proteins with transmembrane domains with protease or carbohydrase activities (Table 1).

Transmission electron microscopy

The TEM images in Fig. 1 revealed (i) the nucleoid structure as a nondelimited electron-lucent area in the middle of the electron-dense cytoplasm, (ii) an electron-dense layer typical from Gram-negative microbes and a periplasmic space, and (iii) cytoplasmic granular-like formations as electron-dense structures, but we did not observed a capsule-like structure. Bacterial cells (1.5 μm × 0.5 μm) were surrounded by a sticky electron-dense extracellular matrix, and spherical-shaped outer membrane vesicles were seen with an electron-dense bilayer membrane and an electron-lucid space inside, with diameters that vary from 50 to 300 nm. We also observed plasma membrane invaginations like vesicular sacs (mesosomes) (Fig. 1).

We observed cytoplasmic granular-like formations as electron-dense structures by TEM; thus, we searched for genes involved in the production of carbon-storage compounds, such as glycogen, polyhydroxyalkanoates and starch. We did not find the genomic information involved in the production of polyhydroxyalkanoates, but the genes involved in the production and degradation of glycogen-like molecules and starch were identified. We found CDSs for the synthesis of glycogen such as a glycogen synthase (EC 2.4.1.21), a phosphoglucomutase (EC 5.4.2.6) and a glycosyltransferase. We also found CDSs for the degradation of glycogen such as a glycogen phosphorylase (EC 2.4.1.1), glycogen debranching enzyme (EC 3.2.1.-), a 1,4-alpha-glucan (glycogen) branching enzyme, GH-13-type (EC 2.4.1.18) and a 4-alpha-glucanotransferase (amylomaltase) (EC 2.4.1.25), with 80–98% identity with related CDSs in *Hymenobacter* spp. Interestingly, we found the genes *sus* (for starch utilization system): *susA* (alpha-amylase, EC 3.2.1.135), *susB* and *susDC*.

We also found the information for the synthesis of trehalose from UDP-glucose, such as the CDSs for the production of the following enzymes: alpha-trehalose-phosphate synthase (UDP-forming) (EC 2.4.1.15) and trehalose-6-phosphate phosphatase (EC 3.1.3.12).

Table 1. The *Hymenobacter* sp. UV11 secretome.

Accession	Most abundant proteins	MoonP	TMM	# Peptides	# PSMs
TFZ68046.1	TonB-dependent receptor	No	No	58	177
TFZ68852.1	TonB-dependent receptor	No	No	43	76
TFZ67628.1	TonB-dependent siderophore receptor	No	No	45	146
TFZ64576.1	TonB-dependent receptor	No	No	37	77
TFZ68246.1	TonB-dependent receptor	No	Yes	28	48

Accession	Proteases	MoonP	TMM	# Peptides	# PSMs
TFZ64495.1	M1 family peptidase	No	No	12	13
TFZ67086.1	TldD/PmbA family protein	No	No	16	28
TFZ65164.1	M13 family peptidase	No	No	12	13
TFZ67145.1	S9 family peptidase	Yes	No	6	6
TFZ67396.1	Insulinase family protein	No	No	2	2
TFZ67450.1	M28 family peptidase	No	No	11	14
TFZ67610.1	M1 family peptidase	Yes	No	6	6
TFZ67931.1	M3 family peptidase	No	No	4	6
TFZ66445.1	M20/M25/M40 family metallo-hydrolase	No	No	11	14
TFZ66147.1	M13 family peptidase	No	No	2	2
TFZ66722.1	S9 family peptidase	No	No	12	14
TFZ65165.1	M13 family peptidase	No	No	7	7
TFZ67101.1	S9 family peptidase	No	No	4	4
TFZ68377.1	Amidohydrolase	No	No	4	4
TFZ67995.1	M1 family peptidase	No	No	6	6
TFZ66465.1	Aminopeptidase	Yes	No	6	6
TFZ64574.1	Serine hydrolase	No	No	5	5
TFZ65168.1	Amidohydrolase family protein	No	Yes	6	8
TFZ64582.1	M20/M25/M40 family metallo-hydrolase	No	No	11	14
TFZ68728.1	Alpha-2-macroglobulin family protein	No	No	1	1
TFZ65530.1	S9 family peptidase	No	No	5	5
TFZ64961.1	Insulinase family protein	No	No	3	3
TFZ66233.1	M28 family peptidase	No	No	1	1
TFZ67460.1	S9 family peptidase	Yes	No	13	15
TFZ65309.1	M1 family peptidase	Yes	No	3	3
TFZ65713.1	S9 family peptidase	Yes	No	0	0
TFZ65063.1	Zinc carboxypeptidase	No	No	4	4
TFZ65378.1	Peptidase M28 family protein	No	No	9	11
TFZ66846.1	Alpha/beta fold hydrolase	No	No	6	6
TFZ67958.1	T9SS type A sorting domain-containing protein	No	No	3	3
TFZ65269.1	Peptidase	No	No	4	4
TFZ65270.1	Alpha/beta hydrolase	Yes	No	4	4
TFZ66309.1	M28 family peptidase	No	No	2	2
TFZ65728.1	LysM peptidoglycan-binding domain-containing protein	No	Yes	1	1
TFZ67622.1	M48 family peptidase	No	No	1	1
TFZ68706.1	Class A beta-lactamase-related serine hydrolase	No	No	1	1
TFZ66830.1	Carboxylesterase family protein	No	No	3	3
TFZ65180.1	Peptidase S8	No	No	0	0
TFZ65150.1	M28 family peptidase	No	No	3	3

Accession	CAZymes	MoonP	TMM	# Peptides	# PSMs
TFZ68161.1	Beta-glucosidase	No	No	17	22
TFZ65940.1	Alpha-amylase	No	No	14	16
TFZ65938.1	Alpha-amylase	No	No	5	5
TFZ64905.1	Glycosyl hydrolase	No	No	18	18
TFZ63464.1	Beta-*N*-acetylhexosaminidase	No	No	5	5
TFZ68143.1	Beta-glucuronidase	No	No	3	3
TFZ63862.1	Beta-glucuronidase	No	No	2	2
TFZ67726.1	Glycogen debranching protein	No	No	5	5
TFZ68018.1	DUF4982 domain-containing protein	No	No	9	9
TFZ63467.1	Hypothetical protein E4631_22590	No	No	2	2
TFZ68160.1	Endoglucanase	No	No	6	7

Table 1. Continued

Accession	CAZymes	MoonP	TMM	# Peptides	# PSMs
TFZ66305.1	Glycoside hydrolase family 92 protein	No	No	0	0
TFZ67807.1	Beta-glucosidase BglX	No	No	5	5
TFZ64519.1	T9SS type A sorting domain-containing protein	No	No	4	4
TFZ65098.1	Carbohydrate-binding protein	No	Yes	5	9
TFZ66456.1	T9SS type A sorting domain-containing protein	No	Yes	2	2
TFZ64904.1	Beta-glycosidase	No	No	3	3
TFZ65270.1	Alpha/beta hydrolase	Yes	No	4	4
TFZ65728.1	LysM peptidoglycan-binding domain-containing protein	No	Yes	1	1
TFZ64643.1	Glycoside hydrolase family 16 protein	No	No	4	5
TFZ68992.1	Glycoside hydrolase family 88 protein	No	No	2	2
TFZ62600.1	Glycoside hydrolase family 32 protein	No	No	1	1
TFZ67475.1	Beta-glucosidase	No	No	0	0
TFZ67810.1	Glycoside hydrolase	No	No	3	3
TFZ67487.1	Glycosyl hydrolase family 43	No	No	4	4
TFZ68162.1	Glycosyl hydrolase	No	No	6	6
TFZ67805.1	Glycoside hydrolase family 5 protein	No	No	6	6
TFZ64577.1	Arabinogalactan endo-1,4-beta-galactosidase	No	No	6	6
TFZ68058.1	T9SS type A sorting domain-containing protein	No	No	2	2

The table shows the CAZymes and proteases, and a few abundant proteins with different functions, found in the UV11 secretome. Proteins with putative transmembrane domains or moonlight function are indicated in the columns 'TMM' and 'MoonP', respectively. The values of peptide-spectrum match (column '# PSMs') and the peptides (column '# Peptides') assigned to each protein are shown.

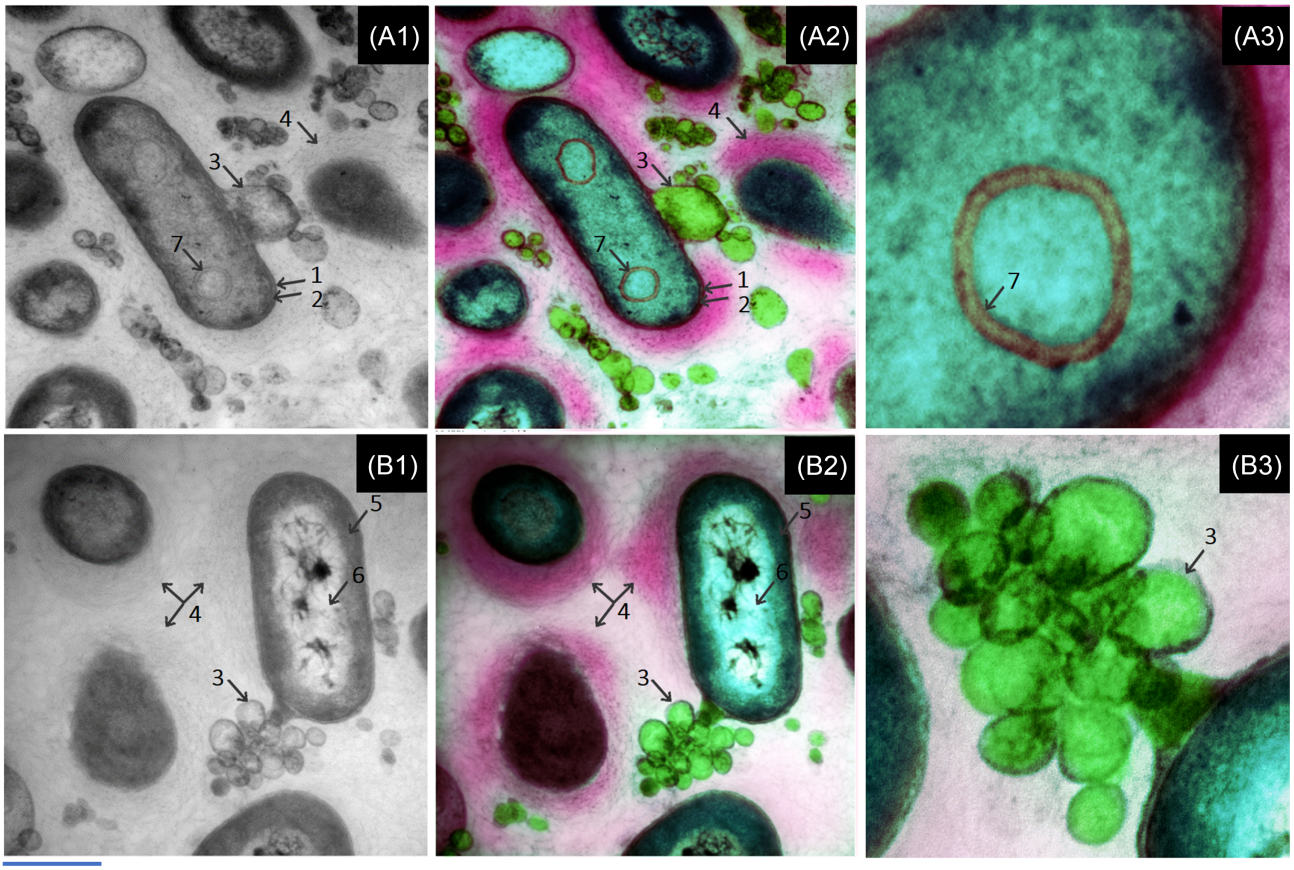

Figure 1. Ultrastructural view of *Hymenobacter* sp. UV11. Ultrastructural view of *Hymenobacter* sp. UV11. **(A1–B1, A2–B2)** Original and colored pictures, respectively. Different structures can be observed. 1 and 2—outer and inner plasma membrane; 3–outer membrane vesicles, new emerging vesicles; 4—extracellular matrix produced by the bacterium; 5—cytoplasm with ribosomes; 6—nucleoid; 7—mesosomes. Scale bar: 500 nm (blue). **(A3, B3)** Zoom-out pictures from (A2) and (B2) showing the double membrane of a mesosome and the outer membrane vesicles emerging from the bacterium.

The resistome analysis: how to deal with the damage induced by UV irradiation

The genomic information regarding UV resistance in strain UV11 was also searched looking for the presence of different systems involved in the repair of the UV-damaged DNA. As it has been previously reported, *Hymenobacter* has a CPD-photolyase (Marizcurrena *et al.* 2017, 2019b), and currently we found that strain UV11 has the UV damage repair endonuclease (UvdE), with 66% and 30% sequence identity compared to UVDE protein of *Hymenobacter swuensis* (WP_044000995.1) and *Deinococcus radiodurans* R1, respectively. Regarding the nucleotide excision repair (NER) system, strain UV11 has three copies of the excinuclease ABC subunits A and C, and a single copy of excinuclease ABC subunit B, and also has the *uvrD* and *polA* (DNA polymerase I).

As found in *D. radiodurans* R1 (Karlowicz *et al.* 2017), the *Hymenobacter* sp. UV11 genome contains two copies of the Lon protease and the components of the Clp protease system (one catalytic ClpP subunit, one subunit of each ClpA and ClpX and two ClpB subunits). The genes were found dispersed throughout the genome.

The characteristic pigment produced by *Hymenobacter* sp. UV11

The HPLC–UV–Vis analysis of the UV11 extract showed (Fig. 2A and B) three minor peaks and a major one. The UV–Vis and ^{1}H-NMR spectra of the colored fraction (Fig. 2C and D) showed these pigments are xanthophyll-like carotenoids, 2′-hydroxyflexixanthin being the main one, a xanthine already reported by Klassen, McKay and Foght (2009) in *Hymenobacter* species. The couplings of the protons of the alpha-hydroxy-carbonyl ring system were clearly observed in the ^{1}H-NMR and COSY spectra of this carotenoid. We also detected the coupling of signal at 5.72 ppm corresponding to 3′ vinyl proton with the 4.04 ppm signal from the 2′ hydroxyl geminal proton by COSY (Fig. 2C and D). The minor xanthophylls, as observed by UV spectra, presumably are compounds related to 2′-hydroxyflexixanthin.

The search on the UV11 genome showed that this bacterium has the genomic information for the synthesis of phytoene synthase (EC 2.5.1.32), phytoene desaturase (EC 1.3.99.28; responsible for the synthesis of lycopene) and many other enzymes such as lycopene beta-cyclase (EC: 5.5.1.19) and beta-carotene 3-hydroxylase (EC: 1.14.15.24).

As shown in Fig. 3, the *in silico* analysis carried on the KAAS-KEGG shows that strain UV11 may produce cathaxanthin, zeaxanthin and astaxanthin. The production of cathaxanthin by strain UV11 was previously demonstrated by FTIR spectra (Montagni *et al.* 2018). We also found the CDSs for the synthesis of dimethylallyltransferase (EC 2.5.1.1), octaprenyl diphosphate synthase (EC 2.5.1.90), beta-carotene hydroxylase, phytoene dehydrogenase (EC 1.14.99.-), beta-carotene ketolase (EC 1.14.-.-), dehydrogenase and related proteins. Bench and *in silico* experiments showed that strain UV11 produces or has the potential to produce a set of carotenoids.

DISCUSSION

In this work, we combined the information obtained in bench and by the sequencing of the genome to decipher some of the genes or pathways involved in a few biochemical properties. This information will allow to better understand the ecological role of *Hymenobacter* sp. strain UV11 in the Antarctic environment and to choose CDSs with potential biotechnological uses.

A general study of the UV11 genome showed that this bacterium has a genome larger than those from other *Hymenobacter* strains (*Hymenobacter* sp. strain IS2118, 5.26 Mb; strain PAMC26628, 5.2 Mb chromosome and one plasmid with 89 596 bp; strain AT01-02, 5.09 Mb; *H. swuensis*, 4.9 Mb; among others) (Jung *et al.* 2014; Ptacek *et al.* 2014; Hansen *et al.* 2016; Oh *et al.* 2016). Larger genome-sized species may dominate in environments where resources are scarce such as the Antarctic environment and suggest an environmental adaptation (Konstantinidis and Tiedje 2004; Land *et al.* 2015). Among potential adaptations, we searched for the production of extracellular hydrolytic enzymes, accumulation of polymeric storage compounds and pigments, and resistance to a few stresses.

We found the information for UV11 endurance in an oligotrophic environment, including the production of extracellular hydrolytic enzymes involved in the degradation of scarce polymeric nutrient molecules, and also accumulation of carbon-storage compounds.

Strain UV11 produced and secreted extracellular hydrolytic enzymes such as carbohydrases and proteases; in addition, the analysis of the genome suggests the enormous potential of strain UV11 for the production of hydrolytic enzymes with potential biotechnological uses. Interestingly, the use of carboxymethylcellulose as sole carbon source (deduced from the detection of cellulases for carboxymethylcellulose degradation) has been reported for *Hymenobacter pallidus* and *Hymenobacter xinjiangensis*; however, *Hymenobacter rigui* and *Hymenobacter gummosus* do not have the ability to hydrolyze carboxymethylcellulose (Chen *et al.* 2017; Sheu *et al.* 2017), suggesting that the production of cellulases is not a common feature among *Hymenobacter* isolates.

TEM analysis suggests that strain UV11 produces outer membrane vesicles, mesosomes and carbon-storage compounds. The release of vesicles from the envelope of growing bacteria allows the extracellular secretion of products involved in colonization, cellular communication, predatory behavior, defense, biofilm formation and the modulation of host defense and response (Kuehn and Kesty 2005; Pérez-Cruz *et al.* 2015; O'Donoghue *et al.* 2017; Nasarabadi, Berleman and Auer 2019). The production and uptake of outer membrane vesicles is a dynamic process that allows the exchange of information in the form of a chemical dialogue, and also allows the exchange of genetic material, which opens the gate for horizontal gene transfer events between bacteria (Boedicker and Tran 2018). UV11 cells could use these vesicles as part of their communicasome, transporting signaling molecules that could modulate the microbial environment and thereby help bacteria to reduce the internal stress by exporting misfolded proteins and/or enable a coordinated behavior between themselves (Kim *et al.* 2015). The formation of mesosome-like structures is commonly associated with cellular processes such as cell division, chromosome segregation and response to stress conditions (Li *et al.* 2008; Murata *et al.* 2008; Hartmann *et al.* 2010; Morita *et al.* 2015). To the best of our knowledge, this is the first report of a *Hymenobacter* isolate that produces this kind of cellular structures.

The results also showed that strain UV11 stores carbon-based compounds, a property that has been associated with the ability of the psychrophilic bacterium *Colwellia* sp. NB097-1 to survive in the cold environment (Zhang, Guo and Wang 2018), and it has also been involved in starvation, desiccation and osmotic stress endurance (Lerner *et al.* 2009). Based on the genomic information, and in agreement with Chen *et al.* (2017)

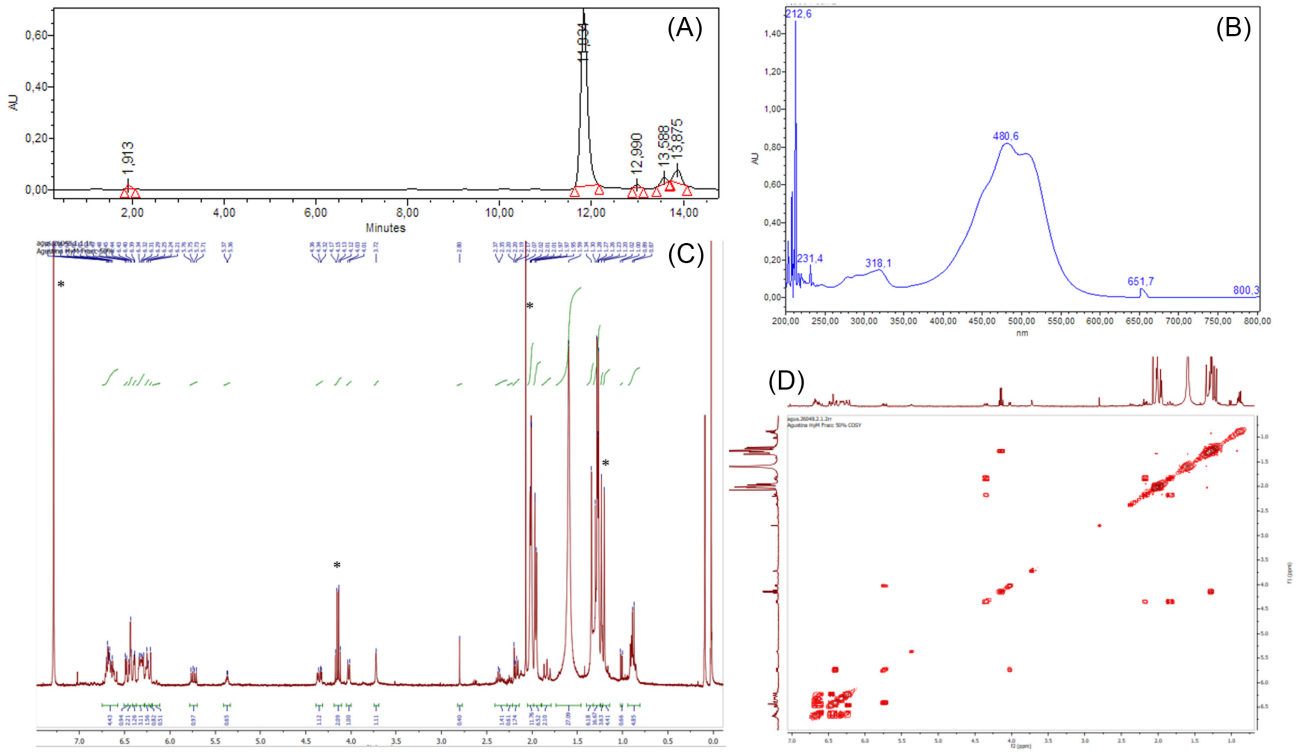

Figure 2. **(A)** HPLC chromatogram of *Hymenobacter* methanolic extract; naftazone was used as internal standard. **(B)** UV–Vis absorption spectra of the major peak: $t = 11.834$. **(C)** ^{1}H-NMR spectra of pigment fraction in $CDCl_3$; solvent residual signals are shown with ∗. **(D)** COSY spectra of pigment fraction in $CDCl_3$.

who worked with *H. gummosus*, we did not find genes involved in the production of polyhydroxyalkanoates. However, Sheu *et al.* (2017) detected the production of polyhydroxyalkanoates by *H. pallidus*. We found genes involved in the production and degradation of glycogen-like molecules and starch, and the *sus* system, essential for the import and degradation of starch. The *sus* genes usually cluster together (*susRABCDEFG*), but many predicted Sus polysaccharide utilization loci do not include obvious *susA* or *susB* genes within the same operon (Foley, Cockburn and Koropatkin 2016) as found in strain UV11. In addition, we found genes involved in the production of the disaccharide trehalose. We did not study whether the strain UV11 produces this disaccharide, but we hypothesize that the accumulation of glycogen and trehalose is involved in bacterial cold adaptation, as it was demonstrated in Antarctic *Penicillium* strains (Miteva-Staleva *et al.* 2017).

UV irradiation induces the production of DNA lesions and protein oxidation, among others. In bacteria, different DNA repair mechanisms have been reported: (i) the direct repair of the damage by photolyases, (ii) the repair of oxidized bases by DNA glycosylases (base excision repair), (iii) the repair of the damage by the UV-damage endonuclease or UVDE, and (iv) the removal and further synthesis of a complete oligonucleotide section that held the damage by the NER system (Goosen and Moolenaar 2008). We previously reported that strain UV11 produces a photolyase, and in this work we report that strain UV11 has the genes for the NER system and the UV damage repair endonuclease (UVDE protein). UVDE provides protection against UV irradiation and can also compensate an NER deficiency (Earl *et al.* 2002). The NER system is the most versatile DNA repair mechanism, and involves different steps: recognition of the DNA damage, incision, excision, DNA synthesis and ligation (Grossman and Kovalsky 2006). The first steps are carried out by the proteins UvrABC, endonucleases that make the 5′ and 3′ incisions around the DNA lesion. Similar to the well-known UV- and radioresistant bacterium *D. radiodurans*, and other *Hymenobacter* isolates (*H. actinosclerus, H. aerophilus*, *H. chitinivorans*, *H. coccineus H. daecheongensis, H. gelipurpurascens*, *H. glacialis, H. lapidaries*, *H. mucosus*, *H. nivis*, *H. norwichensis, H. psychrophilus*, *H. psychrotolerans*, *H. roseosalivarius*, *H. rubripertinctus, H. sedentarius, H. swuensis*, *H. terrenus*), *Hymenobacter* sp. UV11 has the key enzymes involved in DNA recovery after direct and oxidative damage caused by UV radiation. We also found the genes involved in the post-incision steps such as *uvrD* (helicase II; part of the SOS regulon, which is induced by DNA damage) and *polA* (DNA polymerase I) (Grossman and Kovalsky 2006).

We found that strain UV11 produces the Lon and Clp ATP-dependent proteases, which are important cellular components involved in the endurance to physiological stresses (including UV irradiation), since they are able to degrade damaged proteins (Bhattacharjee, Dasgupta and Bagchi 2017). Bacterial ATP-dependent proteases such as Lon and Clp protease systems have already been proposed to be involved in the acclimation to either UV or cold stress as was shown in the cyanobacterium *Synechococcus* (Porankiewicz, Schelin and Clarke 1998) and in the bacterium *D. radiodurans* (Servant *et al.* 2007). Lon is a homohexameric protein and the Clp system contains many components (the proteolytic ClpP and several regulatory ATPase components such as ClpA or ClpC and ClpX, as found in *Escherichia coli*).

Finally, we chemically identified the reddish pigments produced by strain UV11 and the genes involved in the production of carotenoid-like ones. All carotenoids are derived from the colorless carotenes phytoene and phytofluene, the enzyme phytoene synthase being the main one involved in their biosynthesis.

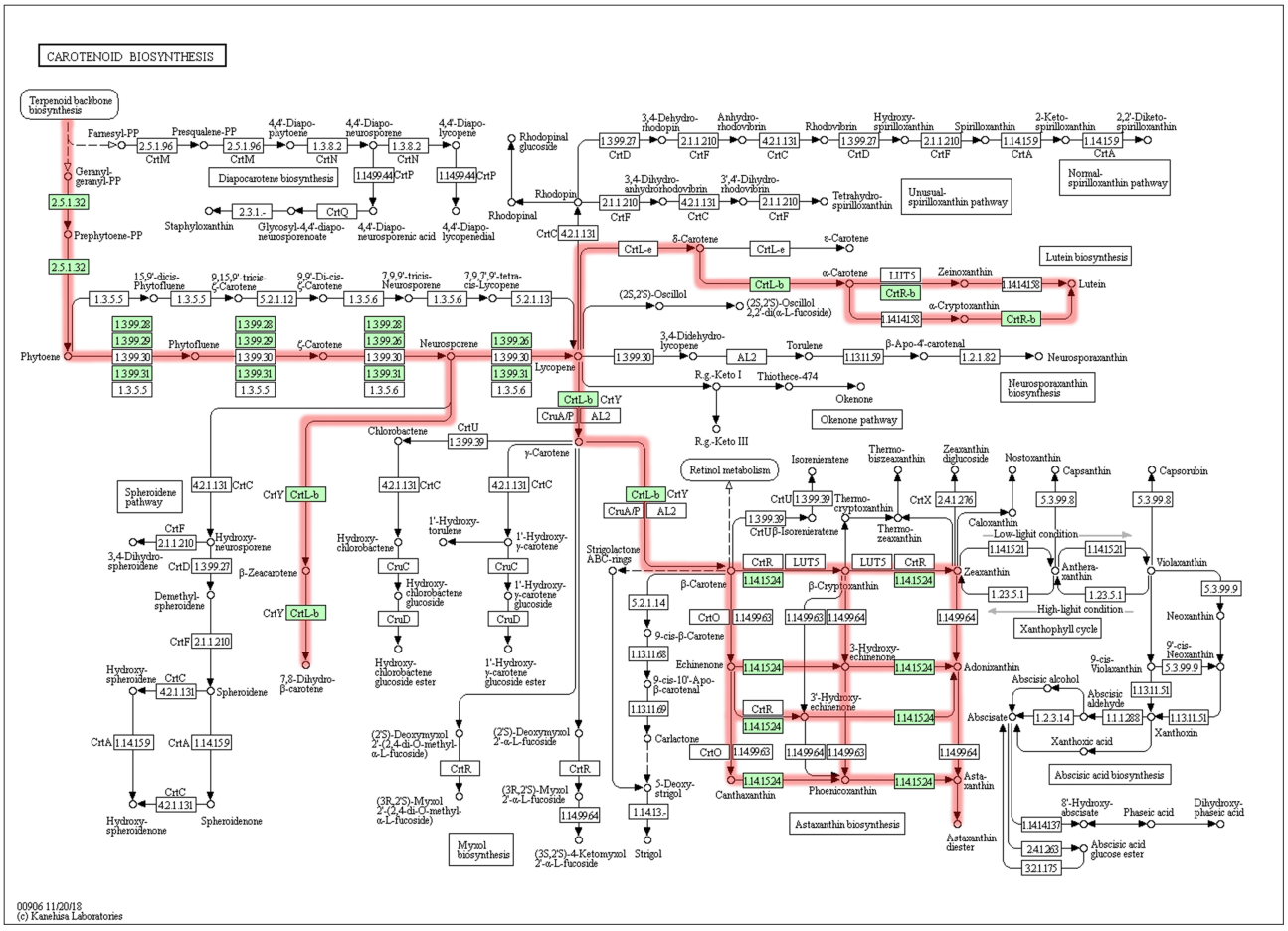

Figure 3. Metabolic pathway for carotenoid biosynthesis. Green boxes shows the enzymes found in the *Hymenobacter* sp. UV11 genome.

Carotenoids and their derivatives are isoprenoid chemical compounds involved in many bacterial functions such as reactive species scavengers, but also in cold stress adaptation, solar irradiation resistance and freeze–thaw cycles (Marizcurrena *et al.* 2019a). These pigments are also produced by other *Hymenobacter* species as it has been previously shown (Klassen and Foght 2008; Klassen, McKay and Foght 2009; Órdenes-Aenishanslins *et al.* 2016).

These results encouraged us to perform a comparative genomic analysis of the *Hymenobacter* genomes available in the databases; this work is under progress and will be the subject of a future work (manuscript in preparation).

CONCLUSIONS

Hymenobacter sp. UV11 is a UVC-resistant bacterium that presents different pathways to cope with the cell damage induced by UV irradiation. This includes the production of a CPD-photolyase, a complete NER system and ATP-dependent proteases such as Lon and Clp proteases. However, the relationship between the xanthophyll-like carotenoid production and UV resistance of strain UV11 still has to be proven by the analysis of deficient pigment-producing bacterium. The information presented here supports the hypothesis that this strain produces pigments probably involved in cold stress adaptation, solar irradiation, freeze–thaw cycles and as reactive species scavengers. Interestingly, strain UV11 produces hydrolytic enzymes with protease and cellulase activities that may extract carbon and nitrogen resources from polymeric substances found in the oligotrophic Antarctic environment. This ability may help this bacterium to survive in oligotrophic lakes such as Uruguay Lake, but the information obtained also suggests that strain UV11 may store glycogen-like and starch molecules. The intracellular accumulation of these molecules and trehalose is commonly involved in bacterial endurance, including cold stress, among others. Interestingly, results from the TEM analysis suggest that strain UV11 produces mesosomes and extracellular vesicles as part of its intercellular communicasome.

Finally, we have found that *Hymenobacter* sp. UV11 has the genetic machinery to cope with the harsh stresses imposed by the Antarctic environment, including UV irradiation, and oxidative and oligotrophic stresses. As cold stress is a huge open chapter in cold-adapted microbes, this subject will be discussed in a future manuscript.

ACKNOWLEDGEMENTS

The authors thank the Uruguayan Antarctic Institute for the logistic support during the stay in the Antarctic Base Artigas. SC-S, DD, AC and JJM are members of the National Research System (SNI, Sistema Nacional de Investigadores).

FUNDING

This work was partially supported by PEDECIBA (Programa de Desarrollo de las Ciencias Básicas) and ANII (Agencia Nacional de Investigación e Innovación, Project FMV_3_2016_1_1226654). The work of JJM and LMH was supported by ANII and CAP (Comisión Académica de Posgrado, UdelaR).

Conflict of interest. None declared.

REFERENCES

Aziz RK, Bartels D, Best A *et al*. The RAST Server: rapid annotations using subsystems technology. *BMC Genomics* 2008;**9**:75.

Bhattacharjee S, Dasgupta R, Bagchi A. A review on the mode of the interactions of bacterial proteases with their substrates. In: *Proteases in Physiology and Pathology*. Singapore: Springer, 2017, 527–48.

Boedicker J, Tran F. Regulation of gene exchange in bacterial outer membrane vesicles. *Bull Am Phys Soc* 2018.

Bradford MM. A rapid and sensitive method for the quantitation of microgram quantities of protein utilizing the principle of protein–dye binding. *Anal Biochem* 1976;**72**:248–54.

Brenner DJ, Krieg NR, Staley JT *et al*. *Bergey's Manual of Systematic Bacteriology: Proteobacteria, Gammaproteobacteria*. Berlin, Germany: Springer, 2005.

Buczolits S, Denner EBM, Vybiral D *et al*. Classification of three airborne bacteria and proposal of *Hymenobacter aerophilus* sp. nov. *Int J Syst Evol Microbiol* 2002;**52**:445–56.

Chen W-M, Chen W-T, Young C-C *et al*. *Hymenobacter gummosus* sp. nov., isolated from a spring. *Int J Syst Evol Microbiol* 2017;**67**:4728–35.

Chung AP, Lopes A, Nobre MF *et al*. *Hymenobacter perfusus* sp. nov., *Hymenobacter flocculans* sp. nov. and *Hymenobacter metalli* sp. nov., three new species isolated from an uranium mine waste water treatment system. *Syst Appl Microbiol* 2010;**33**:436–43.

Collins MD, Hutson RA, Grant IR *et al*. Phylogenetic characterization of a novel radiation-resistant bacterium from irradiated pork: description of *Hymenobacter actinosclerus* sp. nov. *Int J Syst Evol Microbiol* 2000;**50**:731–4.

Earl AM, Rankin SK, Kim KP *et al*. Genetic evidence that the uvsE gene product of *Deinococcus radiodurans* R1 is a UV damage endonuclease. *J Bacteriol* 2002;**184**:1003–9.

Foley MH, Cockburn DW, Koropatkin NM. The Sus operon: a model system for starch uptake by the human gut Bacteroidetes. *Cell Mol Life Sci* 2016;**73**:2603–17.

Garrity GM. *Bergey's Manual of Systematic Bacteriology, 2nd edn, Vol. 2: The Proteobacteria, Part C: The Alpha-, Beta-, Delta-, and Epsilonproteobacteria*. Berlin, Germany: Springer, 2005, 567–71.

Ghio S, Ontañon O, Piccinni FE *et al*. *Paenibacillus* sp. A59 GH10 and GH11 extracellular endoxylanases: application in biomass bioconversion. *BioEnergy Res* 2018;**11**:174–90.

Goosen N, Moolenaar GF. Repair of UV damage in bacteria. *DNA Repair* 2008;**7**:353–79.

Grossman L, Kovalsky O. Nucleotide excision repair in bacteria. In: *Encyclopedia of Life Sciences*. Chichester, UK: Wiley, 2006.

Gurevich A, Saveliev V, Vyahhi N *et al*. QUAST: quality assessment tool for genome assemblies. *Bioinformatics* 2013;**29**:1072–5.

Hansen ACH, Paulino-Lima IG, Fujishima K *et al*. Draft genome sequence of *Hymenobacter* sp. strain AT01-02, isolated from a surface soil sample in the Atacama Desert, Chile. *Genome Announc* 2016;**4**:e01701–15.

Hartmann M, Berditsch M, Hawecker J *et al*. Damage of the bacterial cell envelope by antimicrobial peptides gramicidin S and PGLa as revealed by transmission and scanning electron microscopy. *Antimicrob Agents Chemother* 2010;**54**:3132–42.

Herrera LM, Braña V, Franco Fraguas L *et al*. Characterization of the cellulase-secretome produced by the Antarctic bacterium *Flavobacterium* sp. AUG42. *Microbiol Res* 2019;**223–225**:13–21.

Herrera LM, García-Laviña CX, Marizcurrena JJ *et al*. Hydrolytic enzyme-producing microbes in the Antarctic oligochaete *Grania* sp. (Annelida). *Polar Biol* 2017;**40**:947–53.

Hirsch P, Ludwig W, Hethke C *et al*. *Hymenobacter roseosalivarius* gen. nov., sp. nov. from continental Antarctic soils and sandstone: bacteria of the *Cytophaga/Flavobacterium/Bacteroides* line of phylogenetic descent. *Syst Appl Microbiol* 1998;**21**:374–83.

Jin L, Lee HG, Kim SG *et al*. *Hymenobacter ruber* sp. nov., isolated from grass soil. *Int J Syst Evol Microbiol* 2014;**64**:979–83.

Jung JH, Yang HY, Jeong S *et al*. Complete genome sequence of *Hymenobacter swuensis*, an ionizing-radiation resistant bacterium isolated from mountain soil. *J Biotechnol* 2014;**178**:65–6.

Kanehisa M, Furumichi M, Tanabe M *et al*. KEGG: new perspectives on genomes, pathways, diseases and drugs. *Nucleic Acids Res* 2017;**45**:D353–61.

Kanehisa M, Goto S. KEGG: Kyoto Encyclopedia of Genes and Genomes. *Nucleic Acids Res* 2000;**28**:27–30.

Kanehisa M, Sato Y, Furumichi M *et al*. New approach for understanding genome variations in KEGG. *Nucleic Acids Res* 2019;**47**:D590–5.

Kang JY, Chun J, Choi A *et al*. *Hymenobacter koreensis* sp. nov. and *Hymenobacter saemangeumensis* sp. nov., isolated from estuarine water. *Int J Syst Evol Microbiol* 2013;**63**:4568–73.

Karlowicz A, Wegrzyn K, Gross M *et al*. Defining the crucial domain and amino acid residues in bacterial Lon protease for DNA binding and processing of DNA-interacting substrates. *J Biol Chem* 2017;**292**:7507–18.

Kim JH, Lee J, Park J *et al*. Gram-negative and Gram-positive bacterial extracellular vesicles. *Semin Cell Dev Biol* 2015;**40**:97–104.

Kim MK, Kang MS, Srinivasan S *et al*. Complete genome sequence of *Hymenobacter sedentarius* DG5BT, a bacterium resistant to gamma radiation. *Mol Cell Toxicol* 2017;**13**:199–205.

Klassen JL, Foght JM. Differences in carotenoid composition among *Hymenobacter* and related strains support a tree-like model of carotenoid evolution. *Appl Environ Microbiol* 2008;**74**:2016–22.

Klassen JL, Foght JM. Characterization of *Hymenobacter* isolates from Victoria Upper Glacier, Antarctica reveals five new species and substantial non-vertical evolution within this genus. *Extremophiles* 2011;**15**:45–57.

Klassen JL, McKay R, Foght JM. 2′-Methyl and 1′-xylosyl derivatives of 2′-hydroxyflexixanthin are major carotenoids of *Hymenobacter* species. *Tetrahedron Lett* 2009;**50**:2656–60.

Konstantinidis KT, Tiedje JM. Trends between gene content and genome size in prokaryotic species with larger genomes. *Proc Natl Acad Sci USA* 2004;**101**:3160–5.

Kuehn MJ, Kesty NC. Bacterial outer membrane vesicles and the host–pathogen interaction. *Genes Dev* 2005;**19**:2645–55.

Land M, Hauser L, Jun SR *et al*. Insights from 20 years of bacterial genome sequencing. *Funct Integr Genomics* 2015;**15**:141–61.

Lerner A, Castro-Sowinski S, Lerner H *et al*. Glycogen phosphorylase is involved in stress endurance and biofilm formation

in *Azospirillum brasilense* Sp7. *FEMS Microbiol Lett* 2009;**300**:75–82.

Li X, Feng HQ, Pang XY *et al*. Mesosome formation is accompanied by hydrogen peroxide accumulation in bacteria during the rifampicin effect. *Mol Cell Biochem* 2008;**311**:241–7.

Marizcurrena JJ, Cerdá MF, Alem D *et al*. Living with pigments: the colour palette of Antarctic life. In: *The Ecological Role of Micro-organisms in the Antarctic Environment*. New York: Springer, 2019a, 65–82.

Marizcurrena JJ, Martínez-López W, Ma H *et al*. A highly efficient and cost-effective recombinant production of a bacterial photolyase from the Antarctic isolate *Hymenobacter* sp. UV11. *Extremophiles* 2019b;**23**:49–57.

Marizcurrena JJ, Morales D, Smircich P *et al*. Draft genome sequence of the UV-resistant antarctic bacterium *Sphingomonas* sp. strain UV9. *Microbiol Resour Announc* 2019c;**8**:e01651–18.

Marizcurrena JJ, Morel MA, Braña V *et al*. Searching for novel photolyases in UVC-resistant Antarctic bacteria. *Extremophiles* 2017;**21**:409–18.

Miller GL, Blum R, Glennon WE *et al*. Measurement of carboxymethylcellulase activity. *Anal Biochem* 1960;**1**:127–32.

Miteva-Staleva JG, Krumova ET, Vassilev SV *et al*. Cold-stress response during the stationary-growth phase of Antarctic and temperate-climate *Penicillium* strains. *Microbiology* 2017;**163**:1042–51.

Montagni T, Enciso P, Marizcurrena JJ *et al*. Dye sensitized solar cells based on Antarctic *Hymenobacter* sp. UV11 dyes. *Environ Sustain* 2018;**1**:89–97.

Morel MA, Braña V, Martínez-rosales C *et al*. Five-year biomonitoring of aquatic ecosystems near Artigas Antarctic Scientific Base, King George Island. *Adv Polar Sci* 2015;**26**:102–6.

Morita D, Sawada H, Ogawa W *et al*. Riccardin C derivatives cause cell leakage in *Staphylococcus aureus*. *Biochim Biophys Acta—Biomembr* 2015;**1848**:2057–64.

Murata K, Kawai S, Mikami B *et al*. Superchannel of bacteria: biological significance and new horizons. *Biosci Biotechnol Biochem* 2008;**72**:265–77.

Nasarabadi A, Berleman JE, Auer M. Outer membrane vesicles of bacteria: structure, biogenesis, and function. In: *Biogenesis of Fatty Acids, Lipids and Membranes*. Cham, Switzerland: Springer, 2019, 593–607.

Nishioka T, Elsharkawy MM, Suga H *et al*. Development of culture medium for the isolation of *Flavobacterium* and *Chryseobacterium* from rhizosphere soil. *Microbes Environ* 2016;**31**:104–10.

O'Donoghue EJ, Sirisaengtaksin N, Browning DF *et al*. Lipopolysaccharide structure impacts the entry kinetics of bacterial outer membrane vesicles into host cells. *PLoS Pathog* 2017;**13**:e1006760.

Oh TJ, Han SR, Ahn DH *et al*. Complete genome sequence of *Hymenobacter* sp. strain PAMC26554, an ionizing radiation-resistant bacterium isolated from an Antarctic lichen. *J Biotechnol* 2016;**227**:19–20.

Órdenes-Aenishanslins N, Anziani-Ostuni G, Vargas-Reyes M *et al*. Pigments from UV-resistant Antarctic bacteria as photosensitizers in dye sensitized solar cells. *J Photochem Photobiol B Biol* 2016;**162**:707–14.

Pérez-Cruz C, Delgado L, López-Iglesias C *et al*. Outer-inner membrane vesicles naturally secreted by Gram-negative pathogenic bacteria. *PLoS One* 2015;**10**:e0116896.

Porankiewicz J, Schelin J, Clarke AK. The ATP-dependent Clp protease is essential for acclimation to UV-B and low temperature in the cyanobacterium *Synechococcus*. *Mol Microbiol* 1998;**29**:275–83.

Ptacek T, Swain AK, Andersen DT *et al*. Draft genome sequence of *Hymenobacter* sp. strain IS2118, isolated from a freshwater lake in Schirmacher Oasis, Antarctica, reveals diverse genes for adaptation to cold ecosystems. *Genome Announc* 2014;**2**:e00739–14.

Reddy GSN, Garcia-Pichel F. Description of *Hymenobacter arizonensis* sp. nov. from the southwestern arid lands of the United States of America. *Antonie van Leeuwenhoek, Int J Gen Mol Microbiol* 2013;**103**:321–30.

Servant P, Jolivet E, Bentchikou E *et al*. The ClpPX protease is required for radioresistance and regulates cell division after γ-irradiation in *Deinococcus radiodurans*. *Mol Microbiol* 2007;**66**:1231–9.

Sheu S-Y, Li Y-S, Young C-C *et al*. *Hymenobacter pallidus* sp. nov., isolated from a freshwater fish culture pond. *Int J Syst Evol Microbiol* 2017;**67**:2915–21.

Srinivasan S, Lee J-J, Park KR *et al*. *Hymenobacter terrae* sp. nov., a bacterium isolated from soil. *Curr Microbiol* 2015;**70**:643–50.

Venkateswaran K, Hattori N, La Duc MT *et al*. ATP as a biomarker of viable microorganisms in clean-room facilities. *J Microbiol Methods* 2003;**52**:367–77.

Zhang C, Guo W, Wang Y *et al*. The complete genome sequence of *Colwellia* sp. NB097-1 reveals evidence for the potential genetic basis for its adaptation to cold environment. *Mar Genomics* 2018;**37**:54–57.

Zhang DC, Busse HJ, Liu HC *et al*. *Hymenobacter psychrophilus* sp. nov., a psychrophilic bacterium isolated from soil. *Int J Syst Evol Microbiol* 2011;**61**:859–63.

Zhang L, Dai J, Tang Y *et al*. *Hymenobacter deserti* sp. nov., isolated from the desert of Xinjiang, China. *Int J Syst Evol Microbiol* 2009;**59**:77–82.

Zhang Q, Liu C, Tang Y *et al*. *Hymenobacter xinjiangensis* sp. nov., a radiation-resistant bacterium isolated from the desert of Xinjiang, China. *Int J Syst Evol Microbiol* 2007;**57**:1752–6.

Extremophiles
https://doi.org/10.1007/s00792-018-1059-y

ORIGINAL PAPER

A highly efficient and cost-effective recombinant production of a bacterial photolyase from the Antarctic isolate *Hymenobacter* sp. UV11

Juan José Marizcurrena[1,2,3] · Wilner Martínez-López[2,3] · Hongju Ma[4] · Tilman Lamparter[4] · Susana Castro-Sowinski[1,5]

Received: 6 June 2018 / Accepted: 24 September 2018

Abstract
Photolyases are DNA-repairing flavoproteins that are represented in most phylogenetic taxa with the exception of placental mammals. These enzymes reduce the ultraviolet-induced DNA damage; thus, they have features that make them very attractive for dermatological or other medical uses, such as the prevention of human skin cancer and actinic keratosis. In this work, we identified a 50.8 kDa photolyase from the UVC-resistant Antarctic bacterium *Hymenobacter* sp. UV11. The enzyme was produced by recombinant DNA technology, purified using immobilized metal affinity chromatography and its activity was analyzed using different approaches: detection of cyclobutane pyrimidine dimers (CPDs) by immunochemistry, high-performance liquid chromatography and comet assays using Chinese Hamster Ovary (CHO) and immortalized nontumorigenic human epidermal (HaCat) cells. The information supports that the recombinant protein has the ability to repair the formation of CPDs, on both double- and single-stranded DNA. This CPD-photolyase was fully active on CHO and HaCat cell lines, suggesting that this enzyme could be used for medical or cosmetic purposes. Results also suggest that the UV11 CPD-photolyase uses MTHF as chromophore in the antenna domain. The potential use of this recombinant enzyme in the development of new inventions with pharmaceutical and cosmetic applications is discussed during this work.

Keywords Photolyase · *Hymenobacter* · UV-irradiation · Photorepair · Antarctica

Introduction

Sunlight is the natural light that reaches the Earth's surface. This kind of radiation is reflected, refracted, scattered and partially absorbed by the Earth's atmosphere, with daylight being responsible for the majority of photobiological phenomena. When photobiologists deal with light as waves, it is classified into visible light (range 400–700 nm), ultraviolet radiation (UV; with shorter waves) and infrared radiation (with longer waves). The UV spectrum ranges into ultraviolet A (UVA; 315–400 nm), B (UVB; 290–315 nm) and C (UVC; 220–290 nm). UV radiation produces photo-oxidative DNA damage and different lesions such as cyclobutane pyrimidine dimers (CPDs) and pyrimidine (6–4) pyrimidone adducts (6,4-photoproducts; 6,4PP). These lesions cause bulky DNA backbone distortions that halt RNA polymerase II during transcription or DNA polymerase during replication. When unrepaired, these lesions may lead to skin cancer (UV-photocarcinogenesis) (Seebode et al. 2016). The Nucleotide Excision Repair (NER) pathway is responsible of repairing UV-induced DNA lesions, avoiding UV-induced

Communicated by F. Robb.

Electronic supplementary material The online version of this article (https://doi.org/10.1007/s00792-018-1059-y) contains supplementary material, which is available to authorized users.

✉ Susana Castro-Sowinski
s.castro.sow@gmail.com; scs@fcien.edu.uy

[1] Biochemistry and Molecular Biology, Faculty of Sciences, Universidad de la República (UdelaR), Iguá 4225, 11400 Montevideo, Uruguay

[2] Epigenetics and Genomics Instability Laboratory, Institute Clemente Estable, Av. Italia 3318, 11600 Montevideo, Uruguay

[3] Biodosimetry Service. Institute Clemente Estable, Av. Italia 3318, 11600 Montevideo, Uruguay

[4] Botanical Institute, Karlsruhe Institute for Technology, Fritz Haber Weg 4, 76131 Karlsruhe, Germany

[5] Molecular Microbiology, Institute Clemente Estable, Av. Italia 3318, 11600 Montevideo, Uruguay

Published online: 28 September 2018

cell death and development of melanoma. Patients with NER deficiency (e.g., the genetic disorder Xeroderma Pigmentosum) show skin tumor predisposition, including melanoma (Budden and Bowden 2013). People chronically exposed to solar radiation also display UV-induced actinic keratosis that may progress to nonmelanoma skin cancer (Krutmann et al. 2015). The recommendation for skin cancer protection includes a few strategies, such as DNA photo-damage reduction (avoiding skin sun exposition) and screening (standard examination of skin) (Seebode et al. 2016). Currently, dermatologists recommend the use of sunscreen products, but for patients with high or very high risk of developing skin cancer, the use of sunscreen with DNA repair enzymes is recommended (Krutmann et al. 2015).

Photolyases (EC 4.1.99.3) are monomeric flavoproteins (50–60 kDa) that repair DNA-photoproducts by electron transfer and bond-breaking reactions (Zhong 2015). They have been found widespread in many living organisms, although they are absent in placental mammals (including Human beings) and a few marsupials. It has been shown that the inclusion of photolyases (encapsulated in liposomes) in skin care products reduces skin UV-induced DNA damage (Berardesca et al. 2012; Puig-Butillé et al. 2013; Malvehy 2014; Eibenschutz et al. 2016). In vivo experiments have shown that the topical application of photolyase-containing DNA repair enzyme creams/devices prevents human skin cancer and actinic keratosis. These results have encouraged the search for new highly active photolyases and the development of photolyase-containing products with dermatological or other medical uses.

Photolyases possess an antenna and a DNA-binding domain. The antenna contains a variable chromophore (5,10-methenyl-tetrahydrofolate, MTHF or 8-hydroxy-7,8-didemethyl-5-deazariboflavin, 8-HDF, among others) that absorb blue light and then this energy is transferred by resonance to the Flavin Adenine Dinucleotide (FADH-) redox cofactor. This active cofactor thus transfers the electron to pyrimidine dimers allowing their reparation (Brettel and Byrdin 2010; Wang et al. 2015). Photolyases can be classified according to the photoproduct they repair as CPD-photolyases or 6,4-photolyases. Among CPD-photolyases, they are divided into three classes: I (found in microorganisms, e.g., *Anacystis nidulans* and *Escherichia coli*), II (mainly present in higher eukaryotic organisms, but also in prokaryotes and viruses) and III (closely related to Cryptochromes plant photoreceptors) (Wang et al. 2015). Finally, photolyases are also classified based on the chromophore present in the antenna domain (MTHF or 8-HDF, among others).

It has been proven that Antarctic microorganisms are a novel source of genetic material for the development of new biotechnological exploitation (Martínez-Rosales et al. 2012; Martinez-Rosales et al. 2015; Tucci et al. 2016; Herrera et al. 2017). Due to the continuous depletion of the ozone layer (the sun's harmful UV radiation shield) that affects the Antarctic continent and the ice reflection that can lead to an increased UV intensity, Antarctica may be a hotspot for natural selection of UV-resistant microorganisms (Dugo et al. 2012). In this scenario, microbes probably selected high performance photolyases, among other biomolecules, to keep their physiologic homeostasis. The aim of this work was the recombinant production of a photolyase from the Antarctic isolate *Hymenobacter* sp. UV11, and the characterization of its DNA repair ability, for the future design of cosmetic and/or clinical products with increased photorepair potential. UV11 is an UVC-resistant bacterium isolated from water samples collected in Uruguay Lake, Fildes Peninsula, King George Island, Antarctica (Morel et al. 2015), this bacterium has shown high UVC-LD50 (LD, abbreviation for "lethal dose 50%") (126 J m^{-2}) and photo-reactivation ability (90 J m^{-2}) and produces a Class I CPD-photolyase (Marizcurrena et al. 2017).

Materials and methods

Strains, eukaryotic cell lines and culture conditions

Escherichia coli DH5 alpha and BL21 (DE3) strains (both from Invitrogen, USA) were used for plasmid multiplication and for protein expression, respectively.

CHO (Chinese Hamster Ovary) (Puck 1958) and HaCaT cell lines were used to perform comet assays. "HaCaT" denotes a spontaneously transformed aneuploid immortal keratinocyte cell line from adult human skin with a high capacity for differentiation and proliferation, in vitro (Boukamp et al. 1988). Both cell lines were used to test in vitro the removal of CPDs induced by UVC irradiation by comet assay.

CHO and HaCat cell lines were cultured in McCoy's 5A medium (GIBCO) and Dulbecco's modified Eagle medium (DMEM, GIBCO), respectively. Both media were supplemented with 10% fetal bovine serum (GIBCO), 100 U mL^{-1} of penicillin and 100 U mL^{-1} of streptomycin. Cells were grown at 37 °C in a humidified incubator gassed (95% air and 5% CO_2). Subcultures were obtained by disaggregating the cells with 0.1% trypsin/0.05% ethylenediaminetetraacetic acid (EDTA) solution (final concentration) in Ca^{2+}/Mg^{2+}-free saline phosphate buffer (PBS).

Construction and maintenance of plasmid

The construct (the recombinant plasmid) was synthesized by GenScript (https://www.genscript.com/; USA). The codon optimized for *E. coli* CPD-photolyase Class I gen, from *Hymenobacter* sp. UV11 (GenBank Accession Number

KX118295), was fused into the plasmid vector pET28a(+); the expression vector encodes for the photolyase with an N-terminal 6-His tag. For plasmid maintenance, the construct was transformed to *E. coli* DH5α chemocompetent cells and inoculated on Luria–Bertani (LB) plate containing 50 μg mL^{-1} kanamycin. Plasmids were transformed using the calcium chloride protocol as previously described (Sambrook and Russell 2001). Cells were stored in 15% glycerol at − 80 °C. For ex situ microbial repository purpose in an International Patent Depository (Parc Científic Universitat de Valencia, Spain), under the 1977 Budapest Treaty on the International Recognition of the Deposit of Microorganisms, the expression vector was called PhotoHymeno_pET-28a(+) and the recombinant strain was called *Escherichia coli* BL21 (DE3) strain PhotoUV11 (Depositary Accession Number: CECT 9643).

Production and purification of recombinant photolyase

For the production of the recombinant protein, the recombinant plasmid was transformed into *E. coli* BL21 (DE3) cells. Precultures were obtained by growth on Luria Broth at 37 °C. Cells were transferred to an auto-inductor Zym-5052 medium (Studier 2005), containing Kanamycin (50 mg mL^{-1}), and allowed to grow at different temperatures (14, 20, 37 °C) for 48 h. Cells were harvested, washed twice with PBS, lysed by sonication (40% amplitude, at a relative power output of 10) using sodium phosphate buffer (50 mM, supplemented with NaCl 50 mM, at pH 8), and centrifuged (7000 g at 4 °C, 10 min). The supernatant was labeled TF (Total Fraction). Soluble (SF) and insoluble (IF; including inclusion bodies) fractions were separated by centrifugation (16000 g at 4 °C, 30 min). The insoluble fraction was suspended in the solubilization buffer (50 mM phosphate buffer, 50 mM NaCl, 8 M urea, pH 8.0). All fractions were controlled by Sodium Dodecyl Sulfate-Polyacrylamide Gel Electrophoresis (SDS-PAGE), using 12% acrylamide for the resolving gel and 5% for the stacking gel as described by Laemmli (Laemmli 1970).

The UV11 recombinant photolyase was purified by binding the soluble fraction of proteins with an Ni–NTA affinity resin (Invitrogen) in binding buffer (50 mM phosphate buffer, 50 mM NaCl, 40 mM Imidazole) for 1 h at 4 °C. Afterwards the resin was settled in a purification column. The resin was then washed with binding buffer and the recombinant protein was eluted with binding buffer containing 250 mM Imidazole and further desalted using a PD-10 column (GE Healthcare, 17-0851-01). All fractions were controlled by SDS-PAGE. Protein concentrations were determined by Bradford assay (Amresco, M172), using bovine serum albumin as standard. The identity of the recombinant protein was verified by mass spectrometry MALDI/TOF–TOF analysis in the Analytical Biochemistry and Proteomics Unit of the Institute Pasteur (Montevideo, Uruguay). The protein weight and amino acid composition were found by searching in the NCBI database with peptide m/z values using the MASCOT software. Finally, the recombinant photolyase was stored in PBS buffer supplemented with 50% glycerol at − 20 °C.

Photolyase activity: traditional comet assay or single cell gel electrophoresis (SCGE) with minor modifications

HaCat or CHO cell samples were washed twice with cold PBS, irradiated with a dose of 4 J m^{-2} UVC radiation (254 nm) using a Spectroline lamp (model ENF-260C/FE), washed again, scraped using a rubber policeman and transferred to Eppendorf tubes with 1 mL of PBS. Twenty μL of cell suspension (2×10^6 cells) was gently mixed with 80 μL of 1% low melting-point agarose and directly applied to a 1.5% agarose pre-coated slide. Slides were covered with a coverslip and placed at 4 °C for 5 min. Then, coverslips were removed and slides were submersed in the lysis solution (2.5 M NaCl, 100 mM Na_2EDTA, 10 mM Tris buffer at pH 10, 1% Triton X-100) and incubated at 4 °C for 2 h. Slides were washed twice with buffer NET (100 mM NaCl, 10 mM Tris-HCI, 10 mM EDTA; pH 8.0) for 5 min at room temperature. For treatments with photolyase, 50 μL of recombinant CPD-photolyase at different concentrations (suspended in NET buffer) was applied to the top of gels, irradiated with a UVA lamp (ULTRA-VITALUX OSRAM 300 W) for 10 min in a humidity chamber for photorepair, and then washed twice in NET buffer. All slides were loaded with 50 μL of T4 endonuclease V in NET buffer, covered with a coverslip and incubated in a humidified chamber for 30 min at 37 °C. The endonuclease cleaves the glycosyl bond of the 5′ end of the pyrimidine dimer, whereas unrepaired CPDs are revealed by this enzyme. DNA fragments were resolved by alkaline-electrophoresis (at pH 13 to denature double-stranded DNA), using the following running buffer: 1 mM Na_2EDTA, 0.3 NaOH, at pH 13. DNA was unwound for 15 min and then, the electrophoresis was performed at 0.7 V cm^{-1}, 300 mA for 20 min, in a cold unit at 4 °C. The slides were removed and washed in neutralization buffer (0.4 M Tris–HCl; pH 7.5) for 5 min at room temperature and finally stained with 50 μL ethidium bromide (10 mg mL^{-1}). Slides were analyzed using the Computer Program Comet Imager (MetaSystems). At least 50 nuclei per slide were measured; two slides per treatment or control were analyzed. Three independent biological replicas were performed. Damage was quantified as the comet olive tail moment, which represents the extent of DNA damage in individual cells. Photosomes-V from Barnet was used as control.

Photolyase activity: CPD detection by high performance liquid chromatography (HPLC)

The oligonucleotide t-repair was irradiated for the production of CPD and 6,4-photoproducts; both products were separated by HPLC and used as substrates during a repair assay using the recombinant UV11 photolyase. Repaired and non-repaired products were detected by HPLC as described by Ma et al. (2017). Protocols are described below.

Preparation and purification of photoproducts: a solution of 50 µM oligonucleotide "t-repair" (AGGTTGGC) was prepared in Millipore water, degassed with argon and then poured into a Petri dish as a thin aqueous layer for efficient irradiation, placed on a cooling pack in an irradiation box under argon atmosphere and irradiated for 6 h with a UVC lamp (GE Healthcare, G15T87B, 15 W) located 12 cm above the sample. The irradiated DNA oligonucleotide was then concentrated by vacuum drying and purified by HPLC on a "series 1200 Agilent Technologies system" using a 100-3 C18ec (250 × 10) column (Macherey–Nagel). The separation of oligonucleotides containing CPDs or 6,4-photoproducts was done using a 4–18% gradient of solution B [0.1 M Triethylammonium Acetate (TEAA) prepared in water and acetonitrile (ACN) 20/80] in solution A (0.1 M TEAA in H_2O); the gradient was applied during 45 min and the flow rate was 5 mL min^{-1}. The elution profile was monitored at 260 nm and 325 nm, which is the absorbance maximum of the 6,4-photoproduct. The peak of the CPD photoproduct was identified by the repair assay as described below. CPDs and 6,4-photoproducts fractions were collected and stored at − 20 °C.

For the repair assay, 5 µM CPD or (6–4) photoproducts of the t-repair oligonucleotide were prepared in the following buffer: 50 mM Tris–HCl, 1 mM EDTA, 100 mM NaCl, 5% (w/v) glycerol, 14 mM dithiothreitol (DTT), at pH 7.0. The recombinant photolyase was mixed at 1 or 40 µg mL^{-1} final concentration. The sample was first incubated for 5 min in darkness at 22 °C, and aliquots were irradiated with 400 nm light emitting diodes at an intensity of 250 µmol m^{-2} s^{-1} for 30 min. The reaction was stopped by heating at 95 °C for 10 min. The samples were centrifuged at 13,000 rpm for 10 min and the filtered (0.45 µm pore size) supernatants were subjected to HPLC analysis, using the same Agilent system mentioned above, equipped with a Gemini C18 column of 50 × 4.60 mm, 110 Å (Phenomenex). The HPLC conditions were as previously described by Ma et al. (2017): 7% ACN in 0.1 M TEAA (pH 7.0) for 0–5 min; 7–10% ACN in 0.1 M TEAA (pH 7.0) for 5–35 min; flow rate, 0.75 mL min^{-1}; column temperature, 27 °C; detection wavelengths were 260 nm and 325 nm. The repair efficiency was estimated from the peak areas of damaged DNA and repaired DNA as described earlier (Graf et al. 2015).

Photolyase activity: CPD detection by immunochemistry

Immunochemistry of irradiated Calf thymus DNA was performed to quantify CPDs using the High Sensitivity CPD/Cyclobutane Pyrimidine Dimer ELISA kit from CosmoBio (NM-MA-K001), with modifications as follows. UVC-irradiated calf thymus DNA (50 µL of 0.4 µg mL^{-1} DNA irradiated with 10 Joules) was denatured by incubation at 100 °C for 10 min, followed by ice chilling for 15 min, applied to microtiter wells pre-coated with protamine sulfate and then treated with 150 µL of the recombinant photolyase at different concentrations during 20 min under blue light at room temperature, using the FastGene Blue/Green LED GelPic Imaging System, array of blue/green LEDs, at 515 nm. Control experiments in darkness were also carried out. Then, the photolyase was removed by washing with washing buffer, treated with specific monoclonal anti-CPD antibody clone TDM-2 and washed again. The remaining TDM-2 antibody in each well was then measured by sequential treatment with a secondary biotinylated antibody, streptavidin-peroxidase, and the substrate 3,3′,5,5′-tetramethylbenzidine (TMB). The final product develops a color which was measured at 450 nm. Reactive compounds, including the irradiated calf thymus DNA, antibodies and buffers, were used following manufacturer's instructions (CosmoBio).

Results

The codon-optimized gene encoding the *Hymenobacter* sp. UV11 photolyase was cloned into the a pET28a(+) vector and expressed as a His-tagged protein in the *E. coli* strain BL21(DE3) as described in Materials and Methods. As a fast method to analyze whether the protein was being expressed in active form, photo-reactivation activity assays using the recombinant *E. coli* and the wild-type strains were performed earlier as describe by Marizcurrena et al. (2017). In this assay, the recombinant strain was resistant up to 100 J m^{-2} of photo-reactivation (defined as the amount of the total UVC dose, in J m^{-2}, that the strains tolerate due to the exposure to blue light, in comparison to darkness) whereas the *E. coli* control strain, transformed with the same plasmid but without the UV11 photolyase DNA insert, was resistant at less to 2 J m^{-2}. These results suggest that the enzyme would be produced in an active form, at least while in the cellular environment.

The expression of the recombinant photolyase was analyzed by growing the expression strain in Zym 5052 medium at three different temperatures of 37, 20 and 14 °C. Results showed that the UV11 recombinant photolyase was produced in all tested temperatures. The enzyme was mainly segregated in inclusion bodies at 37 °C; but at lower growth

temperatures the recombinant enzyme was found also in the soluble fraction of proteins (data not shown). For subsequent experiments, the expression strain was grown in Zym 5052 medium at 37 °C until reaching an optical density (O.D.) of 0.6 at 600 nm and then the temperature was reduced to 14 °C during 48 h for proper expression of the recombinant protein in the soluble fraction. The final O.D. was 20. In this condition, the enzyme was also detected in the soluble fraction (Fig. 1a).

The recombinant protein was purified from the soluble fraction by IMAC and analyzed by SDS-PAGE (Fig. 1b) and mass spectrometry (MS) to assure its identity. On SDS-PAGE, the protein runs with a molecular size of 50 kDa, in line with the MS size of 50.8 kDa (protein including the His tag). In addition, a 57.60 kDa molecular chaperone GroEL co-purified with the photolyase (see Fig. 1b; this protein was also identified by MS). The photolyase yield was 42 mg of protein in 6 mL, produced from a 200 mL culture.

The activity of the purified recombinant photolyase was analyzed using three approaches: CPD detection by immunochemistry, HPLC and comet assays using CHO and HaCat cells. It was observed that UVC-irradiated CHO cells that were treated with the recombinant photolyase in the presence of blue light had a significantly lower value of olive tail moment rather than non-photolyase treated cells (Figs. 2a–c and 3a), suggesting that the recombinant enzyme can repair the DNA damage caused by UVC irradiation. Experiments were also done with the commercial photolyase, Photosomes-V. Values of olive tail moment for non-irradiated cells, UVC-irradiated cells and UVC-irradiated cells treated with the commercial photolyase were 1.13, 16.4 and 0.57, respectively. This result would show that, under the assayed conditions, the Photosomes-V (plankton extract and lecithin) produce nucleus shrink (Comet assay in Supplementary material S1).

On view of this result, we faced the analysis of the DNA-repairing ability of the recombinant photolyase on UVC-irradiated human skin HaCat cells (Figs. 2d–f and 3b). HaCat cells that were treated with the recombinant photolyase also showed reduced values of olive tail moments, similar to those values found for the cells that were not exposed to UVC irradiation. These results suggest that under the assay conditions, the recombinant photolyase reduced the UVC induced CPD lesions on the DNA of CHO and HaCat cells almost completely.

The activity of the recombinant UV11 photolyase was also confirmed by the HPLC assay. In these experiments, single-stranded oligonucleotides with a CPD lesion were used as a substrate and the repair activity of two different concentrations of recombinant photolyase was determined. An example for a profile after the repair is given in Fig. 4a–c). The removal of 100% and 90% of CPDs was observed when 40 μg mL^{-1} and 1 μg mL^{-1} of the recombinant photolyase was used, respectively. When the 6,4-photoproduct was used as a substrate, no repair activity was detected.

Immunochemical assay experiments, using monoclonal commercial antibodies that recognize CPDs, also confirmed that the recombinant protein was purified as an active DNA-repairing enzyme. In these experiments, calf thymus DNA, which contains single-stranded DNA, was used as substrate and the recombinant photolyase reduced the presence CPDs completely. In this assay, UVC-irradiated and non-photolyase treated DNA were used as reference or control experiments (Fig. 5). We detected repair activity even using 1 μg mL^{-1} of the recombinant photolyase, which means that the purified enzyme was diluted 5000-fold for this experiment. When experiments were carried out in darkness or when the recombinant enzyme was denatured by heating, we did not detect repair activity (Fig. 5). These results also show that the UV11 recombinant photolyase has been purified as an active enzyme which requires light for its repair activity. As control, we used Photosome-V, but we did not detect activity. The

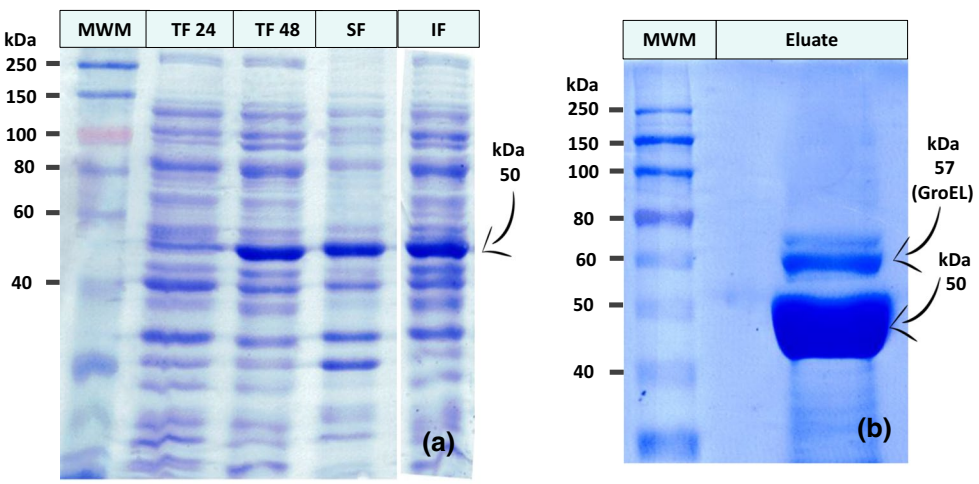

Fig. 1 Expression and purification of UV11 CPD-photolyase. SDS-PAGE analysis of the expression (**a**) and purification by IMAC (**b**) of the CPD-photolyase. The arrow indicates the recombinant enzyme migrating at approximately 50 kDa as expected. Abbreviations are as follows: *MWM* molecular weight marker, *TF 24* total fraction after 24 h growth, *TF 48* total fraction after 48 h growth, *SF* soluble fraction, *IF* insoluble fraction. Eluate is the CPD-photolyase fraction collected after the purification process

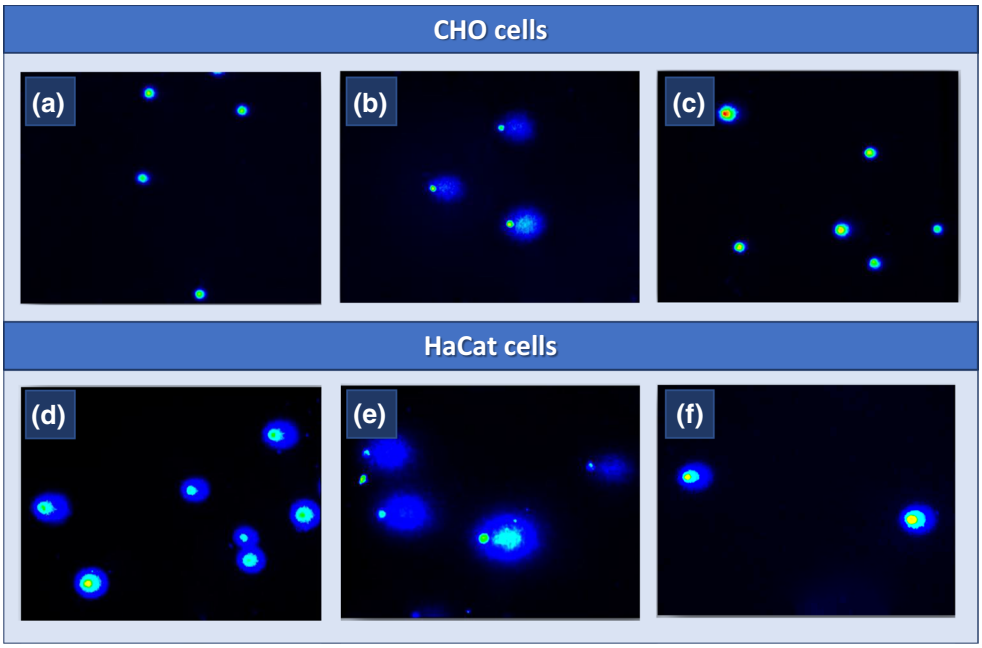

Fig. 2 Repair of DNA damage by UV11 CPD-photolyase in mammalian cells. Comet assay images of CHO (upper figure) and HaCat (below figure) cells. **a** and **d** are non-UVC-irradiated and untreated cells; **b** and **e** are UVC-irradiated cells; **c** and **f** are UVC-irradiated cells treated with the recombinant photolyase

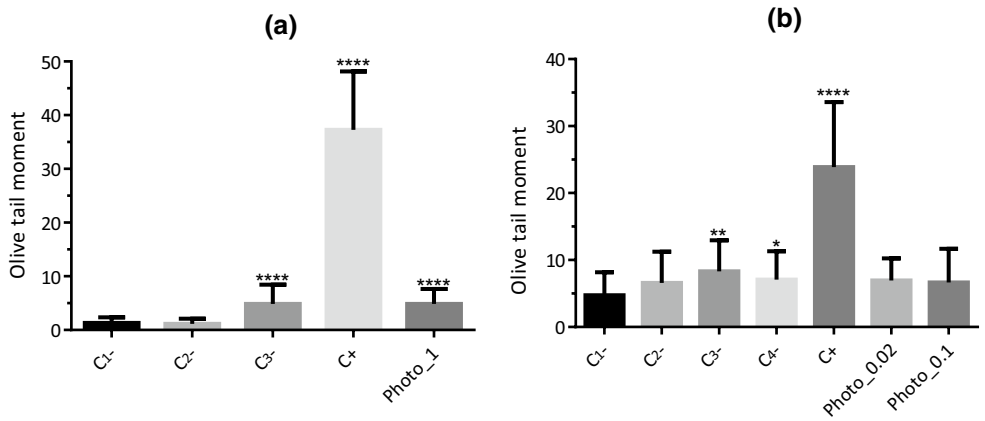

Fig. 3 Quantification of UV11 photolyase activity in mammalian cells. Olive tail moments and statistics. Experiments were performed with CHO (**a**) and HaCat (**b**) line cells. These results were supported by the test statistic (multiple comparison ANOVA assay), where 50 comets per treatment were counted in duplicate. Abbreviations are as follows: C1-, non-irradiated cells (non-damaged DNA); C2-, non-irradiated cells treated with endonuclease T4 V (basal DNA damage under normal conditions); C3-, UVC-irradiated cells (damaged DNA); C4-, non-irradiated cells treated with the recombinant photolyase (potential damage produced by the recombinant photolyase); C+, UVC-irradiated cells treated with endonuclease T4 V (total damage of DNA); Photo_1, Photo_0.1 and Photo_0.02 are cells treated with 50 µl of 1, 0.1 and 0.02 mg/mL recombinant CPD-photolyase

6,4-photoproducts antibodies were also tested in immunochemical assays and these results suggested also that the recombinant photolyase does not repair this kind of DNA lesion (Supplementary materials, S2). We also found by the immunological assay that the repair activity of the recombinant photolyase was not affected by the storage for 1 year at – 20 °C in 50% glycerol (data not shown).

Discussion

The prophylactic use of photolyase-containing liposomes by topical application has shown to provide protection to the UV-exposed human skin (Stege et al. 2000). Working with Caucasian volunteers, Berardesca et al. (2012)

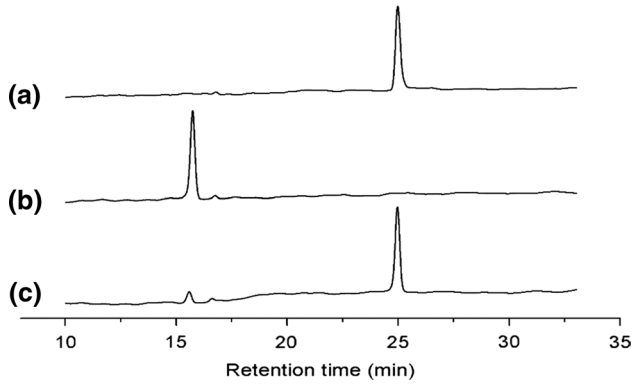

Fig. 4 UV11 CPD-photolyase activity, using UV-irradiated oligonucleotide as substrate, detected by HPLC assay. **a** HPLC assay after CPD DNA repair by the use of 1 µg/mL of the recombinant UV11 photolyase. **a** undamaged t-repair, **b** UVC-irradiated t-repair (the peak represents the CPD photoproduct), **c** UVC-irradiated t-repair treated with the recombinant photolyase

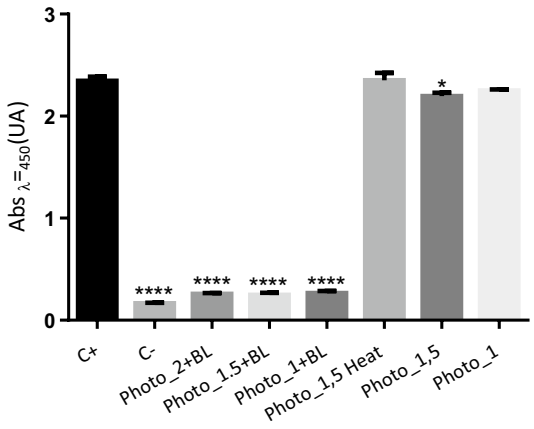

Fig. 5 UV11 CPD-photolyase activity using calf thymus irradiated DNA as substrate, as detected by immunochemistry assay. Results were supported by the statistic test One-way ANOVA ($p < 0.05$). Abbreviations are as follows: C-, non-irradiated calf thymus DNA (non-damaged DNA); C+, 10 Joules m-2 UVC-irradiated DNA (damaged DNA); Photo_1 + BL, Photo_1.5 + BL and Photo_2 + BL are UVC-irradiated DNA treated with 1, 1.5 and 2 µg/mL recombinant CPD-photolyase and blue light (BL); Photo_1,5 and Photo_1 are UVC-irradiated DNA treated with 1,5 and 1 µg/mL recombinant CPD-photolyase in darkness conditions, respectively; Photo_1,5 Heat is UVC-irradiated DNA treated with heat-inactivated recombinant CPD-photolyase

already demonstrated that the use of traditional sunscreen amended with *Anacystis nidulans* photolyase provided a superior protection compared to the use of the sunscreen alone, reducing the formation of CPDs and apoptotic cell death. In addition, histopathological analysis and molecular assessment of CPI-17 gene over-expression, a phosphorylation-dependent inhibitor protein of smooth muscle myosin phosphatase, up-regulated in some cancerous cells, showed that the topical application of a film-forming medical device containing Repairsomes® (photolyase in liposomes and UV filters), in patients with cutaneous field cancerization, restored their skin homeostasis (Puig-Butillé et al. 2013). Currently, there are a few sunscreens containing photolyase: Ladival®Serum Post-Solar Regenerator (Stada Laboratories, with a photolyase extracted from an algae), Eryfotona® AK-NMSC (ISDIN, with liposome-encapsulated photolyase), Celfix DNA™ (PrecisionMD) and DermADN from Dermur (Celsius Laboratories, located in Uruguay), among others. Most of these commercial products contain photolyases from the marine plankton *A. nidulans* (registered as "plankton extract" on the product package).

In this work, we present the recombinant production of a CPD-photolyase from an Antarctic UVC-resistant bacterium, *Hymenobacter* sp. UV11. To the best of our knowledge, this is the first report regarding the recombinant production of a protein from a *Hymenobacter* strain. However, a few other microbial photolyases have been produced by DNA recombinant technology using *E. coli* as host strain and biochemically characterized (Klar et al. 2006; Sancar and Sancar 2006; Scheerer et al. 2015; Su et al. 2015; Munshi et al. 2017). The UV11 recombinant CPD-photolyase was produced with high yield; 42 mg of proteins were obtained from 200 mL of growth culture and showed CPD-repairing activity as demonstrated by comet, HPLC and immunochemistry assays.

The recombinant CPD-photolyase from *Hymenobacter* sp. UV11 was fully active on CHO and human keratinocyte HaCat line cells as shown in Results. In a similar work, Decome et al. (2005) showed that the incubation of UVB-irradiated keratinocytes, in the culture medium, with 0.5% of a photolyase from the commercial product Photosome® (Applied Genetics) induced by 3.3-fold (70% activity) the reparation of CPD lesions. The activity was light dependent because it was observed after the irradiation with 1.2 J cm^{-2} UVA. Notwithstanding that these authors reported positive results, they did not report the composition of the liposome-photolyase preparation from Applied Genetics. In addition, when using photolyases from the *A. nidulans* plankton extracts, the presence of cyanobacterial lipopolysaccharide might induce various human diseases, such as allergy, or respiratory and skin diseases (Stewart et al. 2006). Interestingly, Vernhes et al. (2013) showed that a plant aqueous extract from the endemic Cuban plant, *Phyllanthus orbicularis* Kunth, protects against DNA lesions induced by UVB in human cells by modulation of the NER system. Otherwise, we are producing a photolyase enzymatic preparation that only co-purified with a molecular chaperone (GroEL) (which could be easily removed by size exclusion chromatography if needed), being free of cell debris, other proteins and/or potentially allergenic polysaccharides.

The CPD-repairing activity of the UV11 recombinant CPD-photolyase together with the high yield in the recombinant system suggests that this enzyme could potentially be included in cosmetic products. In addition, it could help to diminish the UVB-induced immunosuppression by restoring the immune competence to UV-irradiated antigen-presenting cells at the skin of patients with Xeroderma Pigmentosum (Stege 2001; Menck et al. 2007). Boros et al. (2013) designed a novel mRNA-based gene therapy method transfecting a lipofectamine-complexed mRNA expressing a photolyase from the marsupial *Potorous tridactylus* in the nuclei of keratinocytes. They found a significantly less amount of CPDs in those cells that were treated with photoreactivating light for activation of photolyase, and induction of IL-6 and inhibition of cell proliferation. This mRNA-based method sounds as a big opportunity for its future application in medicine, but currently the topical use of medical and cosmetic devises containing highly active photolyases might represent a more realistic approach.

Most information regarding photolyases came from the work performed by the Sancar's group, who shared the Nobel Prize in chemistry (2015) with Paul Modrich and Tomas Lindahl for their work on the mechanisms of DNA repair. Probably, photolyases from *A. nidulans* and *E. coli* are the most studied ones. They contain an 8-HDF and MTHF as light-harvesting chromophores, respectively, and have an entire photochemical reaction of ca. 1.2 ns (Tan et al. 2015). Kort et al. (2004) showed that the presence of the 8-HDF is not a prerequisite for the correct folding of the *A. nidulans* photolyase. However, when producing the enzyme by recombinant DNA technology, if *E. coli* is used as host cell factory which is unable to synthesize 8-HDF, the apoenzyme has to be obtained by reconstitution of the chromophore using synthetic 8-HDF (Kort et al. 2004). The inspection of putative metabolic pathways in the draft genome of *Hymenobacter* sp. UV11 (manuscript in preparation) suggested that this bacterium produces MTHF, but not 8-HDF. These results suggested that the recombinant UV11 photolyase could be produced as a fully active enzyme using *E. coli* as factory, without the need of the reconstitution of the antenna chromophore.

Hundreds of inventions related to the use of liposome-encapsulated photolyase from *A. nidulans*, obtained from plankton extract for cosmetic or dermatological uses, or in commercially relevant quantities from *E. coli* for academic purposes (patents and application numbers: US10459339, EP20050017347, US11399728, WO2014011611, KR0180684, US20090117060, CN103212066, CN101144088, CN103212066 CN105087535, CN105062999, CN103966193, CN201310731604, CN1624120 among many others) have been published. However, these inventions inform about the topical cosmetic compositions rather than the production of new photolyases. As far as we could check, the *A. nidulans* photolyase is the only one that has been produced for pharmaceutical and cosmetic uses.

Conclusions

Finally, in this work, we introduced the highly efficient and cost-effective recombinant production of a bacterial photolyase from the Antarctic isolate *Hymenobacter* sp. UV11 and showed its potential as DNA-repairing enzyme, using different approaches. The enzyme was easily produced in a low-cost growing host cell such as *Escherichia coli* and showed repairing activity of UV-induced DNA lesions in CHO and HaCat cell lines, but also in oligonucleotides and calf thymus DNA, showing activity on both double- and single-stranded DNA. We also found a storage condition that assures photolyase integrity and activity at least for 1 year. Our work shows evidence that probably will contribute to the development of new inventions with pharmaceutical and cosmetic applications.

Acknowledgements The authors thank the Uruguayan Antarctic Institute for the logistic support during the stay in the Antarctic Base Artigas. S. Castro-Sowinski, W. Martinez Lopez and J. J. Marizcurrena are members of the National Research System (SNI, Sistema Nacional de Investigadores). This work was partially supported by PEDECIBA (Programa de Desarrollo de las Ciencias Básicas), CSIC (Comisión Sectorial de Investigación Científica; Project C667), ANII (Agencia Nacional de Investigación e Innovación, Project FMV_3_2016_1_1226654) and donations by Celsius Laboratory (http://www.celsius.uy/). The work of JJM was supported by ANII and CAP (Comisión Académica de Posgrado, UdelaR).

Compliance with ethical standard

Conflict of interest The authors declare that they have no conflict of interest.

Ethical approval This article does not contain any studies with human participants or animals performed by any of the authors.

References

Berardesca E, Bertona M, Altabas K et al (2012) Reduced ultraviolet-induced DNA damage and apoptosis in human skin with topical application of a photolyase-containing DNA repair enzyme cream: clues to skin cancer prevention. Mol Med Rep. https://doi.org/10.3892/mmr.2011.673

Boros G, Miko E, Muramatsu H et al (2013) Transfection of pseudouridine-modified mRNA encoding CPD-photolyase leads to repair of DNA damage in human keratinocytes: a new approach with future therapeutic potential. J Photochem Photobiol B Biol. https://doi.org/10.1016/j.jphotobiol.2013.09.010

Boukamp P, Petrussevska RT, Breitkreutz D et al (1988) Normal keratinization in a spontaneously immortalized aneuploid human

keratinocyte cell line. J Cell Biol. https://doi.org/10.1083/jcb.106.3.761
Brettel K, Byrdin M (2010) Reaction mechanisms of DNA photolyase. Curr Opin Struct Biol. https://doi.org/10.1016/j.sbi.2010.07.003
Budden T, Bowden NA (2013) The role of altered nucleotide excision repair and UVB-induced DNA damage in melanomagenesis. Int J Mol Sci. https://doi.org/10.3390/ijms14011132
Decome L, De Méo M, Geffard A et al (2005) Evaluation of photolyase (Photosome®) repair activity in human keratinocytes after a single dose of ultraviolet B irradiation using the comet assay. J Photochem Photobiol B Biol. https://doi.org/10.1016/j.jphotobiol.2004.11.022
Dugo MA, Han F, Tchounwou PB (2012) Persistent polar depletion of stratospheric ozone and emergent mechanisms of ultraviolet radiation-mediated health dysregulation. Rev Environ Health. https://doi.org/10.1515/reveh-2012-0026
Eibenschutz L, Silipo V, De Simone P et al (2016) A 9-month, randomized, assessor-blinded, parallel-group study to evaluate clinical effects of film-forming medical devices containing photolyase and sun filters in the treatment of field cancerization compared with sunscreen in patients after successful photodynamic therapy for actinic keratosis. Br J Dermatol. https://doi.org/10.1111/bjd.14721
Graf D, Wesslowski J, Ma H et al (2015) Key amino acids in the bacterial (6–4) photolyase PhrB from Agrobacterium fabrum. PLoS ONE. https://doi.org/10.1371/journal.pone.0140955
Herrera LM, García-Laviña CX, Marizcurrena JJ et al (2017) Hydrolytic enzyme-producing microbes in the Antarctic oligochaete Grania sp. (Annelida). Polar Biol 40:947–953. https://doi.org/10.1007/s00300-016-2012-0
Klar T, Kaiser G, Hennecke U et al (2006) Natural and non-natural antenna chromophores in the DNA photolyase from Thermus Thermophilus. ChemBioChem. https://doi.org/10.1002/cbic.200600206
Kort R, Komori H, Adachi SI et al (2004) DNA apophotolyase from Anacystis nidulans: 1.8 Å structure, 8-HDF reconstitution and X-ray-induced FAD reduction. Acta Crystallogr Sect D Biol Crystallogr. https://doi.org/10.1107/s0907444904009321
Krutmann J, Berking C, Berneburg M et al (2015) New strategies in the prevention of Actinic Keratosis: a critical review. Skin Pharmacol Physiol. https://doi.org/10.1159/000437272
Laemmli UK (1970) Cleavage of structural proteins during the assembly of the head of bacteriophage T4. Nature. https://doi.org/10.1038/227680a0
Ma H, Zhang F, Ignatz E et al (2017) Divalent cations increase DNA repair activities of bacterial (6–4) photolyases. Photochem Photobiol. https://doi.org/10.1111/php.12698
Malvehy JSP (2014) Field cancerisation improvement with topical application of a film-forming medical device containing photolyase and UV filters in patients with Actinic Keratosis, a pilot study. J Clin Exp Dermatol Res 05:3. https://doi.org/10.4172/2155-9554.1000220
Marizcurrena JJ, Morel MA, Braña V et al (2017) Searching for novel photolyases in UVC-resistant Antarctic bacteria. Extremophiles 21:409–418. https://doi.org/10.1007/s00792-016-0914-y
Martinez-Rosales C, Fullana N, Musto H, Castro-Sowinski S (2012) Antarctic DNA moving forward: Genomic plasticity and biotechnological potential. FEMS Microbiol Lett. https://doi.org/10.1111/j.1574-6968.2012.02531.x
Martinez-Rosales C, Marizcurrena JJ, Iriarte A et al (2015) Characterizing proteases in an Antarctic Janthinobacterium sp. isolate: evidence of a protease horizontal gene transfer event. Adv Polar Sci 1:012. https://doi.org/10.13679/j.advps.2015.1.00088
Menck CFM, Armelini MG, Lima-Bessa KM (2007) On the search for skin gene therapy strategies of xeroderma pigmentosum disease. Curr Gene Ther 7:163–174
Morel MA, Braña V, Martínez-rosales C et al (2015) Five-year biomonitoring of aquatic ecosystems near Artigas Antarctic Scientific Base, King George Island. Adv Polar Sci 26:102–106. https://doi.org/10.13679/j.advps.2015.1.00102
Munshi S, Rajamoorthi A, Stanley RJ (2017) Characterization of a cold-adapted DNA photolyase from C. psychrerythraea 34H. Extremophiles. https://doi.org/10.1007/s00792-017-0953-z
Puck TT (1958) Genetics of somatic mammalian cells: iii. Long-term cultivation of euploid cells from human and animal subjects. J Exp Med. https://doi.org/10.1084/jem.108.6.945
Puig-Butillé JA, Malvehy J, Potrony M et al (2013) Role of CPI-17 in restoring skin homoeostasis in cutaneous field of cancerization: effects of topical application of a film-forming medical device containing photolyase and UV filters. Exp Dermatol. https://doi.org/10.1111/exd.12177
Sambrook J, Russell WD (2001) Molecular cloning: a laboratory manual. Cold Spring Harbour Lab Press, New york. https://doi.org/10.1016/0092-8674(90)90210-6
Sancar GB, Sancar A (2006) Purification and characterization of DNA photolyases. Methods Enzymol. https://doi.org/10.1016/S0076-6879(06)08009-8
Scheerer P, Zhang F, Kalms J et al (2015) The class III cyclobutane pyrimidine dimer photolyase structure reveals a new antenna chromophore binding site and alternative photoreduction pathways. J Biol Chem. https://doi.org/10.1074/jbc.M115.637868
Seebode C, Lehmann J, Emmert S (2016) Photocarcinogenesis and skin cancer prevention strategies. Anticancer Res. https://doi.org/10.21873/anticanres.12334
Stege H (2001) Effect of xenogenic repair enzymes on photoimmunology and photocarcinogenesis. J Photochem Photobiol B Biol. https://doi.org/10.1016/S1011-1344(01)00246-9
Stege H, Roza L, Vink AA et al (2000) Enzyme plus light therapy to repair DNA damage in ultraviolet-B-irradiated human skin. Proc Natl Acad Sci U S A. https://doi.org/10.1073/pnas.030528897
Stewart I, Schluter PJ, Shaw GR (2006) Cyanobacterial lipopolysaccharides and human health—a review. Environ Health. https://doi.org/10.1186/1476-069X-5-7
Studier FW (2005) Protein production by auto-induction in high-density shaking cultures. Protein Expr Purif. https://doi.org/10.1016/j.pep.2005.01.016
Su Z, Lian G, Mawatari K et al (2015) Identification and Purification of the CPD Photolyase in *Vibrio parahaemolyticus* RIMD2210633. Photochem Photobiol 91:1165–1172. https://doi.org/10.1111/php.12481
Tan C, Liu Z, Li J et al (2015) The molecular origin of high DNA-repair efficiency by photolyase. Nat Commun. https://doi.org/10.1038/ncomms8302
Tucci P, Veroli V, Señorale M, Marín M (2016) *Escherichia coli*: the leading model for the production of recombinant proteins. In: Microbial models: from environmental to industrial sustainability. pp 119–147
Vernhes M, González-Pumariega M, Andrade L et al (2013) Protective effect of a Phyllanthus orbicularis aqueous extract against UVB light in human cells. Pharm Biol. https://doi.org/10.3109/13880209.2012.695800
Wang J, Du X, Pan W et al (2015) Photoactivation of the cryptochrome/photolyase superfamily. J Photochem Photobiol C Photochem Rev. https://doi.org/10.1016/j.jphotochemrev.2014.12.001
Zhong D (2015) Electron transfer mechanisms of DNA repair by photolyase. Annu Rev Phys Chem. https://doi.org/10.1146/annurev-physchem-040513-103631

CAPÍTULO III

4. CARACTERIZACIÓN DEL GENOMA DE LA BACTERIA UV-RESISTENTE IDENTIFICADA COMO *SPHINGOMONAS* SP. UV9. PRODUCCIÓN RECOMBINANTE Y CARACTERIZACIÓN DE UNA FOTOLIASA BIFUNCIONAL

El trabajo se finalizó con la secuenciación y la búsqueda de fotoliasas del aislamiento que presentó la mayor capacidad fotorreparadora, *Sphingomonas* sp. UV9, así como la producción recombinante y la caracterización parcial de una de las fotoliasas producida por el mismo (Objetivo específico IV). Se presentan a continuación, los Materiales y Métodos, y los Resultados obtenidos en la forma de un trabajo publicado y otro enviado para su publicación.

4.1. Materiales y Métodos

4.1.1 Crecimiento y secuenciación del genoma

Se creció un cultivo de 3 mL de la cepa *Sphingomonas* sp. UV9 en medio TSA al 10%, y se incubó por 72 h y 200 rpm a 20 ^{o}C. Las células se sedimentaron por centrifugación a temperatura ambiente y 6000 rpm. La extracción genómica, el secuenciado, y la anotación se realizaron de la misma forma como se describió anteriormente para *Hymenobacter* sp. UV11.

Las secuencias codificantes (CDS) para las fotoliasas se identificaron por búsqueda en el genoma anotado, en las bases de datos de la NCBI y del RAST. Además, se buscaron otras secuencias de interés, según se verá en la sección Resultados.

4.1.2 Construcción y mantenimiento del vector de expresión

La secuencia codificante de la fotoliasa de Clase II de *Sphingomonas* sp. UV9 (Número de accseso del GenBank KX118298) se sintetizó con el servicio de Genscript como se describe para *Hymenobacter* sp UV11 (ver sección 3.2.2). El vector de expresión se denominó PhotoSphyngo_pET-28a (+) y la cepa recombinante de *Escherichia coli* BL21 (DE3) se denominó PhotoUV9. La cepa también se encuentra depositada bajo el mismo nombre en el Repositorio Internacional de Patentes de Valencia, España.

4.1.3 Producción, purificación y fotorreducción *in vitro* de la fotoliasa recombinante

La producción y purificación de la fotoliasa se realizó tal cual se describió para *Hymenobacter* sp. UV11 (Ver sección 3.2.3).

Para la fotorreducción *in vitro*, la enzima se incubó a 20 ^{o}C bajo condiciones aerobias hasta alcanzar el estado de máxima oxidación del FAD. Para ello, se realizó una solución de fotoliasa de 1 mg/mL en una cuba de 1 mL, y se colocó en un espectrofotómetro equipado con termostatizador a 20 ^{o}C. Luego se registraron espectros de absorción UV-Vis cada 10 min. La enzima se redujo con la adición de ditiotreitol (DTT) 10mM (99) y con irradiación continua durante 5 min con un LED azul (515 nm, FastGene Blue LED GelPic Imaging System).

4.1.4 Actividad fotoliasa. Detección de CPDs y 6,4-fotoproductos por immunoquímica

La sensibilización, incubación con los anticuerpos primarios y reparación con la fotoliasa, se realizaron de la misma manera que la descrita para *Hymenobacter* sp. UV11. Sin embargo, en esta sección se realizó una modificación del protocolo descrito en 3.2.6, como se describe a continuación. Luego de los lavados de los anticuerpos primarios, se realizó una incubación con una dilución 1/10000 (en tampón ¨Assay Diluent¨, parte del kit de Cosmobio)

del anticuerpo Anti-Ratón IgG–Peroxidasa producido en cabra (Sigma, A0168), durante 30 min a 37 °C. Se lavó cinco veces con tampón de lavado y se incubó con 100 µL de 3,3',5,5'-tetrametilbenzidina (TMB de ThermoFisher, Cat. No. 34028). La reacción se detuvo por la adición de 100 µL de H_2SO_4 2 M, en cada pocillo. El producto final resultante de color amarillo se detectó a 492 nm en un lector de placas Tecan (Infinite 200 PRO, Life Sciences). Los análisis estadísticos se realizaron con One-way ANOVA, con un valor $p < 0.05$.

4.1.5 Predicción de estructura, determinación de bolsillos y acoplamiento molecular

La estructura terciaria de la fotoliasa recombinante se predijo por modelado por homología utilizando el servidor del HHpred (81), utilizando como molde una CPD fotoliasa Clase II de la arquea *Methanosarcina mazei* (PDB ID: 1XRY). La visualización se realizó con el programa ¨Molecular Graphics System PyMOL¨ (número de registro 104107). El área y volumen de los bolsillos se determinaron con el servidor ¨computed atlas of surface topography of proteins¨, CASTp 3.0 (http://sts.bioe.uic.edu/castp/ (100)).

Para los estudios de acoplamiento (docking) molecular, se prepararon lo ligandos CPD y 6,4-FP a partir de los complejos de estructuras ADN-fotoliasa 2XRZ y 3CVU, respectivamente. Luego se realizaron ensayos de acoplamiento molecular en el sitio activo con el modelo de la fotoliasa recombinante. El acoplamiento molecular se realizó con Autodock4 utilizando una ¨grid box¨ de 20 Å, centrada en el sitio activo considerando el dominio α-hélice donde se da la unión al ADN. Se utilizó el algoritmo genérico de Lamarck (101). Las mejores conformaciones para cada ligando se ordenaron tomando en cuenta el criterio de energía de interacción de Autodock. Finalmente, las conformaciones se visualizaron con PyMOL 1.8.

4.2. Resultados

Ver artículos:

- Draft genome sequence of the UV-resistant Antarctic bacterium *Sphingomonas* sp. strain UV9
- A natural occurring bifunctional CPD/6,4-photolyase from the Antarctic bacterium *Sphingomonas* sp. UV9 (listo para enviar para su revision)

MANDALA

Se sembraron y se crecieron las bacterias del género *Sphingomonas* (naranja y amarillo).

AMERICAN SOCIETY FOR MICROBIOLOGY | Microbiology Resource Announcements

GENOME SEQUENCES

Draft Genome Sequence of the UV-Resistant Antarctic Bacterium *Sphingomonas* sp. Strain UV9

Juan J. Marizcurrena,[a] Danilo Morales,[a] Pablo Smircich,[b,c] Susana Castro-Sowinski[a,d]

[a]Section Biochemistry, Faculty of Sciences, Universidad de la República, Iguá, Montevideo, Uruguay
[b]Laboratory of Molecular Interactions, Faculty of Sciences, Universidad de la República, Iguá, Montevideo, Uruguay
[c]Department of Genomics, Instituto de Investigaciones Biológicas Clemente Estable, MEC, Montevideo, Uruguay
[d]Molecular Microbiology, Instituto de Investigaciones Biológicas Clemente Estable, MEC, Montevideo, Uruguay

ABSTRACT We report the draft genome sequence of the Antarctic UV-resistant bacterium *Sphingomonas* sp. strain UV9. The strain has a genome size of 4.25 Mb, a 65.62% GC content, and 3,879 protein-coding sequences. Among others, genes encoding the resolving of the DNA damage produced by the UV irradiation were identified.

Bacteria from the genus *Sphingomonas* are *Alphaproteobacteria* (family *Sphingomonadaceae*) with 127 described species. They are found in a broad range of environments, such as soils, fresh and marine waters, and plants, and in humans acting as opportunistic pathogens (1–6). *Sphingomonas* strains also colonize extreme environments, including Antarctica, volcano lakes, contaminated soils, and highly UV-irradiated places (6–8). They are Gram-negative, rod-shaped, chemoheterotrophic, strictly aerobic, and non-spore-forming bacteria (9).

This work reports the draft genome sequence of the UV-resistant bacterium *Sphingomonas* sp. strain UV9. The isolation and growth conditions for UV9 were previously described (7). Total DNA was extracted using the fungal/bacterial DNA miniprep purification kit (Zymo Research, catalog number D6005). The library preparation was performed using the Accel-NGS 2S PCR-free DNA library kit (Swift Biosciences, MI) and was sequenced at Macrogen using the HiSeq 2000/2500 technology platform with 101-bp paired-end read strategy. At least 13.7 million reads were obtained. Their quality was evaluated with FastQC (https://www.bioinformatics.babraham.ac.uk/projects/fastqc/) and assembled *de novo* using SPAdes (http://cab.spbu.ru/software/spades/) with the repeat resolution and mismatch correction settings enabled. The draft genome consists of ca. 4.25 Mb, including 62 contigs of above 1,000 bp, with a GC content of 65.62% and an N_{50} contig length of 1.26 Mb (L_{50} of 2 Mb) and 40× final coverage. The genome was annotated and the functions of genes were predicted and compared using the Rapid Annotations using Subsystems Technology (RAST) (10) and NCBI Prokaryotic Genome Annotation Pipeline (PGAP) servers. The predicted genes were functionally categorized using the SEED subsystems (11) at the RAST server. Proteins that conserve functional domains were identified using the NCBI conserved domain search service (CD-Search) (12).

The genome was predicted to have at least 3,879 protein-coding sequences (CDS) (1,274 were considered hypothetical, and 1,750 CDSs were classified into 209 subsystems), 50 tRNAs, 1 copy each of 23S rRNA-, 16S rRNA-, and 5S rRNA-encoding genes, and 86 pseudogenes. UV9 has the genomic information for the production of three photolyases, enzymes responsible for photorepairing the DNA damage caused by UV irradiation (13). These include two photolyases that repair the cyclobutane pyrimidine dimers (CPD-photolyase) and one that repairs 6,4 photoproducts (6,4-photolyase); both

Citation Marizcurrena JJ, Morales D, Smircich P, Castro-Sowinski S. 2019. Draft genome sequence of the UV-resistant Antarctic bacterium *Sphingomonas* sp. strain UV9. Microbiol Resour Announc 8:e01651-18. https://doi.org/10.1128/MRA.01651-18.

Editor John J. Dennehy, Queens College

Address correspondence to Susana Castro-Sowinski, scs@fcien.edu.uy.

J.J.M. and D.M. contributed equally to this work.

Received 10 December 2018
Accepted 23 January 2019
Published 14 February 2019

photoproducts halt RNA polymerase II during transcription or DNA polymerase during replication (14). These enzymes may have different functional antenna chromophores, 8-hydroxy-7,8-didemethyl-5-deazariboflavin (MTHF) and/or 6,7-dimethyl-8-ribityllumazine (DMRL), as the biosynthetic pathways were found. UV9 also shows a UvrABC system (14) (excinuclease ABC), as is found in the gamma radiation-resistant *Hymenobacter sedentarius* (15) and *Deinococcus swuensis* (16) bacteria, and an ATP-dependent DNA helicase UvrD/PcrA (essential during replication, recombination, and repair of UV damage) (17). It also contains a copy of the *radA* gene (which fills a gap using the information from the undamaged DNA strand) and the DNA mismatch repair proteins MutL/MutS (which identify and correct errors made during the replication). UV9 has genetic information for the synthesis of bacteriorhodopsin, a light-driven proton pump. Finally, UV9 harbors heavy metal resistance genes, including those for cobalt, zinc, cadmium, chromium, and arsenic, and employs the toxin-antitoxin system (RelEB and VapC), including specific proteases such as Lon, ClpXP, or ClpAP that commonly degrade the antidote (18). Thus, strain UV9 could be a model for studying bacterial UV resistance.

Data availability. This whole-genome shotgun project has been deposited at DDBJ/ENA/GenBank under the accession number SCIN00000000. The version described in this paper is version SCIN01000000.

ACKNOWLEDGMENTS

We thank the Uruguayan Antarctic Institute for logistical support during our stay in the Antarctic Base Artigas. S.C.-S., P.S., and J.J.M. are members of the National Research System (SNI [Sistema Nacional de Investigadores]).

This work was partially supported by PEDECIBA (Programa de Desarrollo de las Ciencias Básicas) and ANII (Agencia Nacional de Investigación e Innovación, project FMV_3_2016_1_1226654). The work of J.J.M. was supported by ANII and CAP (Comisión Académica de Posgrado, UdelaR).

REFERENCES

1. Leung KT, Chang YJ, Gan YD, Peacock A, Macnaughton SJ, Stephen JR, Burkhalter RS, Flemming CA, White DC. 1999. Detection of Sphingomonas spp in soil by PCR and sphingolipid biomarker analysis. J Ind Microbiol Biotechnol 23:252–260. https://doi.org/10.1038/sj.jim.2900677.
2. Asker D, Beppu T, Ueda K. 2007. Sphingomonas jaspsi sp. nov., a novel carotenoid-producing bacterium isolated from Misasa, Tottori, Japan. Int J Syst Evol Microbiol 57:1435–1441. https://doi.org/10.1099/ijs.0.64828-0.
3. Amato P, Parazols M, Sancelme M, Laj P, Mailhot G, Delort AM. 2007. Microorganisms isolated from the water phase of tropospheric clouds at the Puy de Dôme: major groups and growth abilities at low temperatures. FEMS Microbiol Ecol 59:242–254. https://doi.org/10.1111/j.1574-6941.2006.00199.x.
4. Khan AL, Waqas M, Kang SM, Al-Harrasi A, Hussain J, Al-Rawahi A, Al-Khiziri S, Ullah I, Ali L, Jung HY, Lee IJ. 2014. Bacterial endophyte Sphingomonas sp. LK11 produces gibberellins and IAA and promotes tomato plant growth. J Microbiol 52:689–695. https://doi.org/10.1007/s12275-014-4002-7.
5. Ryan MP, Adley CC. 2010. Sphingomonas paucimobilis: a persistent Gram-negative nosocomial infectious organism. J Hosp Infect 75:153–157. https://doi.org/10.1016/j.jhin.2010.03.007.
6. Farias ME, Revale S, Mancini E, Ordoñez O, Turjanski A, Cortez N, Vazquez MP. 2011. Genome sequence of Sphingomonas sp. S17, isolated from an alkaline, hyperarsenic, and hypersaline volcano-associated lake at high altitude in the Argentinean Puna. J Bacteriol 193:3686–3687. https://doi.org/10.1128/JB.05225-11.
7. Marizcurrena JJ, Morel MA, Braña V, Morales D, Martinez-López W, Castro-Sowinski S. 2017. Searching for novel photolyases in UVC-resistant Antarctic bacteria. Extremophiles 21:409–418. https://doi.org/10.1007/s00792-016-0914-y.
8. Merroun ML, Nedelkova M, Ojeda JJ, Reitz T, Fernández ML, Arias JM, Romero-González M, Selenska-Pobell S. 2011. Bio-precipitation of uranium by two bacterial isolates recovered from extreme environments as estimated by potentiometric titration, TEM and X-ray absorption spectroscopic analyses. J Hazard Mater 197:1–10. https://doi.org/10.1016/j.jhazmat.2011.09.049.
9. Brenner D, Krieg N, Staley J. 2005. Bergey's manual of systematic bacteriology, vol. 2: the proteobacteria, part C—the alpha-, beta-, delta-, and epsilonproteobacteria. Springer, New York, NY.
10. Aziz RK, Bartels D, Best A, DeJongh M, Disz T, Edwards RA, Formsma K, Gerdes S, Glass EM, Kubal M, Meyer F, Olsen GJ, Olson R, Osterman AL, Overbeek RA, McNeil LK, Paarmann D, Paczian T, Parrello B, Pusch GD, Reich C, Stevens R, Vassieva O, Vonstein V, Wilke A, Zagnitko O. 2008. The RAST server: Rapid Annotations using Subsystems Technology. BMC Genomics 9:75. https://doi.org/10.1186/1471-2164-9-75.
11. Overbeek R, Begley T, Butler RM, Choudhuri JV, Chuang HY, Cohoon M, de Crécy-Lagard V, Diaz N, Disz T, Edwards R, Fonstein M, Frank ED, Gerdes S, Glass EM, Goesmann A, Hanson A, Iwata-Reuyl D, Jensen R, Jamshidi N, Krause L, Kubal M, Larsen N, Linke B, McHardy AC, Meyer F, Neuweger H, Olsen G, Olson R, Osterman A, Portnoy V, Pusch GD, Rodionov DA, Rückert C, Steiner J, Stevens R, Thiele I, Vassieva O, Ye Y, Zagnitko O, Vonstein V. 2005. The subsystems approach to genome annotation and its use in the project to annotate 1000 genomes. Nucleic Acids Res 33:5691–5702. https://doi.org/10.1093/nar/gki866.
12. Marchler-Bauer A, Derbyshire MK, Gonzales NR, Lu S, Chitsaz F, Geer LY, Geer RC, He J, Gwadz M, Hurwitz DI, Lanczycki CJ, Lu F, Marchler GH, Song JS, Thanki N, Wang Z, Yamashita RA, Zhang D, Zheng C, Bryant SH. 2015. CDD: NCBI's conserved domain database. Nucleic Acids Res 43:D222–D226. https://doi.org/10.1093/nar/gku1221.
13. Sancar GB, Sancar A. 2006. Purification and characterization of DNA photolyases. Methods Enzymol 408:121–156. https://doi.org/10.1016/S0076-6879(06)08009-8.
14. Budden T, Bowden NA. 2013. The role of altered nucleotide excision repair and UVB-induced DNA damage in melanomagenesis. Int J Mol Sci 14:1132–1151. https://doi.org/10.3390/ijms14011132.
15. Kim MK, Kang MS, Srinivasan S, Lee DH, Lee SY, Jung HY. 2017. Complete genome sequence of Hymenobacter sedentarius DG5BT, a bacterium

resistant to gamma radiation. Mol Cell Toxicol 13:199–205. https://doi.org/10.1007/s13273-017-0021-x.
16. Kim MK, Srinivasan S, Back C-G, Joo ES, Lee S-Y, Jung H-Y. 2015. Complete genome sequence of Deinococcus swuensis, a bacterium resistant to radiation toxicity. Mol Cell Toxicol 11:315–321. https://doi.org/10.1007/s13273-015-0031-5.
17. Lee JY, Yang W. 2006. UvrD helicase unwinds DNA one base pair at a time by a two-part power stroke. Cell 127:1349–1360. https://doi.org/10.1016/j.cell.2006.10.049.
18. Buts L, Lah J, Dao-Thi MH, Wyns L, Loris R. 2005. Toxin-antitoxin modules as bacterial metabolic stress managers. Trends Biochem Sci 30:672–679. https://doi.org/10.1016/j.tibs.2005.10.004.

A natural occurring bifunctional CPD/6,4-photolyase from the Antarctic bacterium *Sphingomonas* sp. UV9

Juan José Marizcurrena[1], Silvina Acosta[2], Lucía Canclini[3], Paola Hernández[2], Tilman Lamparter[4], Susana Castro-Sowinski[1*].

From the [1] Biochemistry and Molecular Biology, Faculty of Sciences, University of the Republic. Iguá 4225, 11400, Montevideo, Uruguay; [2] Epigenetics and Genomics Instability Laboratory, Genetic Department, Institute Clemente Estable, Av. Italia 3318, 11600, Montevideo, Uruguay; [3] Genetic Department, Institute Clemente Estable, Av. Italia 3318, 11600, Montevideo, Uruguay; [4] Botanical Institute, Karlsruhe Institute for Technology, Fritz Haber Weg 4, 76131, Karlsruhe, Germany.

Running title: An Antarctic bifunctional CPD/6,4 photolyase

[*]To whom correspondence should be addressed: Susana Castro-Sowinski, Biochemistry and Molecular Biology, Faculty of Sciences, University of the Republic. Iguá 4225, 11400, Montevideo, Uruguay. Email: s.castro.sow@gmail.com

Keywords: Photolyase, Antarctica, Sphingomonas, DNA-damage, photo repair.

Abstract

Photolyases are flavoproteins that repair ultraviolet-induced DNA lesions (cyclobutane pyrimidine dimer or CPD, and pyrimidine (6,4) pyrimidone photoproducts or 6,4-PP), using blue light as an energy source. These enzymes are substrate specific, meaning that a specific photolyase repairs either a CPD or 6-4 photoproduct, but never both. In this work, we produced a Class II photolyase (called as PhrSph98) from the Antarctic bacterium *Sphingomonas* sp. UV9 by recombinant DNA technology and purified the enzyme using immobilized metal affinity chromatography. By using an immunochemistry assay, with monoclonal antibodies against CPD and 6,4-PP photoproducts, we found that PhrSph98 repairs both DNA lesions. The result was confirmed by immunocytochemistry using immortalized non-tumorigenic human keratinocytes (HaCaT). Results from structure prediction, pocket computation and molecular docking analyses showed that PhrSph98 has the two expected protein domains (light-harvesting antenna and a catalytic domain), a larger catalytic site as compared with photolyases produced by mesophilic organisms and that both substrates fit the catalytic domain. The results obtained from predicted homology modelling suggest that the electron transfer pathway may occur following this pathway: Y389-W369-W390-F376-W381/FAD. The evolutionary reconstruction of PhrSph98 suggests that this is a missing link that reflects the transition of 6,4 repair into the CPD repair for the Class II CPD-photolyases. To the best of our knowledge, this is the first report of a naturally occurring bifunctional, CPD and 6,4-PP repairing enzyme.

Light is a source of life, but also could become a source of death. Ultraviolet and visible light cover the range 100 – 400 nm (UVC, UVB and UVA) and 400 to 700 nm, respectively. The spectra required for the giving life photosynthesis phenomenon resides in the visible range. Meanwhile, the exposition to the UV spectra is a source of death due to the production of reactive oxygen species and DNA damage (1, 2). Among both, visible and UV lights (life and death) there are photolyases, enzymes defined as proteins involved in the repair of UV light-induced DNA damage (formation of cyclobutane pyrimidine dimer or CPD, and pyrimidine (6,4) pyrimidone photoproducts or 6,4-PPs).

Photolyases belong to the cryptochrome/photolyase family (CPF), a group of flavoproteins (containing FAD) that use blue light (380-500 nm) photons as an energy source to facilitate the repair of UV-

damaged DNA or to detect external light, respectively. The photolyases are classified according to the photoproduct they repair (CPD-photolyases or 6,4-photolyases). Based on sequence analyses and phylogenetic studies, CPD-photolyases are subdivided into three classes (I, II and III) and single-stranded DNA (ssDNA)-specific ones (3), whereas 6-4 photolyases are divided into eukaryotic and prokaryotic enzymes. Two groups of cryptochromes can be distinguished, the animal cryptochromes that are closely related to the eukaryotic 6-4 photolyases, and the plant cryptochromes that are related to the class III CPD photolyases. There are also several examples for photoreceptor and DNA repair dual function. a 6,4-photolyase (the PtCPF1 protein) from the marine diatom *Phaeodactylum tricornutum* also has activity as a transcriptional repressor of the circadian clock in mammalian cells (4). Another example is the cryptochrome from the green alga *Chlamydomonas reinhardtii* (the protein CraCRY) that additionally has, *in vivo* and *in vitro*, a function as a 6,4-photolyase (5). Recently, Dikbas et al (6) showed that the bacterium *Vibrio cholerae* produces a protein with cryptochrome and 6,4-photolyase activities.

Almost all photolyases have a second chromophore, an antenna chromophore, which can be MTHF (5,10-methenyl-tetrahydrofolate), DMRL (6,7-dimethyl-8-ribityllumazine) or 8-HDF (8-hydroxy-7,8-didemethyl-5-deazariboflavin) (7), whereas plant or animal cryptochromes have no antenna chromophore.

Photolyases have two different protein domains, an antenna domain that holds the chromophore which transfers energy by resonance to FAD, and the photolyase domain that binds FAD which is responsible for removing the UV-induced DNA lesion. The FAD is non-covalently attached at the active site in an unconventional U-shaped conformation and may exist in four different redox states: oxidized (FAD), anionic semiquinone ($FAD^{\bullet-}$), neutral semiquinone ($FADH^{\bullet}$) or anionic hydroquinone ($FADH^{-}$). The hydroquinone, is needed for the enzyme activity. After light absorption by the $FADH^{-}$, electron transfer occurs from an excited reduced and deprotonated $FADH^{-}$ to the flipped-out photolesion for its subsequently repair, and finally, the electron returns to the flavin cofactor to restore the enzyme activity (3). A triad of tryptophans, described first in *Escherichia coli* (Trp^{384}, Trp^{361} and Trp^{308}) is responsible for the electron transfer from the photoactivated reduced FAD to the protein surface. However, an additional fourth Trp and alternative pathways may be involved. Also, Tyr residues can function as electron transmitters in photoreduction. The alternative pathway proposed in *E. coli* includes the amino acids Trp^{384}, Trp^{318} and Trp^{367}, and probably a fourth tryptophan, Trp^{336}, establishing a tryptophan tetrad. Working with a PhrA, a class III CPD photolyase, Holub et al (8) showed that this photolyase uses both charge transfer pathways (triad or tetrad) starting from the same tryptophan and that the alternative pathway is active when the photoreduction of FAD, using the classical triad, is hindered.

It is difficult to bring the different groups of photolyases and cryptochromes in an evolutionary context. It is clear that plant cryptochromes and class III CPD photolyases are sister groups and that these cryptochromes have probably evolved from a common ancestor (9, 10). The animal cryptochromes have probably evolved from eukaryotic 6-4 photolyases. Many photolyases are widely distributed over many groups of organisms. The class II CPD photolyases, the focus of the present study, have been found in bacteria, archaea, various algae, land plants, fungi and animals (11–16). The group of prokaryotic 6-4 photolyases represents probably the most ancient group of photolyases, whereas the class II CPD photolyases stands at the base of all other photolyases and cryptochromes (i.e. plant and animal cryptochromes, class I and class III photolyases and DASH proteins).

This work aimed to perform the characterization of a Class II CPD-photolyase produced by the Antarctic bacterium *Sphingomonas* sp. UV9 (7, 17). We produced the enzyme using DNA recombinant technology and demonstrated that this enzyme has both CPD and 6,4-PP repair activities by immunochemistry and immunocytochemistry for the *in situ* detection of photolyase and DNA-damage. As previously reported, CPD- and 6,4-photolyases cannot repair both 6,4-PPs and CPDs, respectively. However, herein, we report a natural occurring bifunctional CPD/6,4-photolyase.

Results

The codon-optimized gene encoding the *Sphingomonas* sp. UV9 photolyase Class II was cloned into the pET28a (+) vector and expressed as a His-tagged protein in the *E. coli* strain BL21 (DE3) as described in Materials and Methods.

The protein was purified from the soluble fraction by immobilized metal affinity chromatography (IMAC). It was observed as a deep blue/grey protein adsorbed to the resin and as a bluish one in the eluate (**Figure 1A**). Quality control of purification was done by SDS-PAGE, showing that the eluted fraction (eluate) contains a protein with an apparent molecular weight of *c.a* 50 kDa, as expected for the photolyase. The protein was sliced from gel and its identity was verified by mass spectrometry (Maldi-ToF-MS/MS), showing molecular size of 54 kDa and a fragmentation pattern that confirmed the sequence. The enzyme yield was 70 mg of protein from a 200 mL culture. Since now, the photolyase was called PhrSph98.

As shown in Figures 1B and 1C, the full oxidation of PhrSph98 was reached after 140 min incubation at 20 °C under room condition (increased absorbance at 450 nm, fully oxidized FAD; reduced absorbance around 600 nm, probably the bluish semiquinone). The *in vitro* photoreduction of PhrSph98 was achieved after 5 min exposition to DTT and blue light. The spectra (**Figure 1B**) also suggest that recombinant PhrSph98 does not have an additional chromophore; this result was confirmed by analytical HPLC and RMN (data not shown).

The repair activity of the purified recombinant photolyase PhrSph98, was analyzed by immunochemistry assay using commercial monoclonal antibodies that recognize either CPDs or 6,4-PPs. The results showed that PhrSph98 is an active DNA repairing enzyme for both lesions, CPDs and 6,4-PPs (**Figure 2**). As CPD and 6,4 PP repair controls, PhrA photolyase from *Hymenobacter sp* and PhrB from *Agrobacterium tumefaciens*, were used. PhrA showed CPD activity and PhrB showed 6,4 PP activity, as previously reported.

We also performed *in vivo* eukaryotic DNA repair experiments by lipofection of recombinant His-tagged photolyase in a human immortalized keratinocyte cell line. Twenty-four hours after transfection, photolyase subcellular localization was analyzed by immunolocalization using an anti-His-tag antibody. As shown in **Figure 3**, a signal corresponding to PhrSph98 was found in the cytoplasm of HaCaT cells and also in the nucleus with a clear homogenous distribution. Specificity of antibody signal was validated using control cells (not transfected HaCaT cells), where anti-His-tag antibody signal was undetectable (**Figure 3,** inlet).

The possible cytotoxicity effect of lipofection, was analyzed by the resazurin method. HaCaT cell viability results (**Figure 4**) indicate that neither transfection mix (Tmix), PhrSph98 nor both together (PhrSph98 + Tmix) induce cytotoxicity after 24 h of treatment.

Afterward, we assessed the repair ability of PhrSph98 *in vivo*. We first showed that there is a UVC dose-dependent response for CPD formation at 10 and 20 J/m^2 **(Figure 5A)**, and we detected the formation of 6,4-PP at 10, 20 and 40 J/m^2 with no significant difference between them (**Figure 5B**). Thus, we used a dose of 10 and 20 J/m^2 UVC for the *in vivo* DNA photorepair experiments. Then, we evaluated the ability of PhrSph98 to reverse the DNA-damage induced by UVC irradiation in HaCaT cells. Compared with non-transfected cells, transfection of HaCaT cells with PhrSph98 reversed the formation of CPDs (35% and 55%) and 6,4-PP (9% and 24%) when cells were irradiated at 10 and 20 J/m^2, and incubated with blue light for 5 minutes, respectively (**Figure 6**).

Based on these results we wonder if the 3D structure of PhrSph98 may shed light on how this enzyme has both CPD and 6,4-PP repairing activity. Thus, the *in silico* structure of PhrSph98 was predicted and compared with previously reported structures from mesophilic photolyases (highest hits in Swiss-model server) as shown in **Table 1** and **Figure 7**. Results from **Table 1** show that all analyzed mesophilic photolyases have similar catalytic pocket area and volume; however, PhrSph98 displays a larger catalytic pocket (except for the Class III *A. tumefaciens* photolyase).

The closest match in homology modelling was found for the class II CPD photolyase from *Methanosarcina mazei* (PDB code: 2XRY) template. The PhrSph98 model was compared with

the 3D structure of 2XRY (**Figure 7A**). As expected, the PhrSph98 model matched well with 2XRY. Both domains displays a larger C-terminal domain involving α-helixes that buries the catalytic FAD cofactor and an N-terminal domain with a Rossmann-fold topology of α/β heterodimers, probably involved in the binding of the antenna (18). As shown in **Figure 7B**, PhrSph98 may have a semi-conserved triad/cofactor (involving the residues W388-W360-W381/FAD, homologous to those reported for *M. mazei* photolyase and other class II CPD photolyases). However, PhrSph98 has two tryptophans at the positions 369 and 390, and a methionine at the position 397 instead of the expected tryptophan. (**Figure 7B**). Therefore, tryptophan 381 could be involved in the electron transfer, resulting in a different pathway, as the distance from FAD is less than 5 Angstroms.

The results from the docking experiments are shown in **Figure 8**. The *in silico* experiments showed that both substrates successfully fitted the active site pocket with a binding energy of -6.17 kcal/mol and -5.25 kcal/mol for the CPD and the 6,4-PP, respectively. When PhrSph98 was modelled with the closest orthologous 6,4-photolyase from *Arabidopsis thaliana* (3FY4), the docking with the 6,4-PP reached a binding energy of -6.39 kcal/mol (data not shown). These results suggest that both types of lesions could bind in PhrSph98 pocket. The model (see **Figure 8C** and **8F**) predicts that both lesions may be positioned in the active catalytic form by the hydrophobic residues W314 (W305 in *M. mazei*), A430 (W421 in *M. mazei*) and the M388 (M378 in *M. mazei*). Based on (19), E310 and N384 (G375 in *M. mazei*) could also be involved in stabilizing the CPD radical after the electron transfer from the FADH•- and the anionic thymine radical after bond breakage, respectively. Similar changes (G to N) were also reported for plant. animal, and many bacterial Class II photolyases (12), but an asparagine at this position is characteristic in Class I photolyases.

Finally, we assessed the phylogenetic affiliation of PhrSph98 by performing an evolutionary study, using the curated sequences from photolyase and cryptochromes, as shown in **Figure 9**. The result show that our bifunctional photolyase is at the base of Class II photolyases, so suggesting that PhrSph98 may represent a transition protein between CPD- and 6.4-photolyases.

Discussion

Notwithstanding their similar structure and mechanism of action, CPD- and 6,4-photolyases are highly selective enzymes (CPD-photolyases repairs CPD, but not 6,4-PP, and vice versa). However, Yamada et al (20) achieved the functional conversion of the 6,4-photolyase from *Xenopus laevis* by triple mutagenesis. After certain amino acid changes (H354N, L355R, H358M) the protein was also able to repair CPDs. However, the reverse mutation of the three key amino acids did not transform the CPD-photolyase from *E. coli* into a 6,4-PP repairing enzyme. In this work, we report that the Antarctic bacterium *Sphingomonas* sp. UV9 produces a bifunctional photolyase, a naturally occurring CPD and 6,4-PP repairing enzyme. The genome from UV9 has the genomic information for the production of three photolyases (7, 17) and the recombinant photolyase from the Class II showed unexpected results. As shown by performing immunochemistry experiments, PhrSph98 repairs 50% and 20% of CPDs and 6,4-PPs lesions, respectively in 20 minutes, under the assay conditions.

An immunocytochemistry assay also supported the bifunctional activity of PhrSph98. HaCaT cell protein transfection with PhrSph98 showed that the enzyme reaches the nucleus and repairs both kinds of UV-induced lesions. In a pioneer work, Steurer et al (21) showed that lentiviral vectors expressing CPD- or 6,4-photolyases targeted with fluorescent proteins for direct visualization are mainly expressed in the nucleus, without interfering with NER activity. Experiments were performed by FRAP (fluorescence recovery after photo-bleaching) and showed that the photolyases specifically remove either CPD or 6,4-PP lesions. Our enzyme was produced carrying a His-tag for further purification, and the detection into the cell was facilitated using antibodies targeted to the His-tag. We showed that protein transfection, after treatment with lipofectamine, allows the entry of the PhrSph98 photolyase without a nuclear localization signal (NLS)(22–26).

A few reports inform about bifunctional photolyases with 6,4-PP repair and transcriptional

repressor of the circadian clock in mammalian cells activities (4), or 6,4-PP repair and cryptochrome activities (5, 6, 27, 28), or like Cry DASH that repairs CPDs and are also photoreceptors activity (10, 29). So, this is the first report of a bifunctional photolyase able to repair both 6,4-PP and CPD lesions. Based on these reports and the results showed in our work, we think that the common denominator in bifunctional photolyases is the 6,4-PP or CPD repair activity combined with the photoreceptor function. In addition, the work of Zhang et al (30) suggest that 6,4-photolyases branched at the base of the evolution of the Cryptochrome/Photolyase Family (CPF).
Otherwise, phylogenetic analyses suggested that animal and plant cryptochromes are more closely related to 6,4-photolyases and CPD-photolyases, respectively; thus, we wonder, where is the CPD/6,4-PP PhrSph98 photolyase evolutionary located?

The analyses of the protein sequence and phylogenetic studies showed that PhrSph98 is a member of the Class II CPD-photolyases. Our phylogenetic studies showed also that PhrSph98 stands at the base of the Class II photolyases. This finding was obtained with neighbor joining (Figure 9), maximum likelihood, and minimum evolution and parsimony algorithms and is therefore regarded as robust; note also the high bootstrap value at the relevant branches. In the presented tree, the clade of Class II photolyases forms a sister group of prokaryotic 6,4-photolyases and a clade including all other photolyases and cryptochromes. The clade of prokaryotic 6,4-photolyases, also termed FeS-BCP proteins, which are characterized by a specific iron sulfur cluster and other ancient features, is regarded as the most ancient clade of photolyases as discussed earlier (30). In our present phylogenetic studies, where we used slightly different selections of sequences and different algorithms, three different arrangements of clades are at the base of the tree: (i) the present situation as presented in Figure 9 (ii) Class II CPD-photolyases appeared as sister group of prokaryotic 6,4-photolyases and both together a sister group of the clade of all other groups, or (iii) prokaryotic 6,4-photolyases appeared as sister group of all photolyases and cryptochromes, including Class II CPD-photolyases. This pattern is in line with earlier studies and was especially found when PhrSph98 was excluded from the tree construction. Common to all these branch patterns is the positioning of prokaryotic 6,4-photolyases and Class II CPD-photolyases at the base of the evolution of all photolyases. The Class II CPD-photolyases must therefore be the second group in the evolution of photolyases and located at the base of the clade of iron-sulfur-cluster-free photolyases and cryptochromes. How did the transition of the ancient photolyases that were apparently repair enzymes of 6,4-PPs into CPD-photolyases take place? PhrSph98 with the dual function may be regarded as a missing link in this respect. It apparently reflects the transition of 6,4 repair into the CPD repair for the Class II CPD-photolyases. According to the phylogenetic trees, the transition of 6,4 repair into CPD repair must have occurred two more times, for the Cry-DASH proteins (which do repair CPH products) and the Class I + Class III CPD-photolyases. At present, PhrSph98 is the only dual functional photolyase among probably around 100 characterized different proteins. We would rather expect that such an enzyme would have an evolutionary advantage over specialized photolyases, who have to either work as partner in DNA repair or together with nucleotide excision repair.

The predicted 3D structure of PhrSph98 by homology modelling and molecular docking give us interesting information, such as the size of the catalytic pocket, the identification of relevant amino acids and the characteristic changes of this enzyme as compared with the closest related one. PhrSph98 displays a larger catalytic pocket as compared with photolyases produced by mesophilic organisms. This characteristic has been frequently reported for several psychrophilic or cold-adapted enzyme (31, 32). Could this huge catalytic pocket and the amino acids arrange exposed in this site explain the bifunctional activity shown by PhrSph98? In this regard, we performed a partial characterization of PhrSph98, including a protein alignment, the *in silico* 3D structure and docking with CPDs and 6,4-PPs. As reported by Kiontke (12), mutants in W388 in the photolyase from *M. mazei* still have high photoreduction activity, suggesting that the tyrosine residues Y345 and Y380 are potentially involved in electrons channeling. Thus, we propose that Y389 from PhrSph98 (Y380 in *M. mazei*; **Figure 7B**) is

involved in electron transfer. Other amino acids could be involved in the electron transfer, as shown in **Figure 7B** (see black arrows), but based on the predicted homology modelling and the evidence reported by Kiontke (12), we then propose the following electron transfer pathway Y389-W369-W390-F376-W381/FAD (**Figure 7C**). Future work will deal with site directed mutagenesis of catalytic amino acids.

Interestingly, no antenna chromophore seemed to bind to recombinant PhrSph98. This is in line with Kiontke et al (12) did not find the chromophore of *M. mazei* . These authors found later (33) that the photolyase from *M. mazei* binds 8-HDF, a deazaflavin cofactor which is present in prokaryotes but mostly limited to Archaeas, Actinobacterias and algae, and is not produced in the *E. coli* host that is used for protein expression. Regarding the biosynthetic pathways related to chromophore synthesis, *Sphingomonas* sp. UV9 lacks the genomic information that encodes the 8-HDF synthetase. Furthermore, PhrSph98 also lacks the conserved amino acids reported and needed for 8-HDF binding (33).

Our results suggest that the enzyme reaches nucleus and repair the UV-induced lesions; in this scenario, the following step from a biotechnological point of view is the development of a good formulation that addresses the delivery of the enzyme across the stratum corneum and then the cytoplasmic membranes into the cell. The experiments performed by Johnson et al (34) showed that the engineered DNA glycosylase (a DNA repairing enzyme) from Chlorella virus (Cv-pdg), when carrying a nuclear localization sequence and a membrane permeabilization peptide (TAT) delivers the enzyme to the nuclei of keratinocytes and fibroblasts, and to a human skin model. In addition, Cv-pdg rapidly initiated the removal of CPDs, as shown using immunoblot. This report encourages us to face the future engineering of PhrSph98 using the TAT signal and/or using nanoparticles.

Conclusion

In this work, we report the recombinant production and characterization of a bifunctional photolyase from the Antarctic bacterial isolate *Sphingomonas* sp. UV9, with both CPD and 6,4-PP repair activities. This enzyme repaired both lesions in *in vitro* and *in vivo* assays and its evolutionary reconstruction suggests that this is a missing link from 6,4- repair into the CPD repair for the Class II CPD-photolyases.

Experimental Procedures

Strains and culture conditions

Escherichia coli DH5α and BL21 (DE3) strains (both from Invitrogen, USA) were used for plasmid multiplication and for recombinant protein expression, respectively. Strains were maintained in Luria-Bertani (LB) broth and stored in 15% glycerol at -80 °C. For the photolyase recombinant production *E. coli* was grown in the auto-inductor Zym-5052 medium (35) as described below.

Construction and maintenance of the expression vector

The pET28a(+) expression vector containing the coding sequence for the Class II photolyase from *Sphingomonas* sp. UV9 (GenBank Accession Number KX118298) with a 6-His tag fused at the N-terminal was synthesized by GenScript (https://www.genscript.com/, USA). For enhanced expression, the codon adaptation index was optimized for *E. coli*. In order to maintain the expression vector, it was transformed to *E. coli* DH5α chemocompetent cells and grown on LB plates containing 50 μg mL^{-1} Kanamycin. For recombinant production of proteins, the expression vector was transformed to chemocompetent *E. coli* BL21 (DE3) cells. Chemocompetent cells were prepared by the calcium chloride protocol as described by Sambrook et al. (36). For *ex situ* microbial repository purpose in an International Patent Depository (Parc Científic Universitat de Valencia, Spain), under the 1977 Budapest Treaty on the International Recognition of the Deposit of Microorganisms, the expression vector was called PhotoSphyngo_pET-28a (+) and the recombinant strain was called *Escherichia coli* BL21 (DE3) strain PhotoUV9.

Production, purification and in vitro photoreduction of the recombinant photolyase

For the production of the recombinant protein, fresh 2 mL cultures of the recombinant strain were obtained by growth on liquid LB at 37 °C, then transfer to 200 mL auto-inductor Zym-5052

medium, containing 50 mg mL^{-1} of Kanamycin. Cultures were grown for 48 h at 14 °C and 220 rpm. Cells were harvested by centrifugation and suspended in 50 mM sodium phosphate buffer pH 8.0, supplemented with 30 mM NaCl, and lysed by sonication (40% amplitude, at a relative power output of 10). Lysates were clarified by centrifugation at 7000 g, 4 °C, 10 min). A second centrifugation step, at 16000 g, 4 °C for 30 min was performed in order to separate soluble (SF) and insoluble (IF; including inclusion bodies) fractions.

The recombinant photolyase was purified by immobilized metal affinity chromatography (IMAC). The SF was incubated with a Ni-NTA affinity resin (Invitrogen, R907) in binding buffer (50 mM phosphate buffer pH 8.0, 30 mM NaCl, 10 mM Imidazole) for 1 h at 4 °C. After washing, the recombinant protein was eluted with binding buffer containing 150 mM Imidazole. The eluate was desalted using a PD-10 column (GE Healthcare, 17-0851-01). All fractions were controlled by SDS-PAGE (37) and the identity of the recombinant protein was confirmed by mass spectrometry MALDI/TOF-TOF analysis at the Analytical Biochemistry and Proteomics Unit of the Institute Pasteur (Montevideo, Uruguay). Protein concentrations were determined by Bradford assay (Amresco, M172). The purified recombinant photolyase brought in PBS buffer supplemented with 50% glycerol and flash-frozen with liquid nitrogen at -80 °C.

For *in vitro* photoreduction, the enzyme was first incubated at 20 ºC under aerobic conditions until the full oxidation of FAD was reached (evaluated by recording the UV-Abs spectra every 10 min). Then, the enzyme was reduced by the addition of 10 mM dithiothreitol (DTT) and continuous irradiation with the FastGene Blue LED GelPic Imaging System, at 515 nm.

Photolyase in vitro DNA photorepair

The removal of both CPDs and 6,4-PPs was analyzed by immunochemistry experiments, using UVC-irradiated calf thymus DNA as a substrate and monoclonal antibodies from CosmoBio (CAC-NM-DND-001 and CAC-NM-DND-002, respectively). UVC-irradiated calf thymus DNA (10 Joules) samples were denatured by incubation at 100 °C for 10 min, followed by ice chilling for 15 min. DNA samples were fixed to protamine sulfate coated ELISA plates from CosmoBio (CSR-NM-MA-P001) Different concentrations of recombinant photolyase were loaded in the corresponding wells and the photorepair assay was done during 20 min under blue light at room temperature, using the FastGene Blue/Green LED GelPic Imaging System, array of blue/green LEDs, at 515 nm. As negative controls, experiments were also carried out in darkness. As positive controls, a CPD and a 6,4 photolyase from *Hymenobacter sp* and *Agrobacterium tumefaciens*, respectively, were used. Then, the photolyase was removed by washing with PBS-T, followed by the addition of 100 µL monoclonal antibodies diluted in PBS (1/1000 or 1/1500 fold dilutions of CPD or 6,4-PP antibodies per well, respectively) and incubation during 30 min at 37 ˚C. Wells were washed, and then incubated with a 1/10000 fold dilutions of Anti-Mouse IgG–Peroxidase antibody produced in goat (Sigma, A0168) for 30 min at 37 ˚C. Finally, wells were washed and incubated with 3,3',5,5'-tetramethylbenzidine (TMB from ThermoFisher, 34028). The reaction was stopped by H_2SO_4 addition. The final product was measured at 492 nm in a Tecan reader (Infinite 200 PRO, Life Sciences). Statistical analysis was performed using One-way ANOVA, with $p < 0.05$ considered significant.

Photolyase in vivo DNA photorepair

Cell culture and transfection

Immortalized human keratinocytes, HaCaT cells (38) were cultured in DMEM (Dulbecco´s Modified Eagle Medium) containing 10% FBS and 1% penicillin-streptomycin in a humidified incubator at 37 °C and 5% CO_2. Cells were grown on 12 mm coverslips for 24 h and then transfected with the recombinant His-tagged PhrSph98 photolyase with lipofectamine LTX (Invitrogen) transfection mix (lipofectamine LTX, Plus Reagent and Opti-MEM), during 24 h.

Cell viability

The effect of PhrSph98 on cell viability was done as follows: HaCaT cells were seeded in a 96 well plate ($1x10^4$ cells/well) during 24 h; then, the transfection mix and/or PhrSph98 was added in fresh culture medium, and after 24 h the cell viability was assessed by the resazurin method as we previously described (39). Results are shown as

percentage of cell viability as compared with the control without lipofectamine and photolyase (100%). Statistical analysis was performed using One-way ANOVA test and Dunnett's test, with $p < 0.05$ considered significant.

Dose-response UVC damage

HaCaT cells were grown in coverslips as described above, rinsed with PBS and exposed to UVC light (254 nm) at 10, 20 or 40 J/m^2, using a Spectroline lamp (model ENF-260C/FE). Non-irradiated control cells were included. Cells were immediately fixed with 4% paraformaldehyde and then treated with 2 M HCl for DNA denaturation. For photoproduct immunolocalization, cells were permeabilized, blocked and incubated with mouse monoclonal anti-CPD (1500-fold diluted, Cosmo Bio) or anti-6,4-PP (300-fold diluted, Cosmo Bio) overnight, at 4 °C. Samples were washed and incubated with secondary goat anti-mouse AlexaFluor-555 antibody (1000-fold diluted, Invitrogen) plus DAPI (300 nM, Invitrogen) rinsed and mounted with Prolong Glass (Invitrogen). Immunolabeled cells were visualized using a Zeiss LSM800 confocal microscope (Zeiss, Oberkochen, Germany), equipped with a Plan ApoN 63X oil NA 1.4 lens. The antibody signal was quantified using FIJI ImageJ software (40). The mean fluorescence intensity value was calculated and plotted on the graphs. Statistical analysis for photoproducts quantification experiments was performed using One-way ANOVA test and Tukey's test with $p < 0.05$ considered significant, and **** $p \leq 0.0001$.

Immunocytolocalization of PhrSph98

PhrSph98 transfected HaCaT cells were fixed in 4% paraformaldehyde. Cells were permeabilized, blocked and incubated with a mouse-monoclonal anti-His-tag antibody (500-fold diluted, GenScript) overnight at 4 °C. Then, samples were rinsed and incubated with secondary goat anti-mouse AlexaFluor-488 antibody (1000-fold diluted, Invitrogen) plus DAPI (300 nM). Finally, cells were rinsed, mounted and visualized as described above.

In vivo reparation assay

HaCaT cells were grown in coverslips as described above, and the DNA damage was achieved by UVC irradiation at 10 and 20 J/m^2. For photo-reactivation of PhrSph98, cells were slightly covered with HBSS (Hank's balanced salt solution) and placed 10 cm under a white-light lamp (Philips Essential LED 19W, 2300 lumen) for 5 min at 37 °C. Cells were fixed, and treated for photoproducts immunolocalization as was described in the "Dose-response UVC damage" section. Statistical analysis for DNA photorepair experiments was performed using Two-way ANOVA test and Bonferroni's test with $p < 0.05$ considered significant, ** $p \leq 0.01$ and **** $p \leq 0.0001$.

Structure prediction, pocket computation and molecular docking

Tertiary structure of the recombinant protein was predicted by homology modelling using the HHpred server (41) using the Class II CPD photolyase from *Methanosarcina mazei* (PDB ID: 1XRY) as template. Visualization was done using the Molecular Graphics System PyMOL (register number 104107). Pocket area and volume were calculated with the computed atlas of surface topography of proteins, CASTp 3.0 (42).

Molecular docking studies were done using CPD and 6,4-PP as ligands and prepared from the DNA-photolyase complexes 2XRZ and 3CVU, respectively. Then they were docked in the active site of the model from the recombinant protein. Docking was performed with Autodock4 using a grid box sized to 20 Å, centred in the active site comprehended in the α-helix DNA-binding domain, and the generic algorithm of Lamarck (43). The ten best conformations for each ligand were clustered, ranked on the interaction energy criterion by Autodock and visually analyzed using PyMOL 1.8 (44).

Acknowledgements. The authors thank the Uruguayan Antarctic Institute for the logistic support during the stay in the Antarctic Base Artigas. S. Castro-Sowinski, Lucia Canclini and J. J. Marizcurrena are members of the National Research System (SNI, Sistema Nacional de Investigadores). The patent was funded by ANII (Agencia Nacional de Investigación e Innovación, PAT_X_2017_1_140739) & CSIC

(Comisión Sectorial de Investigación Científica). This work was partially supported by PEDECIBA (Programa de Desarrollo de las Ciencias Básicas), CSIC (Project C667), ANII (Project FMV_3_2016_1_1226654), Comisón Honoraria de Lucha Contra el Cáncer and donations by Celsius Laboratory (http://www.celsius.uy/). The work of JJM was supported by ANII and CAP (Comisión Académica de Posgrado, UdelaR).

Conflict of interest: The authors declare that they have no conflicts of interest with the contents of this article.

References

1. Cadet, J., and Richard Wagner, J. (2013) DNA base damage by reactive oxygen species, oxidizing agents, and UV radiation. *Cold Spring Harb. Perspect. Biol.* 10.1101/cshperspect.a012559

2. Kulms, D., Zeise, E., Pöppelmann, B., and Schwarz, T. (2002) DNA damage, death receptor activation and reactive oxygen species contribute to ultraviolet radiation-induced apoptosis in an essential and independent way. *Oncogene*. 10.1038/sj.onc.1205743

3. Zhang, M., Wang, L., and Zhong, D. (2017) Photolyase: Dynamics and Mechanisms of Repair of Sun-Induced DNA Damage. *Photochem. Photobiol.* **93**, 78–92

4. Coesel, S., Mangogna, M., Ishikawa, T., Heijde, M., Rogato, A., Finazzi, G., Todo, T., Bowler, C., and Falciatore, A. (2009) Diatom PtCPF1 is a new cryptochrome/photolyase family member with DNA repair and transcription regulation activity. *EMBO Rep.* **10**, 655–661

5. Franz, S., Ignatz, E., Wenzel, S., Zielosko, H., Ngurah Putu, E. P. G., Maestre-Reyna, M., Tsai, M. D., Yamamoto, J., Mittag, M., and Essen, L. O. (2018) Structure of the bifunctional cryptochrome aCRY from Chlamydomonas reinhardtii. *Nucleic Acids Res.* 10.1093/nar/gky621

6. Dikbas, U. M., Tardu, M., Canturk, A., Gul, S., Ozcelik, G., Baris, I., Ozturk, N., and Kavakli, I. H. (2019) Identification and characterization of a new class of (6-4) photolyase from Vibrio cholerae . *Biochemistry*. 10.1021/acs.biochem.9b00766

7. Marizcurrena, J. J., Morel, M. A., Braña, V., Morales, D., Martinez-López, W., and Castro-Sowinski, S. (2017) Searching for novel photolyases in UVC-resistant Antarctic bacteria. *Extremophiles*. 10.1007/s00792-016-0914-y

8. Holub, D., Lamparter, T., Elstner, M., and Gillet, N. (2019) Biological relevance of charge transfer branching pathways in photolyases. *Phys. Chem. Chem. Phys.* 10.1039/c9cp01609k

9. Oliveri, P., Fortunato, A. E., Petrone, L., Ishikawa-Fujiwara, T., Kobayashi, Y., Todo, T., Antonova, O., Arboleda, E., Zantke, J., Tessmar-Raible, K., and Falciatore, A. (2014) The Cryptochrome/Photolyase Family in aquatic organisms. *Mar. Genomics*. **14**, 23–37

10. Selby, C. P., and Sancar, A. (2006) A cryptochrome/photolyase class of enzymes with single-stranded DNA-specific photolyase activity. *Proc. Natl. Acad. Sci. U. S. A.* 10.1073/pnas.0607993103

11. Slamovits, C. H., and Keeling, P. J. (2004) Class II photolyase in a microsporidian intracellular parasite. *J. Mol. Biol.* 10.1016/j.jmb.2004.06.032

12. Kiontke, S., Geisselbrecht, Y., Pokorny, R., Carell, T., Batschauer, A., and Essen, L. O. (2011) Crystal structures of an archaeal class II DNA photolyase and its complex with UV-damaged duplex DNA. *EMBO J.* 10.1038/emboj.2011.313

13. Petersen, J. L. (2001) A gene required for the novel activation of a class II DNA photolyase in

Chlamydomonas. *Nucleic Acids Res.* 10.1093/nar/29.21.4472

14. Kleiner, O., Butenandt, J., Carell, T., and Batschauer, A. (1999) Class II DNA photolyase from Arabidopsis thaliana contains FAD as a cofactor. *Eur. J. Biochem.* 10.1046/j.1432-1327.1999.00590.x

15. Hitomi, K., Arvai, A. S., Yamamoto, J., Hitomi, C., Teranishi, M., Hirouchi, T., Yamamoto, K., Iwai, S., Tainer, J. A., Hidema, J., and Getzoff, E. D. (2012) Eukaryotic class II cyclobutane pyrimidine dimer photolyase structure reveals basis for improved ultraviolet tolerance in plants. *J. Biol. Chem.* 10.1074/jbc.M111.244020

16. van Oers, M. M., Lampen, M. H., Bajek, M. I., Vlak, J. M., and Eker, A. P. M. (2008) Active DNA photolyase encoded by a baculovirus from the insect Chrysodeixis chalcites. *DNA Repair (Amst).* 10.1016/j.dnarep.2008.04.013

17. Marizcurrena, J. J., Morales, D., Smircich, P., and Castro-Sowinski, S. (2019) Draft Genome Sequence of the UV-Resistant Antarctic Bacterium Sphingomonas sp. Strain UV9 . *Microbiol. Resour. Announc.* 10.1128/mra.01651-18

18. Essen, L. O., and Klar, T. (2006) Light-driven DNA repair by photolyases. *Cell. Mol. Life Sci.* 10.1007/s00018-005-5447-y

19. Masson, F., Laino, T., Rothlisberger, U., and Hutter, J. (2009) A QM/MM investigation of thymine dimer radical anion splitting catalyzed by DNA photolyase. *ChemPhysChem*. **10**, 400–410

20. Yamada, D., Dokainish, H. M., Iwata, T., Yamamoto, J., Ishikawa, T., Todo, T., Iwai, S., Getzoff, E. D., Kitao, A., and Kandori, H. (2016) Functional Conversion of CPD and (6-4) Photolyases by Mutation. *Biochemistry*. 10.1021/acs.biochem.6b00361

21. Steurer, B., Turkyilmaz, Y., van Toorn, M., van Leeuwen, W., Escudero-Ferruz, P., and Marteijn, J. A. (2019) Fluorescently-labelled CPD and 6-4PP photolyases: new tools for live-cell DNA damage quantification and laser-assisted repair. *Nucleic Acids Res.* 10.1093/nar/gkz035

22. Kosugi, S., Hasebe, M., Tomita, M., and Yanagawa, H. (2009) Systematic identification of cell cycle-dependent yeast nucleocytoplasmic shuttling proteins by prediction of composite motifs. *Proc. Natl. Acad. Sci. U. S. A.* 10.1073/pnas.0900604106

23. Kosugi, S., Hasebe, M., Matsumura, N., Takashima, H., Miyamoto-Sato, E., Tomita, M., and Yanagawa, H. (2009) Six classes of nuclear localization signals specific to different binding grooves of importinα. *J. Biol. Chem.* 10.1074/jbc.M807017200

24. Kosugi, S., Hasebe, M., Entani, T., Takayama, S., Tomita, M., and Yanagawa, H. (2008) Design of Peptide Inhibitors for the Importin α/β Nuclear Import Pathway by Activity-Based Profiling. *Chem. Biol.* 10.1016/j.chembiol.2008.07.019

25. Brameier, M., Krings, A., and MacCallum, R. M. (2007) NucPred - Predicting nuclear localization of proteins. *Bioinformatics*. 10.1093/bioinformatics/btm066

26. Almagro Armenteros, J. J., Tsirigos, K. D., Sønderby, C. K., Petersen, T. N., Winther, O., Brunak, S., von Heijne, G., and Nielsen, H. (2019) SignalP 5.0 improves signal peptide predictions using deep neural networks. *Nat. Biotechnol.* 10.1038/s41587-019-0036-z

27. von Zadow, A., Ignatz, E., Pokorny, R., Essen, L. O., and Klug, G. (2016) Rhodobacter sphaeroides CryB is a bacterial cryptochrome with (6–4) photolyase activity. *FEBS J.* 10.1111/febs.13924

28. Ma, H., Holub, D., Gillet, N., Kaeser, G., Thoulass, K., Elstner, M., Krauß, N., and Lamparter, T.

(2019) Two aspartate residues close to the lesion binding site of Agrobacterium (6-4) photolyase are required for Mg2+ stimulation of DNA repair. *FEBS J.* 10.1111/febs.14770

29. Veluchamy, S., and Rollins, J. A. (2008) A CRY-DASH-type photolyase/cryptochrome from Sclerotinia sclerotiorum mediates minor UV-A-specific effects on development. *Fungal Genet. Biol.* **45**, 1265–1276

30. Zhang, F., Scheerer, P., Oberpichler, I., Lamparter, T., and Krauß, N. (2013) Crystal structure of a prokaryotic (6-4) photolyase with an Fe-S cluster and a 6,7-dimethyl-8-ribityllumazine antenna chromophore. *Proc. Natl. Acad. Sci. U. S. A.* 10.1073/pnas.1302377110

31. D'Amico, S., Claverie, P., Collins, T., Georlette, D., Gratia, E., Hoyoux, A., Meuwis, M. A., Feller, G., Gerday, C., Marahiel, M. A., Russell, R., Warren, G., and Davies, P. L. (2002) Molecular basis of cold adaptation. in *Philosophical Transactions of the Royal Society B: Biological Sciences*, 10.1098/rstb.2002.1105

32. Fullana, N., Braña, V., José Marizcurrena, J., Morales, D., Betton, J.-M., Marín, M., and Castro-Sowinski, S. (2017) Identification, recombinant production and partial biochemical characterization of an extracellular cold-active serine-metalloprotease from an Antarctic Pseudomonas isolate. *AIMS Bioeng.* **4**, 386–401

33. Kiontke, S., Gnau, P., Haselsberger, R., Batschauer, A., and Essen, L. O. (2014) Structural and evolutionary aspects of antenna chromophore usage by class II photolyases. *J. Biol. Chem.* **289**, 19659–19669

34. Johnson, J. L., Lowell, B. C., Ryabinina, O. P., Lloyd, R. S., and McCullough, A. K. (2011) TAT-mediated delivery of a DNA repair enzyme to skin cells rapidly initiates repair of UV-induced DNA damage. *J. Invest. Dermatol.* 10.1038/jid.2010.300

35. Studier, F. W. (2005) Protein production by auto-induction in high-density shaking cultures. *Protein Expr. Purif.* 10.1016/j.pep.2005.01.016

36. Sambrook, J., and W Russell, D. (2001) Molecular Cloning: A Laboratory Manual. *Cold Spring Harb. Lab. Press. Cold Spring Harb. NY.* 10.1016/0092-8674(90)90210-6

37. Laemmli, U. K. (1970) Cleavage of structural proteins during the assembly of the head of bacteriophage T4. *Nature*. 10.1038/227680a0

38. Boukamp, P., Petrussevska, R. T., Breitkreutz, D., Hornung, J., Markham, A., and Fusenig, N. E. (1988) Normal keratinization in a spontaneously immortalized aneuploid human keratinocyte cell line. *J. Cell Biol.* 10.1083/jcb.106.3.761

39. Pérez, F., Varela, M., Canclini, L., Acosta, S., Martínez-López, W., López, G. V., and Hernández, P. (2019) Furoxans and tocopherol analogs-furoxan hybrids as anticancer agents. *Anticancer. Drugs*. **30**, 330–338

40. Schindelin, J., Arganda-Carreras, I., Frise, E., Kaynig, V., Longair, M., Pietzsch, T., Preibisch, S., Rueden, C., Saalfeld, S., Schmid, B., Tinevez, J. Y., White, D. J., Hartenstein, V., Eliceiri, K., Tomancak, P., and Cardona, A. (2012) Fiji: An open-source platform for biological-image analysis. *Nat. Methods*. 10.1038/nmeth.2019

41. Zimmermann, L., Stephens, A., Nam, S. Z., Rau, D., Kübler, J., Lozajic, M., Gabler, F., Söding, J., Lupas, A. N., and Alva, V. (2018) A Completely Reimplemented MPI Bioinformatics Toolkit with a New HHpred Server at its Core. *J. Mol. Biol.* 10.1016/j.jmb.2017.12.007

42. Tian, W., Chen, C., Lei, X., Zhao, J., and Liang, J. (2018) CASTp 3.0: Computed atlas of surface

topography of proteins. *Nucleic Acids Res.* 10.1093/nar/gky473

43. Steffen, C., Thomas, K., Huniar, U., Hellweg, A., Rubner, O., and Schroer, A. (2010) AutoDock4 and AutoDockTools4: Automated Docking with Selective Receptor Flexibility. *J. Comput. Chem.* 10.1002/jcc

44. Schrödinger, L. (2015) The PyMol Molecular Graphics System, Versión 1.8. *Thomas Hold.* 10.1007/s13398-014-0173-7.2

45. Robert, X., and Gouet, P. (2014) Deciphering key features in protein structures with the new ENDscript server. *Nucleic Acids Res.* 10.1093/nar/gku316

46. Larkin, M. A., Blackshields, G., Brown, N. P., Chenna, R., Mcgettigan, P. A., McWilliam, H., Valentin, F., Wallace, I. M., Wilm, A., Lopez, R., Thompson, J. D., Gibson, T. J., and Higgins, D. G. (2007) Clustal W and Clustal X version 2.0. *Bioinformatics*. 10.1093/bioinformatics/btm404

47. Kumar, S., Stecher, G., and Tamura, K. (2016) MEGA7: Molecular Evolutionary Genetics Analysis Version 7.0 for Bigger Datasets. *Mol. Biol. Evol.* 10.1093/molbev/msw054

48. Hancock, J. M., Zvelebil, M. J., and Zvelebil, M. J. (2004) UniProt. in *Dictionary of Bioinformatics and Computational Biology*, 10.1002/9780471650126.dob0721.pub2

Table 1. Comparison of the catalytic pockets of PhrSph98 and different crystalized homologues, including bacteria, archaea, plants and animals photolyases. PDB accession numbers are giving in the ID column. Area and volume of pockets were calculated as described in Materials and Methods, using a probe radius of 1.4 Å.

Type	Organism	ID	Area	Volume
Class II	*Sphingomonas* sp.UV9		1140	655
	Methanosarcina mazei	2XRZ	626	536
	Oryza sativa	3UMV	589	508
Class I	*Escherichia coli*	1DNP	607	476
	Anacystis nidulans	1QNF	954	602
	Thermus thermophilus	1IQR	550	396
	Thermus thermophilus	2J09	572	397
Class III	*Agrobacterium tumefaciens*	4U63	983	639
6,4	*Arabidopsis thaliana*	3FY4	528	334
	Agrobacterium tumefaciens	4DJA	774	611
	Drosophila melanogaster	3CVY	683	561

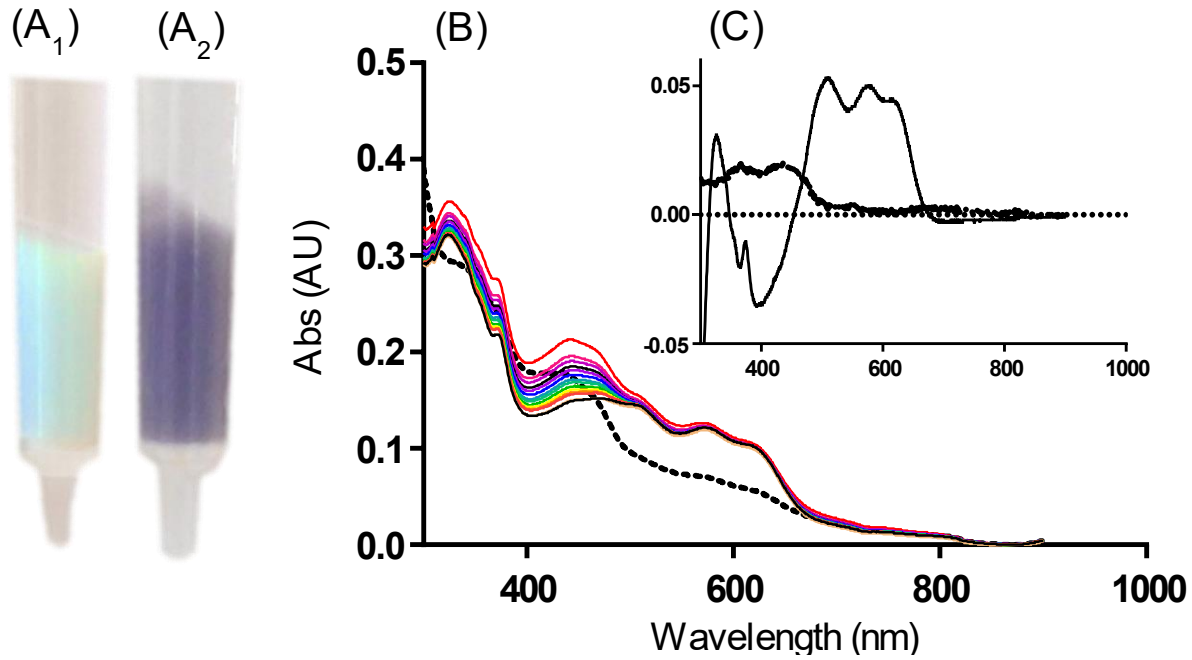

Figure 1. Protein purification and *in vitro* photoreduction. (A) Ni, shows the Ni-NTA resin before the loading of the soluble fraction (A1); Ni + PhrSph98, shows the blue/grey colour observed after the protein binding of the soluble fraction (A2). (B) Photoreduction of PhrSph98; the UV–vis spectra. The photolyase was placed under aerobic conditions to reach the oxidized enzyme (as seen by an increase in the 450 nm peak, corresponding to the oxidized FAD), and spectra where recorded in time. The dashed line shows the spectrum after photoreactivation (by addition of DTT and incubated with 5 min of blue light) of the most oxidized enzyme achieved, in order obtain the fully reduced enzyme. (C) Differential spectra (spectrum from the oxidized enzyme minus the spectrum from the photoreduced enzyme) at 10 min (continuous line) and 140 min (dotted line).

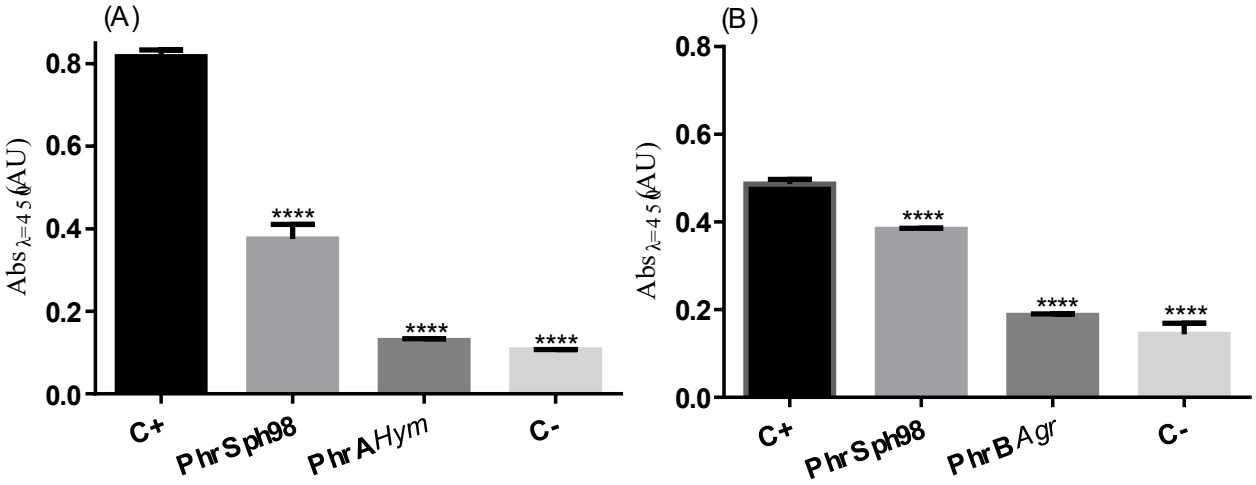

Figure 2. Determination of photolyase activity by immunochemistry assay. (A) CPD-photolyase activity and (B) 6,4-photolyase activity. Abbreviations are as follows: C-, non-irradiated calf thymus DNA (non-damaged DNA); C+, 10 Joules m^{-2} UVC-irradiated DNA (damaged DNA); PhrSph98, PhrA *Hym* and PhrB *Agr* correspond to the DNA-repair activity of 10 Joules m^{-2} UVC-irradiated DNA when using 1µg mL^{-1} recombinant photolyase from *Sphingomonas* sp. UV9, *Hymenobacter* sp. UV11 and *A. tumefaciens*, respectively, in the presence of blue light. Error bars shows the SD of the mean. Each assay was performed with 3 analytical replicates and 2 experimental replicates. Statistical analysis was performed using One-way ANOVA test and Dunnett's test, $p > 0.05$ and **** $p \leq 0.0001$.

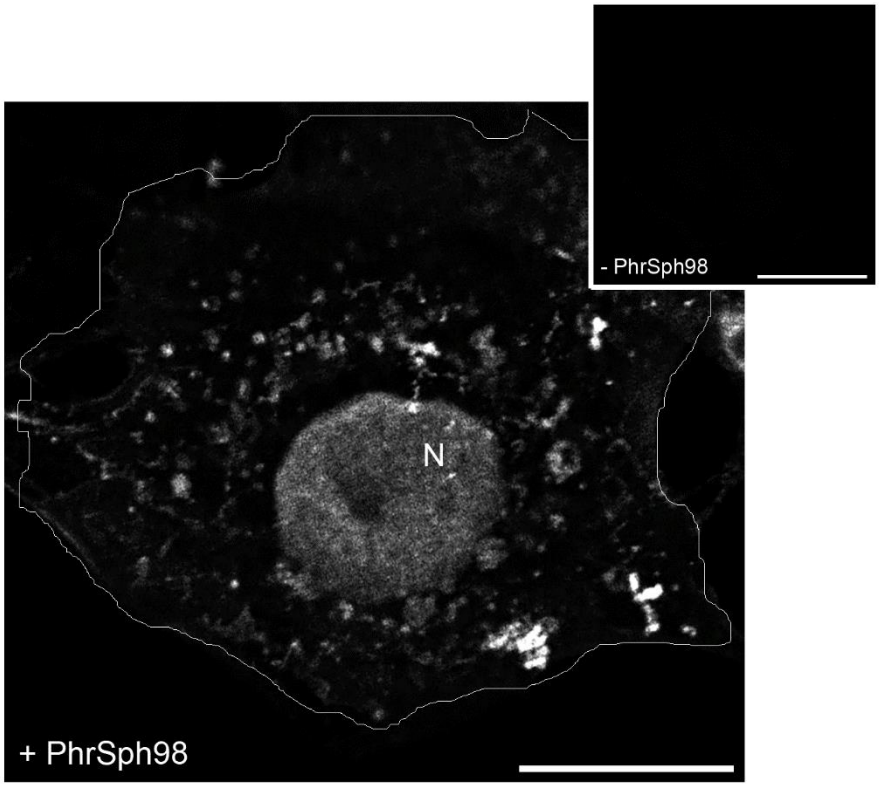

Figure 3. Subcellular localization of transfected-PhrSph98 photolyase. Representative images of HaCaT cells transfected (+ PhrSph98) and not transfected (- PhrSph98, inlet) with photolyase, analyzed by immunocytochemistry using an anti-His-tag antibody. N indicates nucleus. White line represents the cell boundary. Scale bar: 10 μm.

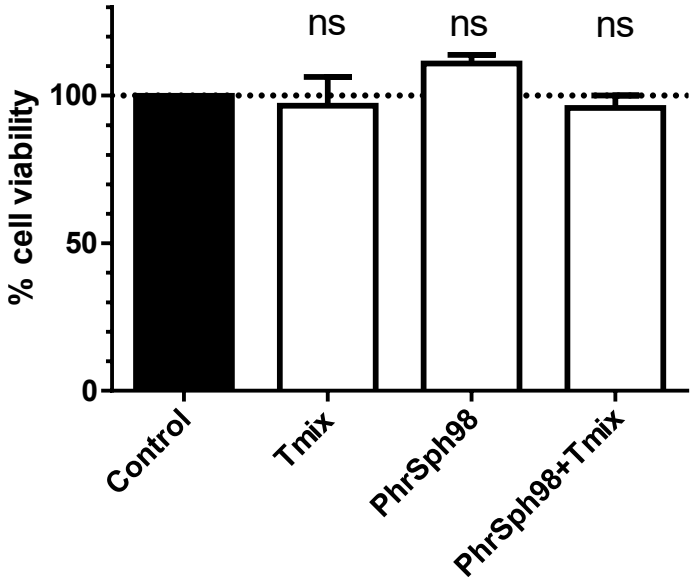

Figure 4. Transfected cell viability with resazurin. Percentage of HaCaT cell viability in presence of transfection mix reagents (Tmix), PhrSph98 or both together (PhrSph98+Tmix). Viability of control cells without treatment is set at 100%. Error bars shows the SD of the mean. N=16. Statistical analysis was performed using One-way ANOVA test, Dunnett's test with no significant difference (ns), $p > 0.05$.

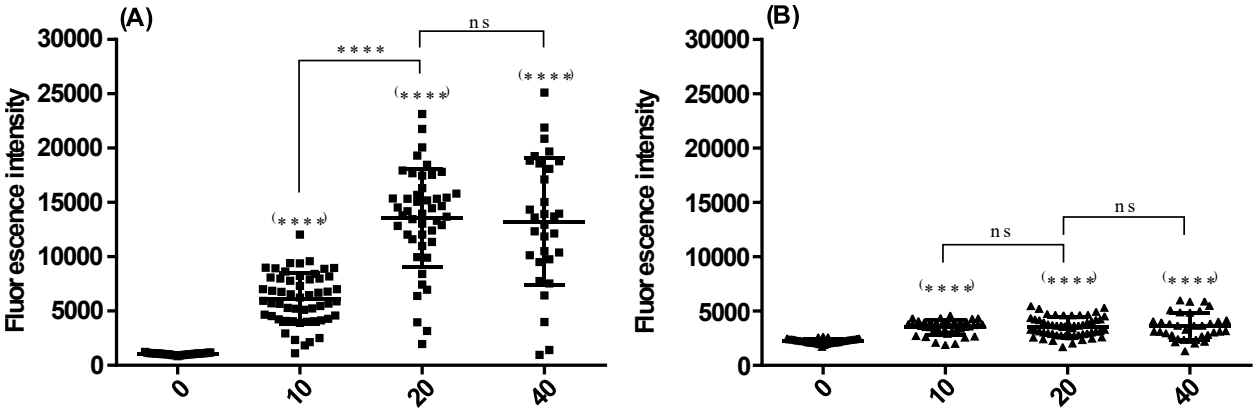

Figure 5. Induction of CPDs and 6,4 PP with UVC. (A) CPD and (B) 6,4-PP photoproducts quantification. Fluorescence intensity of anti-CPD (A) and anti-6,4-PP (B) in HaCaT cells plotted against UVC dose (0, 10, 20, 40 J m^{-2}). The horizontal bars show the media, and the vertical are the error bars corresponding the SD. Each dot represents a cell event. Statistical analysis was performed using One-way ANOVA test, Tukey's test with no significant difference (ns), $p > 0.05$ and **** $p \leq 0.0001$. p values in brackets indicates differences between each condition and the not irradiated control (0 J/m^2).

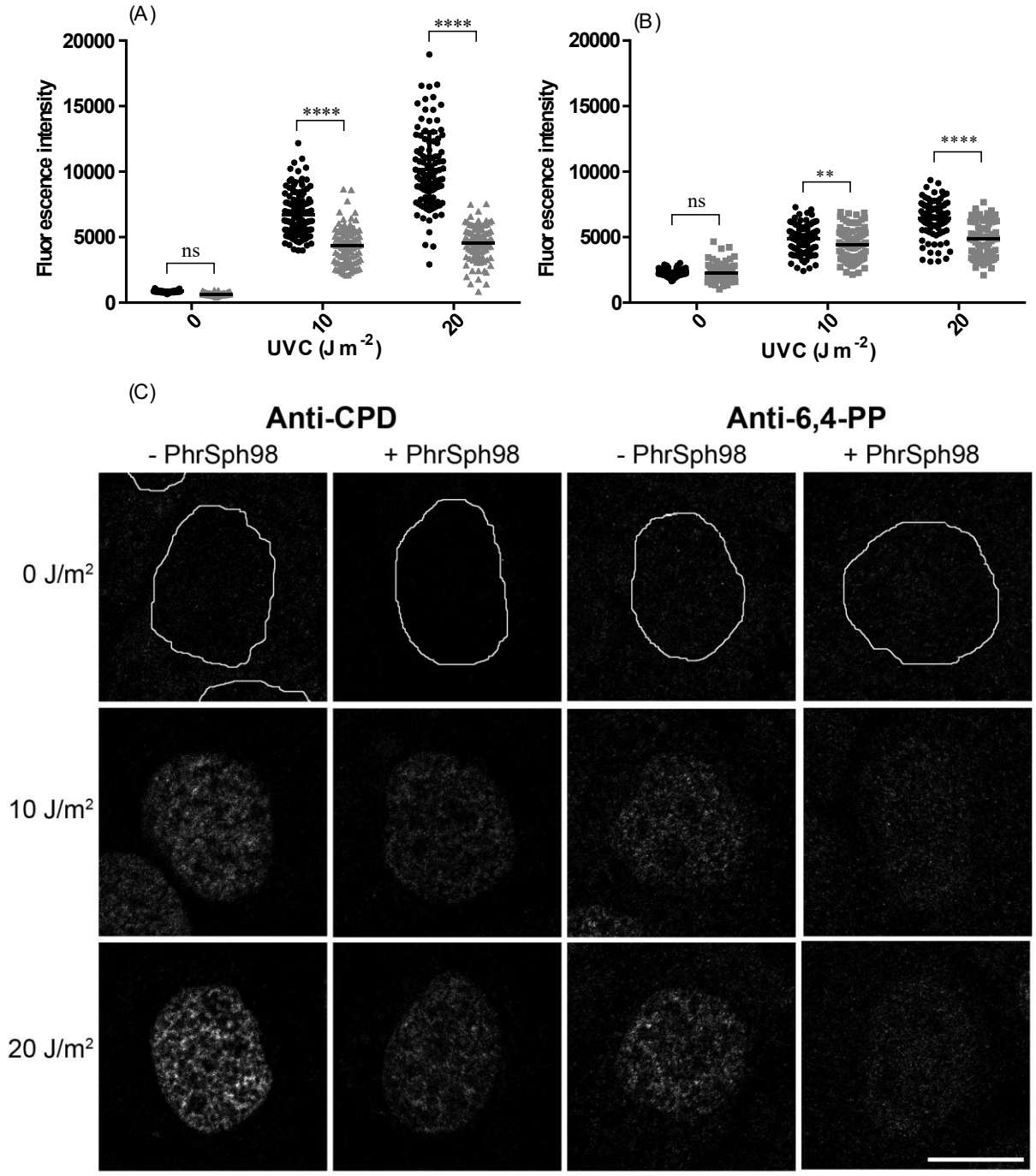

Figure 6. Quantification of CPD and 6,4-PP photoproducts in UVC-irradiated HaCaT cells. Fluorescence intensity of anti-CPD **(A)** and anti-6,4-PP (**B**) in cells treated with (+PhrSph98) or without (-PhrSph98) PhrSph98. The dose of UVC is shown. Each dot represent a cell event. Statistical analysis was performed using Two-way ANOVA test, Bonferroni's test with no significant difference (ns), $p > 0.05$, ** $p \leq 0.01$ and **** $p \leq 0.0001$. **(C)** Representative images of single focal planes of HaCaT cell nuclei from each experimental condition showed in A graphical view. Antibodies recognizing photoproducts (anti-CPD or anti-6,4-PP), transfection condition (+ PhrSph98 or - PhrSph98) and UV dose (0, 10 or 20 J/m^2) used are indicated. White lines represent nuclei boundary where it is not evident by antibody labelling. Scale bar: 10 μm.

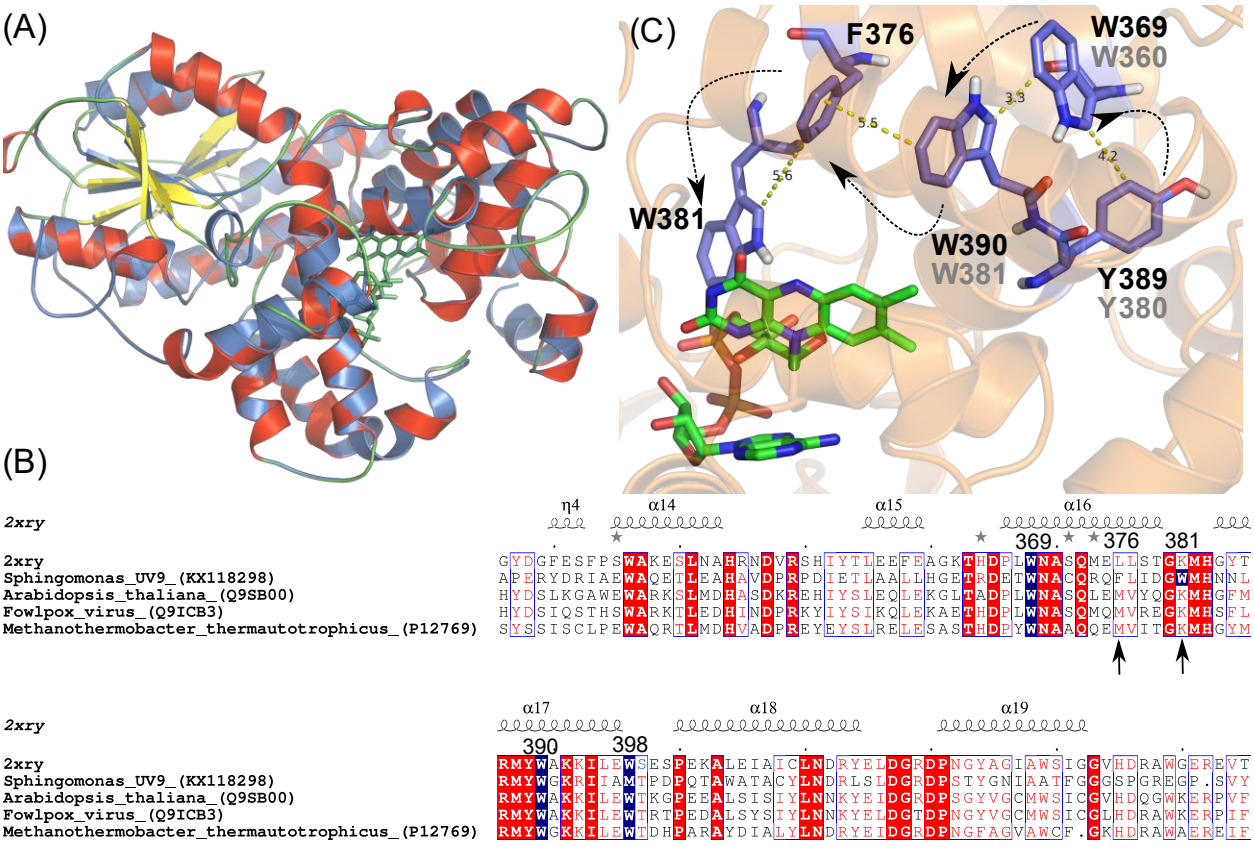

Figure 7. **(A)** Structure superimposition of PhrSph98 (shown in red-yellow) and *M. mazei* class II photolyase 2XRY (shown in blue). **(B)** Structure-based sequence alignment of PhrSph98 and *M. mazei* Class II photolyase 2XRY as a template for secondary structure elements identification. The alignment was done using ENDSCRIPT (http://endscript.ibcp.fr) (45) and included other well-known class II photolyases, such as *Arabidopsis thaliana* (Uniprot Q9SB00), Fowlpox virus (Uniprot Q9ICB3) and *Methanothermobacter thermoautrophicus* (Uniprot P12769). Highly conserved residues are highlighted in red and the conserved tryptophans, probably involved in the electron transfer pathway are shown in blue. Black arrows indicate aromatic amino acid residues that are only present in PhrSph98. These could be involved in the electron transfer pathway. **(C)** *In silico* proposed electron transfer pathway along with the aromatic compounds. The conserved tryptophans W381 and W360 from *M. mazei* (shown in grey) are also present in PhrSph98 (residues W369 and W390). The residue W388 from *M. mazei* was not found in PhrSph98. Aromatic amino acids such as Y389, F376 and the tryptophan W381 could also be involved in the electron transfer as a branch pathway.

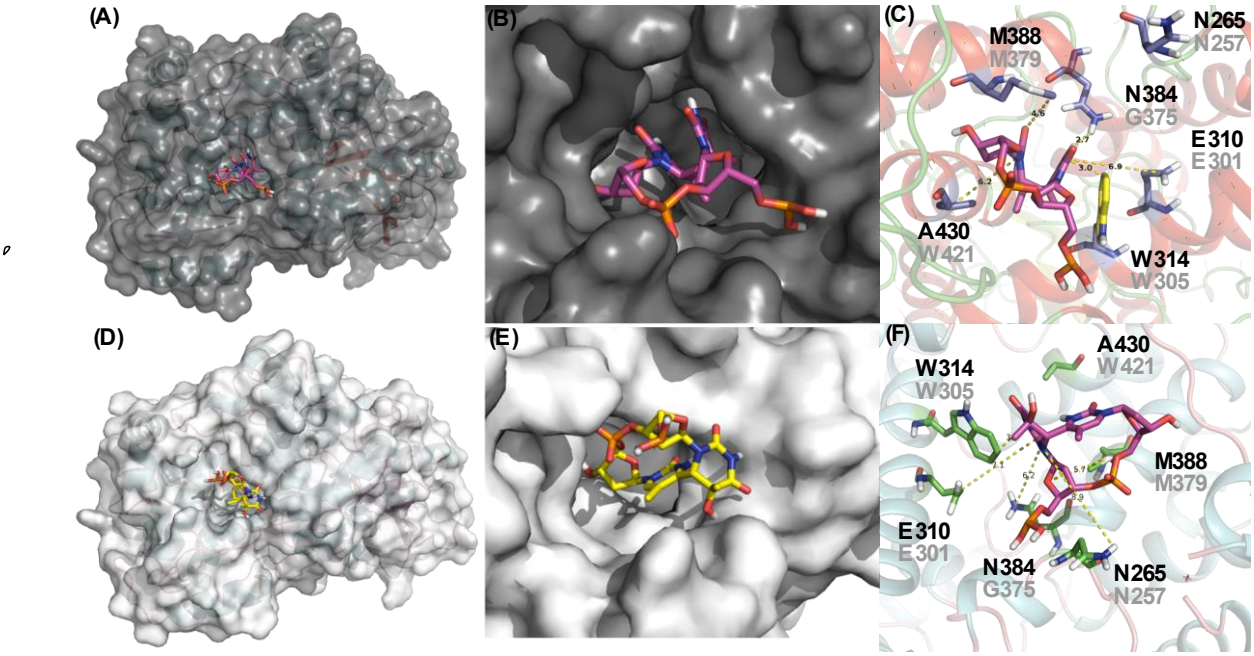

Figure 8. Substrate docking experiments. A) and B) show the docking with CPD. D) and E) show the docking with 6,4-PP. Positions of CPD or 6,4-PP, giving the best energy of binding are shown as sticks. C) and F) show a detailed view of the CPD and the 6,4 photo-lesions within the binding pocket and the amino acid residues involved in the enzyme-substrate interaction (shown in black). In grey are shown the corresponding residues from *M. mazei* CPDII (2XRZ) as reported by (12).

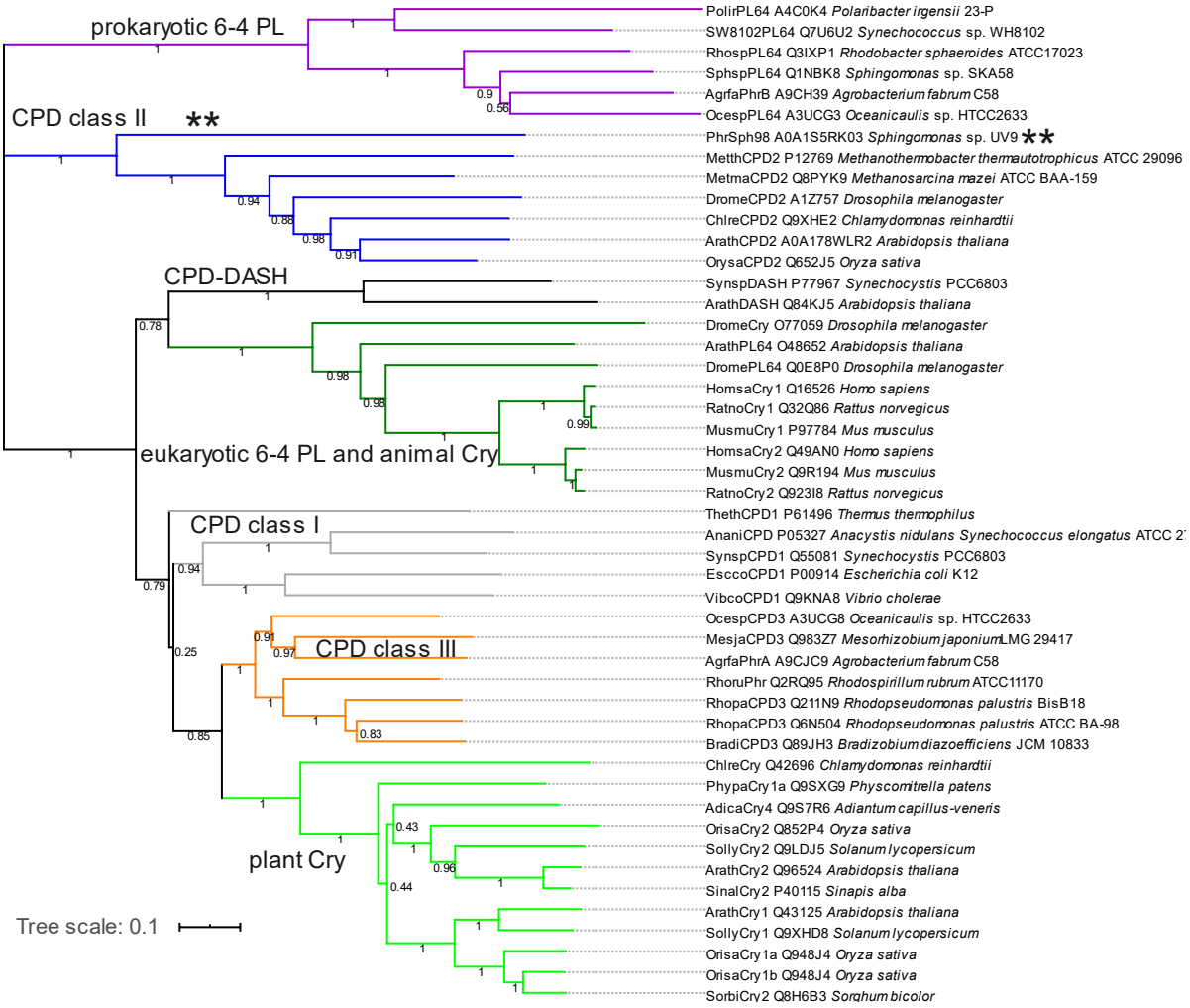

Figure 9. Photolyase and cryptochrome evolution, phylogenetic tree with selected protein sequences. The tree was generated after alignment with Clustal W (46) with the software package Mega-X (47) using the Neighbor Joining algorithm and 100 bootstrap cycles, bootstrap numbers (0-1) are given next to the branches. The proteins are most often denominated by 5 letter code for the species name followed by an abbreviation for the group to which the protein belongs. The protein abbreviation is followed by the Uniprot (48) identifier and the full name of the species or strain. CPD1, CPD2 and CPD3 stand for class I, class II and class III CPH photolyases, 6-4 PL stands for 6-4 photolyase, Cry stands for cryptochromes and CPD DASH stands for Cry-DASH proteins (which are also CPD photolyases). The double asterisks indicate the position of PhrSph98 in the text column and in the tree branches. Note that this is an unrooted tree and the evolutionary base is regarded at the top of the figure.

5. DISCUSIÓN GENERAL

Según la Wold Health Organization (apps.who.int/medicinedocs/en/d/Jh2996e/6.3.html), la bioprospección es "la búsqueda sistemática de nuevas fuentes de compuestos químicos, genes, microorganismos, macroorganismos y otros productos valiosos de la naturaleza. Implica la búsqueda de recursos genéticos y bioquímicos económicamente valiosos de la naturaleza." Curiosamente, la palabra bioprospección no existe en el diccionario de la Real Academia Española (RAE; https://www.rae.es/). En otras palabras, podemos entender la bioprospección como la búsqueda de nuevos o mejores bioproductos o procesos tecnológicos que provienen de fuentes biológicas. En particular, la bioprospección se basa en la provisión de un biorrecurso, como un suministro de biodiversidad novedosa.

Las moléculas derivadas de productos naturales, particularmente aquellas producidas por plantas y microorganismos, tienen un gran historial como fuente de material para el desarrollo de nuevos productos farmacéuticos. Muchos de los productos más valiosos para la industria farmacéutica son derivados directa o indirectamente de fuentes de productos naturales, como por ejemplo el ácido acetil salicílico, proveniente de corteza de sauce blanco, y la penicilina, proveniente del hongo *Penicillium*.

El repertorio de productos de origen microbiano que podemos aprovechar parece ser inagotable. Teniendo en cuenta que se estima que solo conocemos y podemos cultivar un 1% de la diversidad microbiana (102), la bioprospección de microorganismos cultivables se transforma en un gran reto. El descubrimiento y la evaluación de nuevos organismos que aún no se conocen sigue siendo un terreno fértil.

Los microorganismos representan el reservorio más grande de biodiversidad que aún resta por ser descrita, y por tanto posee un gran potencial para el descubrimiento de productos novedosos. Se estima que actualmente la Tierra alberga entre 3 y 30 millones de tipos de organismos. Entre ellos, solamente unos 1,4 millones se describieron por la ciencia (incluyendo aves y mamíferos). Se estima que existen unos 1-1,5 millones de especies de hongos, y entre estos solo 200.000 se encuentran caracterizados (aproximadamente un 13-20%). En bacterias este porcentaje es más bajo, donde se estima que se conocen apenas entre el 1 al 10% de las bacterias cultivables (103, 104).

Uno de los puntos a tener en cuenta al realizar bioprospección (de microorganismos cultivables, o siguiendo técnicas independientes del cultivo como es la metagenómica funcional) es la identificación de nichos de donde aislar microorganismos adaptados a situaciones particulares. En este sentido, ha sido de gran utilidad en el campo de la biotecnología la explotación y la búsqueda de microorganismos en nichos biológicos extremos, como una fuente de una microbiota con propiedades novedosa. Es aquí que podemos destacar a la Antártida, entre otros. La adaptación de los microorganismos al ambiente extremo antártico (baja temperatura, alta irradiación UV, baja disponibilidad de agua, ambiente oligotrófico, etc.), requiere de la adaptación de sus procesos celulares básicos para el crecimiento y la supervivencia en esas condiciones extremas. Estos procesos celulares pueden resumirse en tres categorías básicas: funcionamiento enzimático, transporte de nutrientes y funcionalidad de la membrana (105). Conocer estas adaptaciones de los procesos celulares es de gran interés, pues es en estas moléculas donde existe la novedad y el potencial de explotación biotecnológico.

Por ejemplo, las enzimas adaptadas al frío (enzimas sicrófilas; temperatura máxima de actividad en el entorno de los 40 °C, en comparación con las enzimas mesófilas que tienen

temperaturas máximas de actividad en el entorno de los 60 °C) (106, 107), confieren a los organismos la capacidad de sobrevivir a estos ambientes, y la catálisis a baja temperatura ha sido por lo tanto objeto de estudio con fines de aplicación en diferentes industrias (108). Las enzimas sicrófilas poseen diversas aplicaciones, incluyendo su agregado a detergentes (lavado en frio), procesamiento del cuero, y degradación de compuestos xenobióticos en climas fríos, procesamiento de la comida (fermentación, producción de quesos, panificación, ablandamiento de la carne durante el almacenamiento, entre otras) (109, 110). Específicamente, las enzimas sicrófilas tienen alta constante catalítica a temperaturas inferiores a los 40 °C y usualmente exhiben cierto grado de termolabilidad, lo cual puede ser una ventaja al momento de utilizarlas en procesos industriales donde un aumento de temperatura puede afectar el producto final o cuando se desea detener un proceso por solo un aumento moderado de la temperatura (107).

En los últimos años se han estudiado en mayor profundidad las características estructurales que podrían explicar las adaptaciones de estas enzimas. Por ejemplo, las estructuras terciarias y cuaternarias de las enzimas sicrófilas suelen exhibir mayor flexibilidad respecto a sus homólogas mesófilas, sobre todo a nivel de sus sitios catalíticos. En general estos son de mayor tamaño, lo que explica que tengan menor especificidad por su sustrato. Además, se conoce que las enzimas sicrófilas pierden su actividad antes de desnaturalizarse, lo cual explica su mayor termolabilidad (105, 111).

Sin embargo, la Antártida no se destaca solamente por las bajas temperaturas, sino que también es nicho de otro tipo de microorganismos extremófilos, los radiófilos (resistentes a las radiaciones). Estos son resistentes a altos niveles de radiación ionizante y ultravioleta. Los radiófilos son capaces de tolerar dosis de radiación inclusive 500 veces mayores a las que pueden tolerar los Humanos (112). Un buen ejemplo de radiófilo es la bacteria *Deinococcus*

radiodurans (113), que forma parte del libro de los récords Guinness como ¨la bacteria más dura del mundo¨. *D. radiodurans* posee una marcada resistencia a químicos, daño oxidativo y altos niveles de radiación y deshidratación (114). Esta bacteria posee un espectro de genes que codifican para proteínas involucradas en diferentes mecanismos de reparación del ADN dañado. Dentro de estos genes presentes en el genoma de *D. radiodurans* se encuentran diversas glicosilasas y el gen codificante para una fotoliasa (113).

Durante esta tesis, se eligió el ambiente antártico como nicho estratégico para el aislamiento de microorganismos resistentes a la irradiación UV (potenciales productores de fotoliasas novedosas), y creemos que nuestra estrategia fue acertada. Se identificaron un total de 12 microorganismos UVc-resistentes, con DL50 superiores a las reportadas en otros trabajos (75); siendo los géneros *Hymenobacter* y *Sphingomonas* los más importantes en términos de resistencia total y capacidad fotorreparadora.

De nuestra colección de microorganismos UVc-resistentes, el aislamiento *Hymenobacter* sp. UV11 fue quien mostró mayor resistencia frente a la radiación UVc. La secuenciación del genoma y la caracterización parcial del aislamiento permitió entender mejor las estrategias que posee este microorganismo para lidiar con el daño por UVc. Entre ellos se incluyen la producción de una CPD-fotoliasa, un sistema NER completo y ATPasas capaces de actuar removiendo las proteínas dañadas. También se identificó el pigmento que aporta su característico color rosado y que también podría conferirle resistencia tanto a UV, como a el frío, los ciclos de congelado y descongelado y al estrés oxidativo (115).

Mediante la secuenciación del genoma de UV11, se identificó el gen codificante de una CPD-fotoliasa, lo que permitió acceder a su secuencia codificante para luego expresarla en forma heteróloga. La fotoliasa se produjo con alto rendimiento, y se demostró su actividad mediante diferentes abordajes experimentales (116). Los resultados obtenidos respecto a la

caracterización de esta CPD-fotoliasa recombinante hablan de su potencial uso en la incorporación en productos médicos y cosméticos. Recordando los elementos expuestos en la Introducción de esta tesis, referente al cáncer de piel, esta enzima podría incorporarse en cremas junto con pantallas solares, para así obtener un producto con doble función, protectora ante el daño inducido por la radiación UV y reparadora del daño que no se pudo evitar. En este sentido, este trabajo contribuye al diseño de estrategias de prevención del cáncer de piel.

Por otra parte, el aislamiento *Sphingomonas* sp. UV9, presentó el mayor potencial fotorreparador, sugiriendo que en su genoma podrían estar codificadas posibles fotoliasas de alta eficiencia. La secuenciación de su genoma permitió la identificación de tres fotoliasas (75, 117). Entre ellas se encontraron dos CPD-fotoliasas (de Clase II y III), y una 6,4-fotoliasa. Durante esta tesis de produjo en forma recombinante y se caracterizó la CPD-fotoliasa de Clase II; hasta el momento solo hay reportes de la expresión heteróloga de una fotoliasa de Clase II, proveniente de la bacteria termófila *Methanosarcina mazei* (118, 119). Se logró la producción de una enzima activa, y con un alto rendimiento (resultados del Capítulo 3, presentado como manuscrito). Curiosamente, esta enzima mostró un resultado inesperado, la presencia de actividad reparadora de CPDs y de 6,4-FPs. Hasta el momento no existen reportes de fotoliasas con estas características; al día de hoy se habla de que las CPD-fotoliasas reparan los CPDs y no los 6,4-FP, y *viceversa* (120). La reconstrucción filogenética de esta fotoliasa muestra que la misma se encuentra en la base de la divergencia entre CPD- y 6,4-fotoliasas bacterianas (la enzima se encuentra posicionada en la base del grupo correspondiente a las fotoliasas de Clase II, siendo este grupo a su vez hermano de las 6,4-fotoliasas). Esto podría explicar el remanente de actividad reparadora de 6,4-FP. ¿Se trata de un eslabón perdido? Aún nos queda trabajo a realizar para demostrarlo.

Otra posible explicación es que la doble actividad pudiera estar relacionada a las posibles características sicrófilas de la enzima (tamaño del bolsillo catalítico o la flexibilidad) que le permitiese acoplar ambos sustratos (CPD y 6,4-FP). Los resultados del acoplamiento molecular realizados apoyan la idea de que esta enzima puede acomodar ambos sustratos. Contar con datos estructurales a través de la cristalización podría ayudar a entender mejor esta enzima, además de realizar estudios de actividad de la misma a bajas temperaturas para comprender su carácter sicrófilo. Nosotros sugerimos que ésta sería una fotoliasa recombinante bifuncional, con actividad reparadora de CPDs y 6,4-FPs.

¿Qué se conoce de las 6,4-fotoliasas bacterianas? La respuesta es: muy poco. El grupo del Dr. Lamparter (121) produjo en forma recombinante y caracterizó la que sería la 6,4-fotoliasa más estudiada, la que produce *Agrobacterium tumefaciens* (97–99, 121–123). También existe un reporte sobre una 6,4-fotoliasa Antártica recombinante, pero proveniente de hongos (124). El estudio de 6,4-fotoliasas bacterias de origen antártico, todavía son más escasos. Así que creemos que el estudio de las fotoliasas provenientes de microorganismos adaptados al frío podrían proveer de información que permitiera entender mejor cómo funcionan estas enzimas y como se relacionan evolutivamente con sus homólogas producidas por organismos mesófilos.

Estos resultados derivaron en la presentación de una patente provisional (No 62726780 – Genetically modified bacteria producing two DNA repair enzymes and method for the evaluation of DNA repair activity) y actualmente se encuentra en trámite la PCT (Patent Cooperation Treaty; procedimiento único de solicitud de patentes para proteger las invenciones en todos los países miembros). Entre las patentes actualmente disponibles se encuentra la producción y usos de fotoliasas provenientes de *A. nidulans* (patente 0423214A), así como de formulaciones que la incluyen (WO 2014011611 A1). También se ha patentado

el uso de fotoliasa para el tratamiento de determinadas enfermedades, como es el caso de la queratosis actínica (patente WO2012168401 A1). Es interesante destacar que la fotoliasa de *A. nidulans*, posee un segundo cromóforo tipo 8-HDF. *E. coli* no produce este metabolito, motivo por el cual, luego de la expresión heteróloga de esta enzima, es necesario suplementarla con este metabolito, y así obtener la enzima en forma activa. En nuestro caso, las fotoliasas que producimos en *E. coli* no requieren del agregado de cofactores para su actividad luego de la producción recombinante. Además, producimos estas enzimas en forma muy económica y con alto rendimiento (42 y 70 mg totales de un cultivo proveniente de 200 mL, para la CPD-fotoliasa y fotoliasa bifuncional, respectivamente). Existen empresas que comercializan la fotoliasa recombinante de *A. nidulans* (https://www.mybiosource.com/search/photolyase, (125)), utilizando diferentes hospederos, con un costo elevado (USD 1725 por mg) y sin garantizar la actividad de la misma, con fines académicos. Así que creemos que vamos por un buen camino y podremos ofrecer un producto de bajo costo y alta capacidad reparadora del daño al ADN.

¿Cuál es la factibilidad de producir un desarrollo comercializable agregando fotoliasas, y cuál sería su valor comercial? Existen varios productos en el mercado conteniendo fotoliasas, tanto nacionales como internacionales. A nivel nacional, para la producción de DermADN, Dermur (Celsius) importa una fotoliasa comercial con un costo que supera los 5000 dólares por mg de producto no purificado y que proviene directamente del microorganismo *Anacystis nidulans*. Las fotoliasas producidas en nuestro laboratorio, podrían abaratar los costos de producción de la crema, además de que se estandarizaría el proceso de producción y purificación de la fotoliasa, asegurando la ausencia de contaminantes provenientes de los extractos celulares, que en algunos casos podrían llegar a ser inmunogénicos (116).

Además, la enzima podría luego ser comercializada a nivel internacional. Por ejemplo, la crema Eryfotona AK-NMSC de la empresa ISDYN, contiene fotoliasas en forma de ¨repairsomes¨(126), es de aplicación tópica y se utiliza en el tratamiento de pacientes con queratosis actínicas y cáncer de tipo no melanoma (126). Por otro lado, los fotoprotectores actualmente disponibles en el mercado incorporan fotoliasas capaces de reparar los CPDs, pero no incluyen las enzimas encargadas de reparar los 6,4-FPs. Si bien la formación de los 6,4-FPs representa un 25% del daño en comparación con CPDs (son minoritarios), los estudios recientes muestran que los efectos de los 6,4-FP podrían ser más nocivos que los CPDs.

Una característica química de la formación de un 6,4-FP es que genera un nuevo pico de absorción del ADN a los 320 nm (asociado a la presencia del cromóforo; 5-metil-2-pirimidona). En este contexto, parece factible que la generación del cromofóro de pirimidona dentro de la doble hebra pueda comportarse como un potencial sensibilizador endógeno capaz de absorber energía en el rango UV. Los 6,4-FPs pueden actuar entonces como un caballo de troya, extendiendo el espectro lumínico que genera daño y por lo tanto agravando sus efectos dañinos (127). Por otro lado, un problema que enfrenta el NER durante la reparación de los 6,4-FPs es el reconocimiento del daño por el factor de iniciación UV-DDB (UV-damaged DNA-binding protein complex; quien reconoce la lesión e inicia el mecanismo NER). Las lesiones se reconocen a través de un mecanismo de ‘base flipping’ (arrastre de la base hacia el sitio activo donde se repara), y como el ADN genómico está principalmente asociado a los nucleosomas, el arrastre del 6,4-FP resulta complejo, especialmente si el daño se encuentra en la hebra que contacta con la superficie de la histona (128). Nosotros logramos determinar que al menos la fotoliasa bifuncional recombinante es capaz de resolver ambos tipos de daño en ensayos de citoinmunoquímica, sugiriendo que esta enzima podría ser

efectiva *in vivo*. Faltarían hacer ensayos en piel, y asegurarse que la enzima atraviese el estrato corneo, estudios que serán objeto de trabajos futuros.

Es por eso que los 6,4-FP, si bien son menos abundantes que los CPDs, deberían ser igual o mayormente considerados al momento de valorar el efecto dañino de la irradiación UV, y por tanto resulta de vital importancia un tratamiento sinérgico (reparación de CPDs y 6,4-FP) al momento de reparar las lesiones al ADN luego de la exposición solar, tanto en personas sanas como en aquellas que presentan hipersensibilidad a la radiación UV, motivo por el cual se ha despertado el interés por este tipo de enzimas, a nivel clínico y cosmético.

Además del cáncer de piel, algunas enfermedades genéticas como el xeroderma pigmentosum, tricotiodistrofia y el síndrome de Cockayne están asociadas a los defectos de reparación de los fotoproductos por parte del NER. Para el caso de la formación de los CPDs, se ha demostrado que ratones transgénicos que expresan una CPD-fotoliasa de marsupiales y una 6,4-fotoliasa de plantas presentan una alta resistencia a los efectos causados por la irradiación UV, tales como las quemaduras solares (eritema), hiperplasia epidérmica y apoptosis (129). Aún más importante, la expresión de estas fotoliasas suprimió la formación de carcinomas en la piel. Por supuesto, estamos muy lejos de pensar en Humanos transgénicos.

Por todo lo anteriormente mencionado, creemos que el desarrollo de una formulación conteniendo fotoliasas capaces de remover los CPDs y los 6,4-FPs sería de gran relevancia para la industria médica y cosmética.

6. CONCLUSIONES

Los resultados muestran que el nicho Antártico alberga un grupo diverso de bacterias resistentes a la radiación ultravioleta y que es una fuente de material genético para la identificación de genes codificantes para fotoliasas. La caracterización y secuenciación de los organismos con mayor resistencia y capacidad fotorreparadora, permitieron la identificación de potenciales fotoliasas de alta eficiencia. Se lograron producir una CPD-fotoliasa y una fotoliasa bifuncional de forma sencilla, con un protocolo de purificación de un solo paso, y de forma activa con alta capacidad fotorreparadora. Finalmente, las fotoliasas resultaron ser estables para tiempos mayores a 2 años (almacenadas a – 80 ^{o}C), manteniendo 100% de actividad. Todos estos factores, evaluados en conjunto, hacen de estas enzimas un gran blanco para el desarrollo de una formulación con aplicación en la industria cosmética y médica.

7. PERSPECTIVAS

Como perspectivas desde el punto de vista de investigación aplicada, se plantea seguir adelante en el desarrollo de una formulación que contenga ambas fotoliasas, que permita reparar todos los tipos de daño directo al ADN, que es generado luego de la exposición a luz UV. Las fotoliasas también podrían comercializarse con fines de investigación. También sería interesante definir una unidad enzimática para fotoliasas que permitiesen mejorar la estandarización de los productos.

Desde un punto de vista básico, sería muy interesante abordar la novedad de una fotoliasa bifuncional. Para ello se propone verificar la actividad bifuncional mediante HPLC y realizar experimentos de cristalización de la enzima, y de la enzima co-cristalizada en complejo con ADN conteniendo un CPD y un 6,4-FP. También se propone determinar la

afinidad de unión, y las constantes cinéticas y termodinámicas cuando se utilizan los CPDs y los 6,4-FPs.

8. OTROS TRABAJOS Y COLABORACIONES

Durante el desarrollo de la Tesis de Doctorado, también se publicó un capítulo de libro, artículos en colaboración y se estrecharon vínculos con otras instituciones.

Los ensayos de HPLC se realizaron en Alemania, en el Karlsruher Institute fur Technologie (KIT) en colaboración con un grupo de reconocida experiencia en fotoliasas y a cargo del Dr. Tilman Lamparter. Se utilizaron fondos del programa de movilidad e intercambio de CSIC para la realización de dicha pasantía, lo que permitió establecer en vínculo estrecho con el grupo del Dr.

También generamos una vinculación a través de un proyecto de la Comisión Honoraria de Lucha Contra el Cáncer con las Dras. Paola Hernández y Lucía Canclini, donde continuamos con el estudio la internalización de las fotoliasas en queratinocitos humanos y a futuro en melanocitos.

Finalmente, se estableció una colaboración con el Laboratorio de Biomateriales de la Facultad de Ciencias, el Laboratorio de Espectroscopía y Fisicoquímica Orgánica, Litoral Norte, y el Departamento de Química Orgánica de la Facultad de Química, donde se estudió el uso del pigmento producido por *Hymenobacte*r sp. UV11 para su utilización en celdas fotoeléctricas.

A continuación, se detallan las publicaciones generadas, aparte de las que forman parte de los capítulos de la tesis.

2018 - Montagni T, Enciso P**, Marizcurrena JJ**, Castro-Sowinski S, Fontana C, Davyt D and Cerdá MF. Dye sensitized solar cells based on Antarctic *Hymenobacter* sp. UV11 dyes. *Environ Sust* **1**: 89-97

2017 - Herrera LM, García-Laviña CX, **Marizurrena JJ**, Volonterio O, Ponce de León R and Castro-Sowinski S. Hydrolytic enzyme-producing microbes in the Antarctic oligochaete *Grania* sp. (Annelida). *Polar Biol* 40: 947-953.

2017 - Fullana N, Braña V, **Marizcurrena JJ**, Morales D, Betton JM, Marín M and Castro-Sowinski, S. Identification, recombinant production and partial biochemical characterization of an extracellular cold-active serine-metalloprotease from an Antarctic *Pseudomonas* isolate. *AIMS Bioengin* 4: 386-401.

2019 - **Marizcurrena JJ**, Cerdá MF, Alem D and Castro-Sowinski S. Living with Pigments: The Colour Palette of Antarctic Life. In: The Ecological Role of Micro-organisms in the Antarctic Environment (pp. 65-82). Springer, Cham. ISBN 978-3-030-02786-5

9. BIBLIOGRAFÍA

1. World Health Organisation (2017) WHO | Skin cancers. *Who*. **9**, 607–622
2. Ferlay, J., Colombet, M., Soerjomataram, I., Mathers, C., Parkin, D. M., Piñeros, M., Znaor, A., and Bray, F. (2019) Estimating the global cancer incidence and mortality in 2018: GLOBOCAN sources and methods. *Int. J. Cancer*. **144**, 1941–1953
3. Narayanan, D. L., Saladi, R. N., and Fox, J. L. (2010) Ultraviolet radiation and skin cancer. *Int. J. Dermatol.* 10.1111/j.1365-4632.2010.04474.x
4. Seebode, C., Lehmann, J., and Emmert, S. (2016) Photocarcinogenesis and Skin Cancer Prevention Strategies. *Anticancer Res.* 10.21873/anticanres.12334
5. Youssef, K. K., Van Keymeulen, A., Lapouge, G., Beck, B., Michaux, C., Achouri, Y., Sotiropoulou, P. A., and Blanpain, C. (2010) Identification of the cell lineage at the origin of basal cell carcinoma. *Nat. Cell Biol.* 10.1038/ncb2031
6. Graham, G. F., and Tuchayi, S. M. (2016) Squamous cell carcinoma. in *Dermatological Cryosurgery and Cryotherapy*, 10.1007/978-1-4471-6765-5_131
7. Stoff, B., Salisbury, C., Parker, D., and O'Reilly Zwald, F. (2010) Dermatopathology of skin cancer in solid organ transplant recipients. *Transplant. Rev.* 10.1016/j.trre.2010.05.002
8. Se detectan ocho casos de cáncer de piel por día en Uruguay [online] https://www.elobservador.com.uy/nota/se-detectan-ocho-casos-de-cancer-de-piel-por-dia-en-uruguay-201911104044 (Accessed January 24, 2020)
9. Quinet, A., Lerner, L. K., Martins, D. J., and Menck, C. F. M. (2018) Filling gaps in translesion DNA synthesis in human cells. *Mutat. Res. - Genet. Toxicol. Environ. Mutagen.* 10.1016/j.mrgentox.2018.02.004
10. Hogg, M., Wallace, S. S., and Doublié, S. (2005) Bumps in the road: How replicative DNA polymerases see DNA damage. *Curr. Opin. Struct. Biol.* 10.1016/j.sbi.2005.01.014
11. Jacobs, A. L., and Schär, P. (2012) DNA glycosylases: In DNA repair and beyond. *Chromosoma*. **121**, 1–20
12. Coste, F., Ober, M., Carell, T., Boiteux, S., Zelwer, C., and Castaing, B. (2004) Structural basis for the recognition of the FapydG lesion (2,6-diamino-4-hydroxy-5-formamidopyrimidine) by formamidopyrimidine-DNA glycosylase. *J. Biol. Chem.*

10.1074/jbc.M405928200

13. Krishnamurthy, N., Haraguchi, K., Greenberg, M. M., and David, S. S. (2008) Efficient removal of formamidopyrimidines by 8-oxoguanine glycosylases. *Biochemistry*. 10.1021/bi701619u
14. Stevnsner, T., Thorslund, T., De Souza-Pinto, N. C., and Bohr, V. A. (2002) Mitochondrial repair of 8-oxoguanine and changes with aging. in *Experimental Gerontology*, 10.1016/S0531-5565(02)00142-0
15. Cleaver, J. E., Lam, E. T., and Revet, I. (2009) Disorders of nucleotide excision repair: The genetic and molecular basis of heterogeneity. *Nat. Rev. Genet.* 10.1038/nrg2663
16. Hoeijmakers, J. H. J. (2001) Genome maintenance mechanisms for preventing cancer. *Nature*. 10.1038/35077232
17. Hanawalt, P. C. (2000) The bases for Cockayne syndrome. *Nature*. 10.1038/35013197
18. KEGG PATHWAY: Mismatch repair [online] https://www.genome.jp/kegg-bin/show_pathway?map=ko03430&show_description=show (Accessed January 24, 2020)
19. Bailey, S., and Grossman, A. (2008) Photoprotection in cyanobacteria: Regulation of light harvesting. in *Photochemistry and Photobiology*, 10.1111/j.1751-1097.2008.00453.x
20. Purcell, E. B., and Crosson, S. (2008) Photoregulation in prokaryotes. *Curr. Opin. Microbiol.* 10.1016/j.mib.2008.02.014
21. Propst Ricciuti, C., and Lubin, L. B. (1976) Light induced inhibition of sporulation in Bacillus licheniformis. *J. Bacteriol.*
22. White, D., Shropshire, W., and Stephens, K. (1980) Photocontrol of development by Stigmatella aurantiaca. *J. Bacteriol.*
23. Briggs, W. R., Beck, C. F., Cashmore, A. R., Christie, J. M., Hughes, J., Jarillo, J. A., Kagawa, T., Kanegae, H., Liscum, E., Nagatani, A., Okada, K., Salomon, M., Rüdiger, W., Sakai, T., Takano, M., Wada, M., and Watson, J. C. (2001) The phototropin family of photoreceptors. *Plant Cell*. 10.1105/tpc.13.5.993
24. Gomelsky, M., and Klug, G. (2002) BLUF: A novel FAD-binding domain involved in sensory transduction in microorganisms. *Trends Biochem. Sci.* 10.1016/S0968-0004(02)02181-3
25. Hitomi, K. (2000) Bacterial cryptochrome and photolyase: characterization of two

photolyase-like genes of Synechocystis sp. PCC6803. *Nucleic Acids Res.* 10.1093/nar/28.12.2353

26. Pattison, D. I., and Davies, M. J. (2006) Actions of ultraviolet light on cellular structures. *EXS*. 10.1007/3-7643-7378-4_6
27. Sancar, A. (2004) Photolyase and cryptochrome blue-light photoreceptors. *Adv. Protein Chem.* 10.1016/S0065-3233(04)69003-6
28. Rosato, E., Tauber, E., and Kyriacou, C. P. (2006) Molecular genetics of the fruit-fly circadian clock. *Eur. J. Hum. Genet.* 10.1038/sj.ejhg.5201547
29. Losi, A. (2007) Flavin-based blue-light photosensors: A photobiophysics update. *Photochem. Photobiol.* 10.1111/j.1751-1097.2007.00196.x
30. Herrou, J., and Crosson, S. (2011) Function, structure and mechanism of bacterial photosensory LOV proteins. *Nat. Rev. Microbiol.* 10.1038/nrmicro2622
31. Nash, A. I., McNulty, R., Shillito, M. E., Swartz, T. E., Bogomolni, R. A., Luecke, H., and Gardner, K. H. (2011) Structural basis of photosensitivity in a bacterial light-oxygen-voltage/ helix-turn-helix (LOV-HTH) DNA-binding protein. *Proc. Natl. Acad. Sci. U. S. A.* 10.1073/pnas.1100262108
32. Swartz, T. E., Tseng, T. S., Frederickson, M. A., Paris, G., Comerci, D. J., Rajashekara, G., Kim, J. G., Mudgett, M. B., Splitter, G. A., Ugalde, R. A., Goldbaum, F. A., Briggs, W. R., and Bogomolni, R. A. (2007) Blue-light-activated histidine kinases: Two-component sensors in bacteria. *Science (80-.).* 10.1126/science.1144306
33. Sancar, A. (2003) Structure and function of DNA photolyase and cryptochrome blue-light photoreceptors. *Chem. Rev.* **103**, 2203–2237
34. Lin, C., and Shalitin, D. (2003) C RYPTOCHROME S TRUCTURE AND S IGNAL T RANSDUCTION . *Annu. Rev. Plant Biol.* **54**, 469–496
35. Cashmore, A. R. (2003) Cryptochromes: Enabling plants and animals to determine circadian time. *Cell*. **114**, 537–543
36. Todo, T. (1999) Functional diversity of the DNA photolyase/blue light receptor family. *Mutat. Res. - DNA Repair*. **434**, 89–97
37. Kanai, S., Kikuno, R., Toh, H., Ryo, H., and Todo, T. (1997) Molecular evolution of the photolyase-blue-light photoreceptor family. *J. Mol. Evol.* **45**, 535–548
38. Lin, C., and Todo, T. (2005) The cryptochromes. *Genome Biol.* 10.1186/gb-2005-6-5-220

39. Ahmad, M., and Cashmore, A. R. (1993) HY4 gene of A. thaliana encodes a protein with characteristics of a blue-light photoreceptor. *Nature*. **366**, 162–166

40. Lin, C., Robertson, D. E., Ahmad, M., Raibekas, A. A., Jorns, M. S., Dutton, P. L., and Cashmore, A. R. (1995) Association of flavin adenine dinucleotide with the Arabidopsis blue light receptor CRY1. *Science (80-.).* **269**, 968–970

41. Malhotra, K., Kim, S. T., Batschauer, A., Dawut, L., and Sancar, A. (1995) Putative Blue-Light Photoreceptors from Arabidopsis thaliana and Sinapis alba with a High Degree of Sequence Homology to DNA Photolyase Contain the Two Photolyase Cofactors but Lack DNA Repair Activity. *Biochemistry*. **34**, 6892–6899

42. Park, H. W., Kim, S. T., Sancar, A., and Deisenhofer, J. (1995) Crystal structure of DNA photolyase from Escherichia coli. *Science (80-.).* 10.1126/science.7604260

43. Brautigam, C. A., Smith, B. S., Ma, Z., Palnitkar, M., Tomchick, D. R., Machius, M., and Deisenhofer, J. (2004) Structure of the photolyase-like domain of cryptochrome 1 from Arabidopsis thaliana. *Proc. Natl. Acad. Sci. U. S. A.* **101**, 12142–12147

44. Brudler, R., Hitomi, K., Daiyasu, H., Toh, H., Kucho, K. I., Ishiura, M., Kanehisa, M., Roberts, V. A., Todo, T., Tainer, J. A., and Getzoff, E. D. (2003) Identification of a new cryptochrome class: Structure, function, and evolution. *Mol. Cell*. 10.1016/S1097-2765(03)00008-X

45. Kelner, A. (1949) Effect of visible light on the recovery of Streptomyces griseus conidia. *Proc. Natl. Acad. Sci. United States*. **35**, 73–79

46. Kelner, A. (1949) Photoreactivation of ultraviolet-irradiated Escherichia coli, with special reference to the dose-reduction principle and to ultraviolet-inuced mutation. *J. Bacteriol.* **58**, 511–22

47. Rupert, C. S. (1960) Photoreactivation of transforming DNA by an enzyme from bakers' yeast. *J. Gen. Physiol.* **43**, 573–595

48. Rupert, C. S., Goodgal, S. H., and Herriott, R. M. (1958) Photoreactivation in vitro of ultraviolet-inactivated Hemophilus influenzae transforming factor. *J. Gen. Physiol.* **41**, 451–471

49. Rupert, C. S. (1962) Photoenzymatic repair of ultraviolet damage in DNA. I. Kinetics of the reaction. *J. Gen. Physiol.* **45**, 703–724

50. Wulff, D., research, C. R.-B. and biophysical, and 1962, undefined Disappearance of thymine photodimer in ultraviolet irradiated DNA upon treatment with a

photoreactivating enzyme from baker's yeast. *Elsevier*. [online] https://www.sciencedirect.com/science/article/pii/0006291X6290181X (Accessed December 9, 2019)

51. Sancar, A. (2016) Mechanisms of DNA Repair by Photolyase and Excision Nuclease (Nobel Lecture). *Angew. Chemie - Int. Ed.* **55**, 8502–8527
52. Sancar, A., and Rupert, C. S. (1978) Cloning of the phr gene and amplification of photolyase in Escherichia coli. *Gene*. **4**, 295–308
53. Sancar, A., and Sancar, G. B. (1984) Escherichia coli DNA photolyase is a flavoprotein. *J. Mol. Biol.* 10.1016/S0022-2836(84)80040-6
54. Sancar, A., Smith, F. W., and Sancar, G. B. (1984) Purification of Escherichia coli DNA photolyase. *J. Biol. Chem.*
55. Jorns, M. S., Sancar, G. B., and Sancar, A. (1984) Identification of a Neutral Flavin Radical and Characterization of a Second Chromophore in Escherichia coli DNA Photolyase. *Biochemistry*. 10.1021/bi00307a021
56. Payne, G., Sancar, A., Heelis, P. F., and Rohrs, B. R. (1987) The Active Form of Escherichia coli DNA Photolyase Contains a Fully Reduced Flavin and Not a Flavin Radical, both in Vivo and in Vitro. *Biochemistry*. 10.1021/bi00396a038
57. Johnson, J. L., Hamm-Alvarez, S., Payne, G., Sancar, G. B., Rajagopalan, K. V., and Sancar, A. (1988) Identification of the second chromophore of Escherichia coli and yeast DNA photolyases as 5,10-methenyltetrahydrofolate. *Proc. Natl. Acad. Sci. U. S. A.* 10.1073/pnas.85.7.2046
58. Tan, C., Guo, L., Ai, Y., Li, J., Wang, L., Sancar, A., Luo, Y., and Zhong, D. (2014) Direct determination of resonance energy transfer in photolyase: Structural alignment for the functional state. *J. Phys. Chem. A*. **118**, 10522–10530
59. Sancar, G. B., Jorns, M. S., Payne, G., Fluke, D. J., and Rupert, C. S. (1987) Action mechanism of Escherichia coli DNA photolyase. III. Photolysis of the enzyme-substrate complex and the absolute action spectrum. *J. Biol. Chem.*
60. Heelis, P. F., Payne, G., and Sancar, A. (1987) Photochemical Properties of Escherichia coli DNA Photolyase: Selective Photodecomposition of the Second Chromophore. *Biochemistry*. 10.1021/bi00389a007
61. Payne, G., and Sancar, A. (1990) Absolute Action Spectrum of E-FADH2 and E-FADH2-MTHF Forms of Escherichia coli DNA Photolyase. *Biochemistry*. 10.1021/bi00485a021

62. Kavakli, I. H., and Sancar, A. (2004) Analysis of the role of intraprotein electron transfer in photoreactivation by DNA photolyase in vivo. *Biochemistry*. 10.1021/bi0478796

63. Liu, Z., Tan, C., Guo, X., Kao, Y. T., Li, J., Wang, L., Sancar, A., and Zhong, D. (2011) Dynamics and mechanism of cyclobutane pyrimidine dimer repair by DNA photolyase. *Proc. Natl. Acad. Sci. U. S. A.* 10.1073/pnas.1110927108

64. Zhong, D. (2015) Electron Transfer Mechanisms of DNA Repair by Photolyase. *Annu. Rev. Phys. Chem.* 10.1146/annurev-physchem-040513-103631

65. Kao, Y. T., Saxena, C., Wang, L., Sancar, A., and Zhong, D. (2005) Direct observation of thymine dimer repair in DNA by photolyase. *Proc. Natl. Acad. Sci. U. S. A.* 10.1073/pnas.0506586102

66. Tan, C., Liu, Z., Li, J., Guo, X., Wang, L., Sancar, A., and Zhong, D. (2015) The molecular origin of high DNA-repair efficiency by photolyase. *Nat. Commun.* 10.1038/ncomms8302

67. Sancar, A. (1994) Structure and Function of DNA Photolyase. *Biochemistry*. 10.1021/bi00167a001

68. Yarosh, D. B., Rosenthal, A., and Moy, R. (2019) Six critical questions for DNA repair enzymes in skincare products: A review in dialog. *Clin. Cosmet. Investig. Dermatol.* 10.2147/CCID.S220741

69. Sambandan, D. R., and Ratner, D. (2011) Sunscreens: An overview and update. *J. Am. Acad. Dermatol.* 10.1016/j.jaad.2010.01.005

70. Stege, H. (2001) Effect of xenogenic repair enzymes on photoimmunology and photocarcinogenesis. *J. Photochem. Photobiol. B Biol.* 10.1016/S1011-1344(01)00246-9

71. Stege, H., Roza, L., Vink, a a, Grewe, M., Ruzicka, T., Grether-Beck, S., and Krutmann, J. (2000) Enzyme plus light therapy to repair DNA damage in ultraviolet-B-irradiated human skin. *Proc. Natl. Acad. Sci. U. S. A.* 10.1073/pnas.030528897

72. Berardesca, E., Bertona, M., Altabas, K., Altabas, V., and Emanuele, E. (2012) Reduced ultraviolet-induced DNA damage and apoptosis in human skin with topical application of a photolyase-containing DNA repair enzyme cream: Clues to skin cancer prevention. *Mol. Med. Rep.* 10.3892/mmr.2011.673

73. Kawanishi, M., Matsukawa, K., Kuraoka, I., Takamura-Enya, T., Totsuka, Y., Matsumoto, Y., Watanabe, M., Zou, Y., Tanaka, K., Sugimura, T., Wakabayashi, K., and Yagi, T. (2007)

Molecular evidence of the involvement of the nucleotide excision repair (NER) system in the repair of the mono(ADP-ribosyl)ated DNA adduct produced by pierisin-1, an apoptosis-inducing protein from the cabbage butterfly. *Chem. Res. Toxicol.* 10.1021/tx600360b

74. Morel, M. A., Braña, V., Martínez-rosales, C., Cagide, C., and Castro-sowinski, S. (2015) Five-year bio-monitoring of aquatic ecosystems near Artigas Antarctic Scientific Base , King George Island. *Adv. Polar Sci.* **26**, 102–106
75. Marizcurrena, J. J., Morel, M. A., Braña, V., Morales, D., Martinez-López, W., and Castro-Sowinski, S. (2017) Searching for novel photolyases in UVC-resistant Antarctic bacteria. *Extremophiles*. 10.1007/s00792-016-0914-y
76. Miller, J. (1972) Experiments in molecular genetics. *Astrophys. Space Sci.*
77. Eker, A. P. M., Yajima, H., and Yasui, A. (1994) DNA photolyase from the fungus Neurospora crassa. Purification, characterization and comparison with other photolyases. *Photochem. Photobiol.* **60**, 125–133
78. Johnson, M., Zaretskaya, I., Raytselis, Y., Merezhuk, Y., McGinnis, S., and Madden, T. L. (2008) NCBI BLAST: a better web interface. *Nucleic Acids Res.* 10.1093/nar/gkn201
79. Bankevich, A., Nurk, S., Antipov, D., Gurevich, A. A., Dvorkin, M., Kulikov, A. S., Lesin, V. M., Nikolenko, S. I., Pham, S., Prjibelski, A. D., Pyshkin, A. V., Sirotkin, A. V., Vyahhi, N., Tesler, G., Alekseyev, M. A., and Pevzner, P. A. (2012) SPAdes: A New Genome Assembly Algorithm and Its Applications to Single-Cell Sequencing. *J. Comput. Biol.* 10.1089/cmb.2012.0021
80. Aziz, R. K., Bartels, D., Best, A., DeJongh, M., Disz, T., Edwards, R. A., Formsma, K., Gerdes, S., Glass, E. M., Kubal, M., Meyer, F., Olsen, G. J., Olson, R., Osterman, A. L., Overbeek, R. A., McNeil, L. K., Paarmann, D., Paczian, T., Parrello, B., Pusch, G. D., Reich, C., Stevens, R., Vassieva, O., Vonstein, V., Wilke, A., and Zagnitko, O. (2008) The RAST Server: Rapid annotations using subsystems technology. *BMC Genomics*. 10.1186/1471-2164-9-75
81. Zimmermann, L., Stephens, A., Nam, S. Z., Rau, D., Kübler, J., Lozajic, M., Gabler, F., Söding, J., Lupas, A. N., and Alva, V. (2018) A Completely Reimplemented MPI Bioinformatics Toolkit with a New HHpred Server at its Core. *J. Mol. Biol.* 10.1016/j.jmb.2017.12.007
82. Larkin, M. A., Blackshields, G., Brown, N. P., Chenna, R., Mcgettigan, P. A., McWilliam,

H., Valentin, F., Wallace, I. M., Wilm, A., Lopez, R., Thompson, J. D., Gibson, T. J., and Higgins, D. G. (2007) Clustal W and Clustal X version 2.0. *Bioinformatics*. 10.1093/bioinformatics/btm404

83. Kumar, S., Stecher, G., and Tamura, K. (2016) MEGA7: Molecular Evolutionary Genetics Analysis Version 7.0 for Bigger Datasets. *Mol. Biol. Evol.* 10.1093/molbev/msw054
84. Ghio, S., Ontañon, O., Piccinni, F. E., Marrero Díaz de Villegas, R., Talia, P., Grasso, D. H., and Campos, E. (2018) Paenibacillus sp. A59 GH10 and GH11 Extracellular Endoxylanases: Application in Biomass Bioconversion. *BioEnergy Res.* **11**, 174–190
85. Yin, Y., Mao, X., Yang, J., Chen, X., Mao, F., and Xu, Y. (2012) DbCAN: A web resource for automated carbohydrate-active enzyme annotation. *Nucleic Acids Res.* 10.1093/nar/gks479
86. Rawlings, N. D., Barrett, A. J., and Bateman, A. (2009) MEROPS: The peptidase database. *Nucleic Acids Res.* 10.1093/nar/gkp971
87. Mani, M., Chen, C., Amblee, V., Liu, H., Mathur, T., Zwicke, G., Zabad, S., Patel, B., Thakkar, J., and Jeffery, C. J. (2015) MoonProt: A database for proteins that are known to moonlight. *Nucleic Acids Res.* 10.1093/nar/gku954
88. Krogh, A., Larsson, B., Von Heijne, G., and Sonnhammer, E. L. L. (2001) Predicting transmembrane protein topology with a hidden Markov model: Application to complete genomes. *J. Mol. Biol.* 10.1006/jmbi.2000.4315
89. Puck, T. T., Cieciura, S. J., and Robinson, A. (1958) Genetics of somatic mammalian cells: iii. Long-term cultivation of euploid cells from human and animal subjects. *J. Exp. Med.* **108**, 945–956
90. Boukamp, P., Petrussevska, R. T., Breitkreutz, D., Hornung, J., Markham, A., and Fusenig, N. E. (1988) Normal keratinization in a spontaneously immortalized aneuploid human keratinocyte cell line. *J. Cell Biol.* 10.1083/jcb.106.3.761
91. Gibson, D. G. (2012) *Genscript, Gene Synthesis*, 10.1007/978-1-61779-564-0
92. Sambrook, J., and W Russell, D. (2001) Molecular Cloning: A Laboratory Manual. *Cold Spring Harb. Lab. Press. Cold Spring Harb. NY*. 10.1016/0092-8674(90)90210-6
93. Studier, F. W. (2005) Protein production by auto-induction in high-density shaking cultures. *Protein Expr. Purif.* 10.1016/j.pep.2005.01.016
94. Laemmli, U. K. (1970) Cleavage of structural proteins during the assembly of the head of bacteriophage T4. *Nature*. 10.1038/227680a0

95. Dyrlund, T. F., Poulsen, E. T., Scavenius, C., Sanggaard, K. W., and Enghild, J. J. (2012) MS Data Miner: A web-based software tool to analyze, compare, and share mass spectrometry protein identifications. *Proteomics*. 10.1002/pmic.201200109

96. Photosomes V – ProTec Ingredia [online] https://protecingredia.com/products/barnet/photosomes.html (Accessed February 3, 2020)

97. Ma, H., Zhang, F., Ignatz, E., Suehnel, M., Xue, P., Scheerer, P., Essen, L. O., Krauï¿½, N., and Lamparter, T. (2017) Divalent Cations Increase DNA Repair Activities of Bacterial (6-4) Photolyases. in *Photochemistry and Photobiology*, 10.1111/php.12698

98. Graf, D., Wesslowski, J., Ma, H., Scheerer, P., Krauß, N., Oberpichler, I., Zhang, F., and Lamparter, T. (2015) Key amino acids in the bacterial (6-4) photolyase PhrB from Agrobacterium fabrum. *PLoS One*. 10.1371/journal.pone.0140955

99. Oberpichler, I., Pierik, A. J., Wesslowski, J., Pokorny, R., Rosen, R., Vugman, M., Zhang, F., Neubauer, O., Ron, E. Z., Batschauer, A., and Lamparter, T. (2011) A photolyase-like protein from agrobacterium tumefaciens with an iron-sulfur cluster. *PLoS One*. 10.1371/journal.pone.0026775

100. Tian, W., Chen, C., Lei, X., Zhao, J., and Liang, J. (2018) CASTp 3.0: Computed atlas of surface topography of proteins. *Nucleic Acids Res.* 10.1093/nar/gky473

101. Steffen, C., Thomas, K., Huniar, U., Hellweg, A., Rubner, O., and Schroer, A. (2010) AutoDock4 and AutoDockTools4: Automated Docking with Selective Receptor Flexibility. *J. Comput. Chem.* 10.1002/jcc

102. Benbelgacem, F. F., Bellag, O. A., Salleh, H. M., and Batcha, I. A. N. (2019) Functional Diversity of Biocatalysts: Whether to Bioprospect or Bioengineer? *Biol. Nat. Resour. Eng. J.* **2**, 64–84

103. Bull, A. (1992) Biodiversity As A Source of Innovation in Biotechnology. *Annu. Rev. Microbiol.* 10.1146/annurev.micro.46.1.219

104. Bull, A. T., Ward, A. C., and Goodfellow, M. (2000) Search and Discovery Strategies for Biotechnology: the Paradigm Shift. *Microbiol. Mol. Biol. Rev.* 10.1128/mmbr.64.3.573-606.2000

105. Feller, G., and Gerday, C. (1997) Psychrophilic enzymes: Molecular basis of cold adaptation. *Cell. Mol. Life Sci.* 10.1007/s000180050103

106. Gerday, C., Aittaleb, M., Arpigny, J. L., Baise, E., Chessa, J. P., Garsoux, G., Petrescu, I.,

and Feller, G. (1997) Psychrophilic enzymes: A thermodynamic challenge. *Biochim. Biophys. Acta - Protein Struct. Mol. Enzymol.* 10.1016/S0167-4838(97)00093-9

107. Feller, G., and Gerday, C. (2003) Psychrophilic enzymes: Hot topics in cold adaptation. *Nat. Rev. Microbiol.* 10.1038/nrmicro773
108. Gerday, C., Aittaleb, M., Bentahir, M., Chessa, J. P., Claverie, P., Collins, T., D'Amico, S., Dumont, J., Garsoux, G., Georlette, D., Hoyoux, A., Lonhienne, T., Meuwis, M. A., and Feller, G. (2000) Cold-adapted enzymes: From fundamentals to biotechnology. *Trends Biotechnol.* 10.1016/S0167-7799(99)01413-4
109. Zakhia, F., Jungblut, A. D., Taton, A., Vincent, W. F., and Wilmotte, A. (2008) Cyanobacteria in cold ecosystems. in *Psychrophiles: From Biodiversity to Biotechnology*, 10.1007/978-3-540-74335-4_8
110. Margesin, R., and Schinner, F. (2001) Potential of halotolerant and halophilic microorganisms for biotechnology. *Extremophiles*. 10.1007/s007920100184
111. Feller, G. (2003) Molecular adaptations to cold in psychrophilic enzymes. *Cell. Mol. Life Sci.* 10.1007/s00018-003-2155-3
112. Daly, M. J. (2000) Engineering radiation-resistant bacteria for environmental biotechnology. *Curr. Opin. Biotechnol.* 10.1016/S0958-1669(00)00096-3
113. Rothschild, L. J., and Mancinelli, R. L. (2001) Life in extreme environments. *Nature*. 10.1038/35059215
114. Daly, M. J. (2012) Death by protein damage in irradiated cells. *DNA Repair (Amst).* 10.1016/j.dnarep.2011.10.024
115. Marizcurrena, J. J., Herrera, L. M., Costábile, A., Morales, D., Villadóniga, C., Eizmendi, A., Davyt, D., and Castro-Sowinski, S. (2019) Validating biochemical features at the genome level in the Antarctic bacterium Hymenobacter sp. strain UV11. *FEMS Microbiol. Lett.* **366**, 1–10
116. Marizcurrena, J. J., Martínez-López, W., Ma, H., Lamparter, T., and Castro-Sowinski, S. (2019) A highly efficient and cost-effective recombinant production of a bacterial photolyase from the Antarctic isolate Hymenobacter sp. UV11. *Extremophiles*. **23**, 49–57
117. Marizcurrena, J. J., Morales, D., Smircich, P., and Castro-Sowinski, S. (2019) Draft Genome Sequence of the UV-Resistant Antarctic Bacterium Sphingomonas sp. Strain UV9 . *Microbiol. Resour. Announc.* 10.1128/mra.01651-18

118. Kiontke, S., Geisselbrecht, Y., Pokorny, R., Carell, T., Batschauer, A., and Essen, L. O. (2011) Crystal structures of an archaeal class II DNA photolyase and its complex with UV-damaged duplex DNA. *EMBO J.* 10.1038/emboj.2011.313

119. Ignatz, E., Geisselbrecht, Y., Kiontke, S., and Essen, L. O. (2018) Nicotinamide Adenine Dinucleotides Arrest Photoreduction of Class II DNA Photolyases in $FADH^{\cdot}$ State. *Photochem. Photobiol.* 10.1111/php.12834

120. Yamada, D., Dokainish, H. M., Iwata, T., Yamamoto, J., Ishikawa, T., Todo, T., Iwai, S., Getzoff, E. D., Kitao, A., and Kandori, H. (2016) Functional Conversion of CPD and (6-4) Photolyases by Mutation. *Biochemistry*. 10.1021/acs.biochem.6b00361

121. Zhang, F., Scheerer, P., Oberpichler, I., Lamparter, T., and Krauß, N. (2013) Crystal structure of a prokaryotic (6-4) photolyase with an Fe-S cluster and a 6,7-dimethyl-8-ribityllumazine antenna chromophore. *Proc. Natl. Acad. Sci. U. S. A.* 10.1073/pnas.1302377110

122. Ma, H., Holub, D., Gillet, N., Kaeser, G., Thoulass, K., Elstner, M., Krauß, N., and Lamparter, T. (2019) Two aspartate residues close to the lesion binding site of Agrobacterium (6-4) photolyase are required for Mg2+ stimulation of DNA repair. *FEBS J.* 10.1111/febs.14770

123. Holub, D., Lamparter, T., Elstner, M., and Gillet, N. (2019) Biological relevance of charge transfer branching pathways in photolyases. *Phys. Chem. Chem. Phys.* 10.1039/c9cp01609k

124. An, M., Zheng, Z., Qu, C., Wang, X., Chen, H., Shi, C., and Miao, J. (2018) The first (6-4) photolyase with DNA damage repair activity from the Antarctic microalga Chlamydomonas sp. ICE-L. *Mutat. Res. - Fundam. Mol. Mech. Mutagen.* 10.1016/j.mrfmmm.2018.03.004

125. Photolyase - Search Results - MyBioSource [online] https://www.mybiosource.com/search/photolyase (Accessed February 14, 2020)

126. Puviani, M., Barcella, A., and Milani, M. (2013) Efficacy of a photolyase-based device in the treatment of cancerization field in patients with actinic keratosis and non-melanoma skin cancer. *G. Ital. di Dermatologia e Venereol.*

127. Vendrell-Criado, V., Rodríguez-Muñiz, G. M., Cuquerella, M. C., Lhiaubet-Vallet, V., and Miranda, M. A. (2013) Photosensitization of DNA by 5-methyl-2-pyrimidone deoxyribonucleoside: (6 - 4) photoproduct as a possible trojan horse. *Angew. Chemie* -

Int. Ed. 10.1002/anie.201302176

128. Osakabe, A., Tachiwana, H., Kagawa, W., Horikoshi, N., Matsumoto, S., Hasegawa, M., Matsumoto, N., Toga, T., Yamamoto, J., Hanaoka, F., Thomä, N. H., Sugasawa, K., Iwai, S., and Kurumizaka, H. (2015) Structural basis of pyrimidine-pyrimidone (6-4) photoproduct recognition by UV-DDB in the nucleosome. *Sci. Rep.* 10.1038/srep16330

129. Jans, J., Schul, W., Sert, Y. G., Rijksen, Y., Rebel, H., Eker, A. P. M., Nakajima, S., Van Steeg, H., De Gruijl, F. R., Yasui, A., Hoeijmakers, J. H. J., and Van Der Horst, G. T. J. (2005) Powerful skin cancer protection by a CPD-photolyase transgene. *Curr. Biol.* 10.1016/j.cub.2005.01.001